DEVELOPMENT OF A LOW COST DESIGN TOOLKIT FOR SIZING AIR-COOLED HEAT EXCHANGERS USING OPEN SOURCE HEAT TRANSFER CORRELATIONS.

A THESIS SUBMITTED IN PARTIAL FULFILLMENT OF THE REQUIREMENTS FOR THE DEGREE

OF

MASTER OF PHILOSOPHY

IN

MECHANICAL ENGINEERING

BY

UGONNA CHIDERA MBAEZUE

REG. NO: 201384951

Department of Mechanical and Aerospace Engineering

University of Strathclyde

Glasgow

2019

SUPERVISOR: Dr. WILLIAM DEMPSTER

Declaration

This thesis is the result of the author's original research. It has been composed by the author and has not been previously submitted for the examination which has led to the award of a degree.

The copyright of this thesis belongs to the author under the terms of the United Kingdom Copyright Acts as qualified by the University of Strathclyde Regulation 3.50. Due acknowledgement must always be made of the use of any material contained in, or derived from, this thesis

Signed: *Ugonna Chidera Mbaezue*   Date: 06/06/2019

Abstract:

The exorbitant costs associated with heat exchanger design software e.g. ASPEN EDR, HTRI X-Suite etc., means that most engineering firms especially SMEs, struggle to purchase and use these tools for in-house design purposes. Therefore, heat exchanger design for these engineering firms is dependent on charts, graphs and 'passed down' knowledge. Unfortunately in most cases, the accuracy of these design data sources cannot be verified which means that every heat exchanger designed, is not sized correctly to deliver the heat duty required.

The aim of this project was to build a low cost toolkit capable of designing and rating Circular – Fin, Tube-in-Plate Fin and Plain Tube Heat Exchangers air-cooled heat exchangers.

Heat transfer correlations were obtained from publicly available data and the validation process involved designing air-cooled heat exchangers using these correlations. Thereafter, the design process was repeated using the industry standard software, ASPEN Exchanger Design & Rating (EDR). The results were then compared. The outcome indicated that when geometrical characteristics and operating conditions stayed within the boundaries specified by the open source correlations, the largest deviation will occur in the Tube-in-Plate heat exchanger with an over-prediction of 14% of the area ratio (Gas side vs. Fluid side of the heat exchanger) when compared with the ASPEN EDR results. The Plain Tube heat exchanger showed a 7.5% over-prediction for the staggered tube layout and an 8% over-prediction for the inline tube layout. The Circular-Fin heat exchanger gave the best result with a 6% over-prediction for the compared area ratios.

Based on these results, the toolkit was developed using the Excel Visual Basic for Applications (VBA) programming language. The NIST Reference fluid Properties (REFPROP) database was used to obtain the thermophysical properties of the interacting fluids and was also integrated into the toolkit using the VBA programming language.

Table of Contents

List of Figures

List of Tables

Nomenclature

The dimensions for each symbol are represented in SI units.

A or A_T	Total heat transfer surface area, m^2
A_f	Total fin surface area, m^2
A_p	Primary surface area of bare tubes alone, m^2
A_o	Total heat transfer area based on outside dimensions of heat exchanger ($A_f + A_p$), m^2
A_r	Area at fin root diameter, m^2
A_{fr}	Frontal area, m^2
A_{min}	Minimum flow area, m^2
C^*	Thermal capacity ($\dot{m}c_p$) J/Sec. K
c_p	Specific heat capacity of fluid, J/kg. K
D_h	Hydraulic diameter, m
d_c	Internal diameter, m
d_e	Fin tip diameter, m
d_i	Internal diameter, m
d_o	Outer diameter, m
d_r	Fin root diameter, m
f	Fanning frictional factor, dimensionless
G	Mass velocity, $kg/m^2.s$
g	Gravitational acceleration, m/s^2
g_c	proportionality constant in Newton's second law of motion, g_c = 1 and dimensionless in SI units
Hg	Hagen number, Dimensionless
h	Heat transfer coefficient, $W/m^2.K$
h_f	Fin height, m
J	Colburn factor, $(h/Gc_p).Pr^{2/3}$, dimensionless
k	Thermal conductivity, W/m. K
l	Fin height, m
L_1	Tube length, m
L_2	Flow length, m
L_3	Stack height, m
Lq	Lévêque number
$\dot{m}$	Fluid mass flow rate, kg/s
m	Fin surface parameter
N_t	Total number of tubes in exchanger
N_f	Number of fins per unit length, m^{-1}
N_r	Number of rows in flow direction
Nu	Nusselt number, dimensionless
NTU	Number of Transfer Units
Pr	Prandtl number, dimensionless
P_t	Transverse pitch, perpendicular to gas-side fluid flow, m
P_l	Longitudinal pitch, parallel to gas-side fluid flow, m
p_f	Fin pitch, $1/N_f$, m
Δp	Fluid static pressure drop on either tube-side or gas-side of heat exchanger, Pa
Q	Heat duty, kW
Re	Reynolds number based on hydraulic diameter, dimensionless

Re_d	Reynolds number based on tube outside diameter, dimensionless
Re_{dc}	Reynolds number based on tube collar diameter, dimensionless
R_w	Tube wall resistance, $W/m^2 \cdot K$
s	mean gap between fins, $(p_f - \delta)$ m
T_1	Inlet fluid temperature, ^0C
T_2	Outlet fluid temperature, ^0C
ΔT_{LMTD}	Log-mean temperature difference, ^0C
U	Overall Heat transfer coefficient, $W/m^2 \cdot K$
X_t	Transverse pitch, perpendicular to gas-side fluid flow, m
X_l	Longitudinal pitch, parallel to gas-side fluid flow, m
X_d	Diagonal pitch, $(X_t^2 + X_l^2)$, m
X_t^*	Ratio of the transverse pitch to the tube outer diameter, in a circular tube bank, X_t/d_0, dimensionless
X_l^*	Ratio of the longitudinal pitch to the tube outer diameter, in a circular tube bank, X_l/d_0, dimensionless
X_d^*	Ratio of the diagonal pitch to the tube outer diameter, in a circular tube bank, X_d/d_0
x	Steam quality
δ	Fin thickness, m
μ	Fluid dynamic viscosity, Pa. s
ρ	Fluid density, kg/m^3
σ	Ratio of free flow area to frontal area, A_0/A_{fr}, dimensionless
η	Efficiency
ε	ratio of external surface area to external bare surface area at fin root diameter
∈	Thermal effectiveness

Subscripts

LMTD	Logarithmic mean
f	fluid
fb	fin bond
fo	fouling
g	gas – side
in	inline
st	staggered
r	root
s	surface
t	tube - side
o	overall
o	outside surface
i	Inside surface
l	liquid (condensate)
lam	laminar
turb	turbulent
w	wall
cr	critical
con	condensation
sat	Saturation

vap	vaporisation
1	inlet
2	outlet

Chapter 1

1.1   Introduction:

Chapter 1 consists of an introduction to heat exchangers. It further expands to describe circumstances under which heat exchangers are used, how they are classified and the types that fall under each category. Further on, the objective of the project is explained and the chapters constituting the thesis are also outlined.

1.2   Background:

The Department of Energy and Climate Change (2012), estimates that heat constitutes up to 80% of the energy needs of every industry. This heat is often generated as a by-product of activities such as combustion of fuels for energy generation. BCS Incorporate (2008) suggests that 20 − 50% of generated heat is eventually discharged into the atmosphere as waste and is hardly ever reused. However, the latest drive to reduce carbon emissions by as much as 70% by 2050 by countries such as the UK (Department of Energy & Climate Change, 2012), has seen the urgent need to improve process efficiency through the reuse of generated heat. For example, heat designated as waste could be used to preheat boiler feed water. This not only improves the efficiency of the initial process that generates the heat, but also improves the efficiency of the boiler since less work is needed to raise the temperature of the feed water. Though the aim to improve process efficiency via heat addition is important, the need to extract it is equally as important especially in industries where heat generating chemical reactions occur as part of the process. An example is seen in the automobile industry, where vehicle engines reach extremely high temperatures as a result of combustion and need to be cooled to prevent damage to the engine.

A heat exchanger is therefore any device or equipment which has been designed to utilise a combination of all the modes of heat transfer (conduction, convection and radiation) to convey generated heat energy between interacting fluids, surfaces or a combination of a surface and a fluid. Whatever the case maybe (heat addition or heat extraction), a temperature gradient must exist between the interacting fluids, surfaces or fluids and surfaces for the heat to flow.

Therefore, as a fundamental part of any thermal system, the strategic position of heat exchangers in industrialisation becomes easily apparent. In fact, it is predicted that by 2020, the global market for heat exchangers will hit the $24.3 billion mark (A Global Strategic Business Report, 2016). To cater to this ever growing market, several multinational companies such as GEA Heat Exchangers Group, Alfa Laval AB, SPX Flow etc. have sprung up in the last few years and have equally seen unprecedented growth in sales and revenue. Unfortunately, the extent of growth predicted and seen in the heat exchanger industry for both use and manufacture has not been matched by equivalent growth in the heat exchanger design software market. This could be down to the significant investment in time and

finances needed for research to fully understand the complex nature of fluid flow and heat transfer interaction in heat exchangers. A good understanding of this interaction will ensure that an engineer can design and select the appropriate unit to match his unique process conditions. Poor specification will lead to problems such as inability of the heat exchanger to either extract or transfer the required heat to another process and this could be due to several factors such as fouling, disproportionate areas, initial design data inaccuracy etc. According to Ibrahim (2012), 15% of total expenditure in any industry is eventually traced to the maintenance and replacement of heat exchangers alone. Besides the added expenditure, other issues such as plant shutdowns, production and revenue losses can also be traced to poor heat exchanger design and selection.

Refs 66-79, show that over the past years, in-depth experimental and numerical research in the heat transfer process has grown and credit must be given for the amount of work invested in this area. However, very little progress has been made in harmonising all this data into a single design tool suited to any heat exchanger. This could possibly be attributed to the different skillset needed for computer programming purposes. This factor then constitutes the difficult part for any thermal design engineer who is left with the difficult task of trawling through several pages of scientific journals to find design data that exactly matches his unique process conditions. In instances where a heat exchanger software design tool is available, the design engineer is likely to be confronted with either the excessive costs associated with owning the software or the accuracy of the software design tool is called into question due to lack of access to the design correlations with which they have been built.

1.3   Classification of Heat Exchangers

Heat exchangers can be classified according to area of application, nature of the fluids & interacting surfaces, method of contact between the transfer surfaces, surface compactness, etc. However, the one common characteristic they all share is that in all cases, there is no external heat or work interaction generated during their use.

The categories include:

- **Classification according to heat transfer process**
  - **Indirect – Contact Heat Exchangers:** Indirect – contact heat exchangers are identified by the presence of a separating surface between the interacting fluids. Heat is usually transferred between the fluids across the dividing wall mainly via conduction. In most cases, simultaneous fluid flow of both fluids is required. These heat exchangers are referred to as direct transfer heat exchangers or recuperators. Examples include tubular or extended surface heat exchangers.

In another scenario, heat is first transferred to one medium (e.g. a permeable solid material) by the hot fluid and then, the cooler fluid is allowed to flow through the material for the heat transfer to occur. These heat exchangers are referred to as storage type heat exchangers or regenerators. An example of the latter is the storage type exchanger.

In the final category of indirect-contact heat exchangers, you have the Fluidized-Bed Heat Exchangers. In these heat exchangers, a side of the heat transfer unit is buried in a bed of fine material, e.g. sand or coal. The second fluid is then allowed to flow in an upward direction through this bed of fine particles. If the velocity of flow is low, the fine particles remain fixed in their position and the gas simply flows through. However, if flow velocity is high, the fine particles are suspended acting almost as fluids. This characteristic is referred to as the fluidized state. In this state, the cold fluid is given more time to interact with the hot fluid within the confines of the bed, thus high heat transfer coefficients are common in these beds. Where coal is used as the packed bed, chemical reactions could occur in the form of combustion with by-products tapped off at the bottom of the heat transfer unit. The possibility of combustion or chemical reactions further adds to the complexity in the design of these units.

- **Direct – Contact Heat Exchangers:** In the direct-contact type, the interacting fluids are allowed to mix, exchange heat and are then separated. They are characterised by mass transfer in addition to the heat transferred and possibly a phase change in the fluids. The direct contact between the interacting fluids accounts for the very high heat transfer rates achieved especially where one interacting fluid (e.g. steam) is at a high enthalpy.   Further classification of direct contact heat exchangers include: Liquid-Vapour Exchangers (steam is partially or fully condensed using cold water through direct contact of the two fluids), Gas-Liquid Exchangers (heat is transferred between a gas and a low pressure liquid) and Immiscible Fluid Exchangers (two immiscible fluids are brought in contact for heat transfer to occur. An example is the condensation of oil vapours with air or water)

- **Number of interacting fluids:**

    In most heat exchangers, heat transfer is predominantly between two fluids. However, Sekulić and Shah (2003) points out that chemical processes e.g. air-separation systems utilise as much as 12 fluid streams in heat transfer processes. As the number of interacting fluids increases, so does the complexity involved in the design of these heat exchangers.

- **Surface compactness:** Compact heat exchangers refer to exchangers with a much larger heat transfer surface area per unit volume of the heat exchanger. This arrangement produces a unit with less energy requirements, less space, better heat transfer design and weight when compared to heat exchangers such as shell and tube heat exchangers where the per unit volume is much more than the heat transfer surface available.

    Compact exchangers are common where one fluid has very poor heat transfer properties (i.e. heat transfer coefficient) in comparison to the other fluid. The larger surface area therefore serves to improve the ability of the poorer heat transfer fluid to either reject or acquire heat during the heat exchange process, thereby reducing the overall surface needed for heat transfer. An example is a gas-to-fluid heat exchanger which has a heat transfer surface area per unit volume greater than $700m^2/m^3$ in the gas stream and $400m^2/m^3$ for operating in the fluid stream. In comparison, shell and tube heat exchangers will have a surface area per unit volume of less than $100m^2/m^3$ on the side with plain tubes and two or three times that on the high fin density side (Sekulić and Shah 2003). Compact heat exchangers are not entirely restricted to gas-to-fluid heat transfer processes. They are also common in gas-to-liquid and gas-to-phase change heat exchangers, so long as one fluid has a heat transfer coefficient significantly less than the other fluid.

- **Construction features:** Examples under these include; tubular, plate-type, extended surface and regenerative heat exchangers.

    The tubular type exchangers are made predominantly of cylindrical tubes which are arranged in any configuration ranging from spiral, straight or rectangular to elliptical. Tubular heat exchangers are used mainly in high pressure environments or conditions where high pressure differences exist between the interacting fluids. Their application covers liquid-to-liquid, liquid-to-phase change, gas-to-liquid or gas-to-gas heat transfer processes.

Examples include; shell & tube heat exchangers and double-pipe heat exchangers.

Plate-type heat exchangers are made from channels bored through flat thin plate. Tubes are inserted in these channels and interacting fluids flow through these tubes on either side of the plate. Heat is thus transferred from one fluid to the other as a result of the plates being in contact with the tubes. Examples include: gasketed, welded or brazed, spiral plate, lamella and platecoil heat exchangers. Due to the weak nature of the plates used, these heat exchangers are never reliable in high pressure or temperature conditions.

In operations where high exchanger effectiveness is required, especially when one or both of the interacting fluids has poor heat transfer coefficients, an extended surface heat exchangers will provide an effective solution. To achieve this, the surface area of a tubular heat exchanger is increased during construction. This is achieved by attaching 'fins' on either side of the tube to effectively increase the surface area of interaction between the fluids. When a 'fin' is attached, heat is conducted along the fins, and then further convected or radiated depending on the unit being used for a heating or cooling application. Common types of extended surface heat exchangers are the plate-fin and tube-fin heat exchanger.

In the plate-fin extended surface heat exchanger, triangular or rectangular shaped fins are used as spacers between parallel arranged flat plates. This allows an uninterrupted flow passage for one side of the interacting fluid which is almost always a gas. The second fluid is then passed through a header attached at either end of the flat plates. The heat is thus transferred through the flat plates to interact with the gas and further enhanced by the addition of the fins.

In the tube-fin extended surface heat exchanger, fins are directly attached to the tubes by a tension winding, welding, brazing or tight mechanical fitting process. In some cases, the tubes are individually finned, with the fins running in a spiral formation around the tube (these are referred to as circular-fin heat exchangers), straight along the longitudinal length of the tube. In another scenario, several tubes are assembled to share a common fin which is usually a flat thin plate made of good heat transfer material such as copper or aluminium. The latter type of arrangement is referred to as

either plate-fin & tube; plate finned tube or tube-in-plate fin heat exchangers.

- **Flow arrangements:** Fluid flow in heat exchangers can be split into either the single or multi-pass flow arrangement. The decision on pass arrangement, is usually dependent on design restrictions such as, minimum and maximum flow velocities, temperature levels, maximum pressure drops etc. In the single pass, each fluid makes a single sweep through the heat exchanger in its full length, while in the multi-pass arrangement, the flow is reversed and the fluid makes another pass through the heat exchanger section.

  The single or multi-pass arrangement can be further split to describe the counter-current flow, co-current flow and the cross flow arrangement. In the counter-flow arrangement, the interacting fluids flow parallel, but in opposite directions to each other. This arrangement is considered to be very efficient for heat transfer purposes, as the cold fluid does not give up any of the heat acquired from the hot fluid as it travels across the exchanger. In the co-current arrangement, the interacting fluids enter and exit the heat exchanger from the same direction. The thermal effectiveness of such heat exchangers is usually very poor. Finally, in the cross flow fluid arrangement, the fluids flow in directions normal or perpendicular to each other. This arrangement is common in extended surface heat exchangers with banks of tubes. The thermal effectiveness of cross flow heat exchangers is considered to be between the counter current flow type arrangement and the co-current flow type arrangement.

- **Heat transfer mechanism:** classification under heat transfer mechanism refers to the mode of heat transfer employed by the interacting fluids during the transfer process. The tube-side fluid is usually able to give up its thermal energy to the tube wall through single-phase convection (forced or free), two-phase convection (via condensation or evaporation, by forced or free convection), and combined convection and radiation heat transfer. Examples include vehicle radiators where single phase convection heat transfer occurs on one side while two-phase convection occurs on the other side of the tubes. Radiation heat transfer is also seen to be the main mode for heat transfer in steam generators and other fired heat exchangers.

1.4   Objectives of thesis:

The overall objective of this project is to create a low cost design toolkit suitable for use in the design of air-cooled heat exchangers. The project objective will be achieved by reviewing publicly available heat transfer data with the aim of collating those design correlations that fit closest to a range of geometrical dimensions obtained from an actual engineering design firm. These heat transfer correlations will then be used to build the toolkit. The process of achieving the project objective will include:

- A description of the heat transfer process and the methods through which heat is transferred (conduction, convection and radiation). The link between the heat transfer processes and heat exchanger design is then discussed and established.

- An analysis of extended surface air cooled heat exchangers with particular reference to circular-fin and plate-in-tube air cooled heat exchangers is conducted along with a literature review of available research to emphasise the benefits of extended surfaces in the heat transfer process.

- A further in-depth review of available heat transfer literature is then conducted, with the aim of collating convective and conductive heat transfer correlations specific to the types of heat exchangers under consideration.

- A validation exercise which involves comparing results produced with the collated heat transfer correlations to the results produced using the ASPEN EDR thermal design software. This exercise will aim to validate the results obtained using the collated heat transfer correlations by comparing them with results obtained using ASPEN EDR results for the same design conditions. This will be the benchmark for selection of any heat transfer correlation for use in the final assembly of the heat exchanger design toolkit.

- Applying an optimization process in the design of a circular fin air-cooled heat exchanger to determine the minimum possible values for the geometrical characteristics (Tube OD, Tube Length, etc.) of the heat exchanger used in the validation exercise described above. The result of the optimization exercise see a reduction in the overall heat transfer surface of the circular-fin heat exchanger required to achieve the desired thermal duty. A reduced overall surface area has been selected as the optimization objective because of the following reasons:

  o **Cost of labour and materials:** because they have the most direct impact on the final price of the heat exchanger. Therefore, because these two cost streams are directly proportional to the overall surface area of the heat exchanger, the cost of manufacturing the heat exchanger can be significantly reduced by minimising the overall size of the designed heat exchanger. The reduction in manufacturing costs,

will allow the manufacturer either make more profit from sales or become more competitive by reducing the cost of sale of his heat exchanger units.

- o **End-user requirements:** The argument to support the selection of the overall heat transfer surface area as the optimization (minimization) objective has been further strengthened by the observation that the heat exchanger industry is predominantly a bespoke manufacturing industry. This means that the overall size of each heat exchanger unit is solely dependent on the operating conditions or dimensional constraints specified by the end user. Therefore, the requirement to minimise operational factors such as pressure drop will vary from unit to unit and in some cases, will not be marked as a criterion by the end user. This is because air-cooled heat exchanger components such as fans and duct transitions are only specified and purchased based on the final overall size of the heat exchanger. In addition to this, the requirement for a reasonably sized heat exchanger unit which still delivers the desired thermal duty will always be important to the end user because of issues such as space constraint and manual handling.

- o **Sizing:** Lastly, optimizing the overall heat transfer surface area of the air cooled heat exchanger unit will eliminate the issue of oversizing heat exchangers at the design stage. The issue of heat exchanger oversizing will always lead to an increase in costs for both labour and materials. In addition to an increase in cost of labour and material, an oversized heat exchanger will deliver a heat duty outside of the requirements of the overall system and eventually lead to an imbalanced system.

- An outline of technical specifications which will show the step-by-step approach required for data input, data analysis and data output when the toolkit is used for the thermal design of air cooled heat exchangers.

- Development of the toolkit using a widely available, easy access programming language such as Microsoft Excel visual basic for applications (VBA).

1.5 Outline of thesis:

- Chapter 1 (Introduction): discusses means of improving plant efficiency through the use of heat exchangers to recycle heat developed during a process. This discussion thus establishes the importance of heat exchangers in most plant processes. Once the need for heat exchangers has been established, chapter 1 then discusses the results of investigations carried out in an attempt to find a low cost thermal design tool that can accurately design heat exchangers. These investigations show that although there has been in-depth research into heat transfer, little or no effort has been made towards developing low cost tools for the

design of heat exchangers. This gap in the market thus justifies the need to develop a low cost thermal design tool, which forms the foundation of the project.

Finally, Chapter 1 discusses the methods of classification of heat exchangers, describes the objectives of the project and provides an outline of the structure of the thesis.

- Chapter 2 (Air-Cooled Heat Exchanger): this chapter focuses on air-cooled heat exchangers which have been selected for the project. This chapter begins by describing the method of heat transfer in air cooled heat exchangers, the advantages of air-cooled heat exchangers and the types of configuration of these units. Chapter 2 goes on to describe methods of improving heat transfer through the use of extended surfaces in air-cooled heat exchangers. Types of extended surfaces are presented and discussed along with results of a literature research conducted to validate the argument that extended surfaces improve heat transfer.

- Chapter 3 (Convective Heat Transfer Coefficient for Forced Convective Heat Transfer): marks the start of the toolkit design process by identifying the elements of the heat transfer process that must be calculated in every heat exchanger design. The chapter begins with providing the reader with an in-depth analysis of the process of heat transfer between the tube-side and the gas-side fluids with respect to the heat transfer coefficient of the interacting fluids. The gas-side fluid (e.g. air) is identified as possessing the poorer thermal conductivity and thus requires more accurate prediction of its heat transfer capabilities when it interacts with the tube-side fluid. Empirical and numerically derived heat transfer correlations for the prediction of the gas-side heat transfer coefficient are then presented and discussed in detail. These correlations cover the types of air-cooled heat exchangers under review and were obtained from research data available in the public domain. Attempts were also made to select those correlations that cover a wide range of design conditions and geometry. Heat exchanger geometry equations needed to calculate the overall heat transfer area of heat exchangers are finally presented.

- Chapter 4 (Validation of Heat Transfer Correlations): ASPEN Exchanger Design and Rating (ASPEN EDR) was selected as the industry standard software against which the results obtained using open source correlations will be validated. Therefore, chapter 4 begins with a description of the physical layout of the ASPEN EDR software. The subsequent sub-section then describes in detail, the sources and validation process for the air-side heat transfer correlations used in ASPEN EDR. To test the accuracy of the open source heat transfer correlations, a case study was selected for circular-fin, tube-in-plate fin and plain tube heat exchangers. Thermal design calculations of the selected case studies were conducted using both ASPEN EDR and the open source correlations. Results from these calculations are discussed in the final section of this chapter.

- Chapter 5 (Heat Exchanger Design Optimization): Since the open source heat transfer correlations have been validated in the preceding chapter, an attempt is made to optimize the process of air-cooled heat exchanger design using the GRG non-linear solver available in Microsoft Excel. The optimization exercise, concentrates on optimising the geometric dimensions of a circular-fin heat exchanger without forfeiting the desired heat duty. A literature review is carried out prior to the onset of the optimization exercise and results are presented in the first half of this chapter. A comparison between the results obtained using the GRG non-linear solver and the conventional design process, is presented and then discussed in the concluding section of the chapter.

- Chapter 6 (Conclusion and Recommendations): involves further discussion of the results obtained in the validation section and the development process of the tool. Recommendations for further development of the tool are discussed in the final section of this chapter.

- Appendix A (Heat Exchanger Design): describes in detail, the process of heat transfer and the heat exchanger design methodology. Design theories such as the ε-NTU and the LMTD method are also presented and discussed.

- Appendix B (Toolkit Specification): The specifications and requirements of the toolkit are outlined and discussed. The structure of the graphic user interface (GUI) and the step-by-step calculation process required from the fully developed tool are discussed in detail.

- Appendix C (Toolkit Design and Development): outlines a step-by-step process for carrying out design calculations using the developed tool. The graphic user interface (physical layout) of the complete design tool is described along with the functionality of each section. A heat exchanger design example is carried out using the tool, and the results presented. A trouble shooting section is included as the last section in this chapter.

Chapter 2

Air-Cooled Heat Exchangers

2.1   Introduction:

These heat exchangers predominantly utilise ambient air to cool or condense the tube-side fluid which is in contrast to using a liquid as seen in shell and tube heat exchanger where water or any other liquid is used. The advantages of air cooling lies in its free availability, where little or no added investment is required to accommodate it. Conditions such as fouling are also non-existent on the air-side of air-cooled heat exchangers, which means that maintenance costs are kept at the very minimum. Lestina and Robert, 2014, [14] state that although the capital cost of air cooled heat exchangers has been known to be quite high, operating cost has however been found to be significantly lower than that of the water-cooled heat exchanger.

In air-cooled heat exchangers, the hot fluid is channelled through the tubes while the cold fluid (mostly air) is allowed to flow on the outside of banks of tubes. In single phase heat transfer, these tubes banks are aligned in the horizontal and in cases where condensation could occur, tube banks are arranged in an A-Frame, to allow for the collection of steam condensate at the heat exchanger bottom header. When tube bundles are aligned horizontally in condensation heat transfer, the condensed fluid tends to lie within the tubes and could lead to an onset of tube corrosion.

In a bid to improve the heat transfer process, a fan assembly can be used to increase the volume of air flow through these heat exchangers. Two types of arrangement exist and they are:

- Forced draft: in this arrangement, the fans are located below the heat exchanger unit and air forcefully pushed across the unit. This arrangement ensures that the fan assembly is kept clear of the hot air generated from the heat transfer process in addition to giving easy access for the inspection and maintenance of the fan assembly. The downside to this arrangement lies in their susceptibility to hot air recirculation as indicated by Lestina and Robert, 2014, [14]. Hot air recirculation tends to reduce the capacity of the exchanger unit leading to the requirement of higher air flow rates or even greater heat transfer surface area.
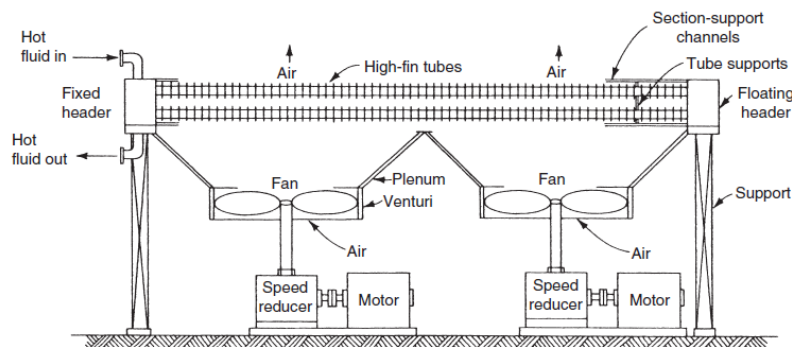
Figure 1: Forced draft air-cooled heat exchanger [Source: Kraus, Aziz & Welty, 2001]

- Induced draft: In the induced draft assembly, the fan is mounted above the heat exchanger bundle, and ambient air drawn across the unit. More power is consumed in this arrangement as a result of the hot air generated during the heat transfer process which has to be handled by the fans (Lestina and Robert, 2014 [14]). However, more uniform flow distribution is achieved and there exists a lesser possibility of hot air recirculation as opposed to the forced draft fan arrangement. Minto, 1991, [26] states that owing to this advantage; induced-draft fan assemblies sometimes require less power than the forced-draft fan assemblies. In the induced draft assembly, the fan drive could be placed below the heat exchanger unit. However, this arrangement sees the drive shaft pass through the tube bank which means that a few tubes will be omitted in the bundle and could effectively reduce the capacity of the unit.
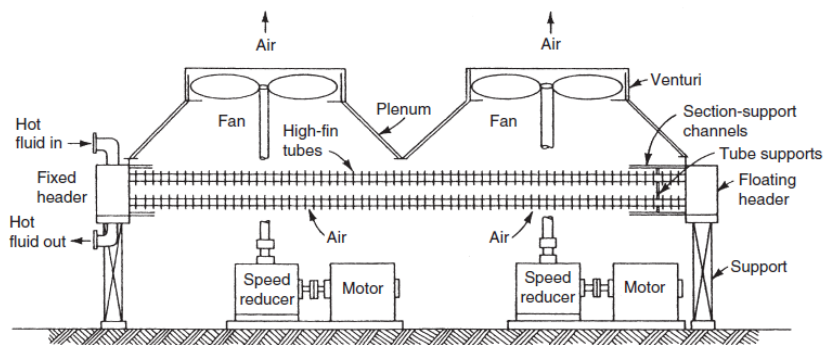
Figure 2: Induced draft air-cooled heat exchanger [Source: Kraus, Aziz & Welty, 2001]

2.2 Heat Transfer Enhancement:

To overcome air-side thermal resistance and improve the overall efficiency of the heat transfer process, several methods have been employed and several more being researched. Ref. [17] describes these methods as either active or passive heat transfer enhancement methods. In the active process, external power is used to improve and sustain the heat transfer process e.g. via stirring or constant surface vibration. Karmatskii, Nesis and Shatalov (1994) [18] and Hagge and Junkhan (1975), [19] give examples of active methods that can be used to improve the heat transfer process. In the passive method, the heat exchanger unit does not require the use of an external power to improve or sustain the heat transfer process. Abdulhafiz, Boukhary, Khaled and Siddique, 2010, [20] provide examples where the passive method is applied which include the use of treated surfaces, extended surfaces, fluid additives or rough surfaces on either the tubes or on the extended surfaces, use of surface tension devices, displaced enhancement devices etc.

In the use of extended surfaces, the surface area of the heat exchanger tubes in contact with the gas of lesser or poorer heat transfer capability is increased through the use of fins. These fins are designed to induce turbulence or better mixing in fluid flow on the gas-side of the heat exchanger. They are also designed to give the gas-side fluid more contact surface to interact with the tube-side

fluid. As a result of their usefulness, fins have found application in several industries such as electronics, gas turbine blade cooling, the automobile industry, thermal storage systems which include phase change materials Refs. [21-24] etc.

Extended surfaces are available in various forms; however the ones of importance to this project have been described below along with studies which have been conducted to show the advantage they present in heat transfer.

2.1.0   Circular or High-Fin Heat Exchangers:

Most ACHE tubes have fins attached to them (hence the term extended surface). This is done, to compensate for the poor heat transfer coefficient of the cooling air. These fins could be rectangular, annular or triangular as seen in Lestina and Robert (2014). Only the circular or High-Fin arrangement on the tubes will be discussed. Several configurations of the circular fin exist and they include:

- Integrally finned: Also referred to as K-fin tubing, fins are extruded from the body of the tube itself. This ensures full thermal contact between the fin and the tube at all operating conditions. These fins are common on metals that are easily worked, e.g. copper and aluminium.
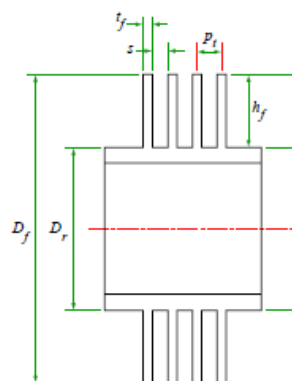
Figure 3: Integral finned heat exchanger tube (Source: ESDU 86022, 1998)

- Bimetallic fins: Also referred to as E-fin tubing, this arrangement consists of an outer and inner layer. The inner layer could be made from any regular tubing material (steel, copper etc.). However, the outer layer or tube is integrally finned and usually made from an aluminium alloy. The outer tube acts as sheath over the inner tube, with the main advantage being that the outer layer can be replaced without damage to the inner tubes. However, thermal contact is poor due to the gap that exists between the two layers. Bell and Muller (2001) showed that although this is negligible at low temperatures, it can account for between 10 − 20% of the total thermal resistance in heat transfer involving high tube-side temperatures.
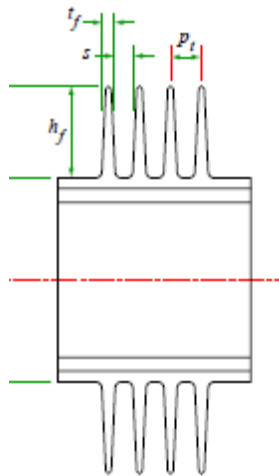
Figure 4: Bimetal fin heat exchanger tube (Source: ESDU 86022, 1998)

- Tension-wound or spiral fins: These are the commonly used fin types due to their low cost and ease of manufacture. They are formed by tension winding a strip of metal round a potential heat exchanger tube. The strip can be left in straight alignment (I-fin) or bent at the root to form an L (L-fin) which ensures better thermal contact with the tube. The disadvantage in this arrangement is that the tubes can be loosened while operating in high temperature environments. Therefore they are only used in operations where temperatures do not exceed 200°C (Robert and Lestina, 2014). The possibility of moisture collection in the gap between the fin and the tube also greatly increases the onset of corrosion in tension wound tubes. The onset of this corrosion can then further expand and attack the tubes directly.
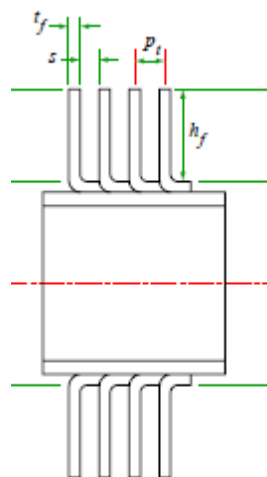
Figure 5: Tension-wound L-shape fin heat exchanger tube (Source: ESDU 86022, 1998)

- Embedded-fin: Also referred to as G-fin, these are much similar to the tension wound. However, the fins are inserted in helical grooves marked around the surface of the tube. This ensures that the fins maintain full contact with the tubes even in high temperature applications. The thermal resistance observed in tension wound tubes, almost disappears in

14

this case, due to insertion of the thin fins in these helical grooves. Robert and Lestina (2014), show they can be used in high temperature conditions as high as 400^{0}C.
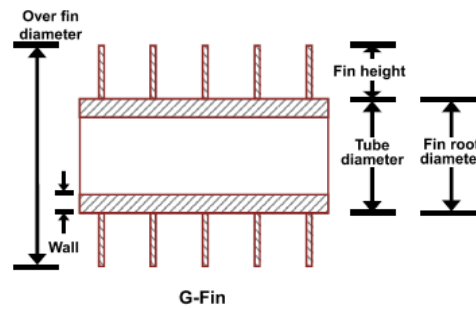
Figure 6: Embedded G-fin heat exchanger tube (Source: Ref. [14])

- Brazed-fin: is made by firstly tension winding the metal strip to the tube, and then brazing them together to ensure full contact as well as reduce thermal contact resistance. When copper fins are used, temperatures as high as 537^{0}C can be accommodated, while stainless steel fins can accommodate a temperature region as high as 816^{0}C (Robert and Lestina, 2014).

High-fin diameters usually range from 12.7mm to 203.2mm with fin heights ranging from 6.35mm to 38.1mm. Average fin thicknesses can be between 0.3mm and 0.9mm, while the number of fins per tube metre, can range from 78 fins per metre of tube, to 472 fins per metre of tube (Robert and Lestina, 2014). A triangular layout is used in the arrangement of tubes if a staggered arrangement is desired, the most common staggered arrangement being the equilateral triangle layout. If the inline arrangement is to be used, a simple 90^0 tube layout is used.

Circular fins have far reaching effects on the performance of heat exchangers and this is observed simply by modifying their surface design (plain, crimped, serrated etc.) or arrangement (inline or staggered). For example, Fukano, Hamakawa, Kudo, Nakashima and Nishida, (2008), studied the vortex shedding effect from a circular cylinder with a spiral fin. As part of their results, they found that in using plain surface spiral-finned tubes, the heat transfer coefficient improved when compared to cases where individual circular fins were used. This result they have stated could possibly be due to the spiral vortices created by the fins. When using serrated spiral fins, Naess (2010), studied the effects of fin pitch and fin outer diameter on heat transfer in a staggered tube heat exchanger layout. Results showed that an increase in fin pitch caused a proportional increase in heat transfer but the fin OD had negligible effect on the heat transfer coefficient. Nuntaphan, Kiatsiriroat and Wang (2005), found that in using crimped spiral fins for an inline heat exchanger, pressure drop increased as tube outer diameter and fin height increased with a decrease in the heat transfer coefficient occurring. However, with a staggered arrangement, the heat transfer greatly improved, along with a decrease in the effect of the fin height on pressure drop. Tang, Wang and Zeng (2009), studied fin design effect on heat transfer and fluid flow using crimped spiral fin, plain fin, slit fin, vortex

generator fins (with longitudinal delta wings) and mixed fin (6 front row vortex generators and 6-rear row slit fins). Observations showed that the crimped spiral fin provided better heat transfer and pressure drop than the other fin designs. Using L-footed spiral fins, Tang, Wang and Zeng, (2009), as well as Pikulkajorn, Pongsoi, and Wongwises, (2013), studied the effect of the fin outside diameter and pitches on a heat exchanger with a multi-pass parallel and counter cross-flow at high air-side Reynolds numbers. Observations indicated that fin pitch had negligible effect on the air-side heat transfer coefficient and Colburn factor, but significantly featured on the rate of heat transfer, pressure drop across the heat exchanger and the frictional factor. Observations also showed that fin OD had a significant effect on the pressure drop, as it increased proportionally with the former. Kiatpachai, Pikulkajorn and Wongwises (2015) also studied the impact serrated welded spiral fins had on heat transfer. Their observations showed that fin pitch had a significant impact on both the heat transfer coefficient and the Colburn factor (j) at high Reynolds numbers. Pressure drop was also found to increase as fin pitch increased. They concluded that serrated welded spiral fins produced higher Colburn factors and frictional factors than any other circular fin. In contrast, Anoop, Balaji, and Velusamy (2015) studied the heat transfer properties of serrated finned tubes and conclusions showed that serrating the fins did not show any improvement to heat transfer when compared to the solid fins. The only advantage they state is the reduction in weight of the heat exchanger as a result of the fin serrations. Cho, Ha, Jung, and Lee (2012) studied the effect of punching holes directly on the circular fins. For 2-hole punched fins, heat transfer improved by 3.55% while for the 4-hole punched fins, heat transfer improved by 3.31%. As for pressure drop, an increase of 0.68% and 2.08% was observed in the 2-hole and 4-hole fins respectively. They attributed the improvement in the heat transfer coefficient to the presence of holes on the fins which reduced the effect of recirculation zones created at flow separation regions on the fins. Joo, Kang, Kim, and Lee, (2011), studied the heat transfer properties of a spiral coiled finned tube under frost conditions by varying the fin pitch and number of tube rows in the heat exchanger. Their observations showed that pressure drop per unit increase in tube length, increased as the fin pitch increased. They also showed that the rate of heat transfer increased as fin pitch decreased and number of tube rows increased. The latter, they attributed to the increase in available heat transfer surface area.

To indicate the effectiveness of a solid circular fin in transferring heat in a given application, the term fin efficiency is used. It follows the form as indicated by McQuiston, and Tree (1972) for fins with plane parallel sides on a flat surface with mean thickness:

$$Fin\ efficiency = \frac{actual\ heat\ transferred}{heat\ which\ would\ be\ transferred\ if\ entire\ fin\ area\ were\ at\ base\ temperature} = \eta_f \qquad .1$$

$$= \frac{\tanh mL}{mL} \qquad\qquad .2$$

16

$$m = \sqrt{\frac{2h}{k_f \delta_f}} \qquad\qquad .3$$

$$L = \frac{d_o}{2}\left(\frac{D}{d_o} - 1\right)\left[1 + 0.35ln\left(\frac{D}{d_o}\right)\right] \qquad\qquad .4$$

The above equations are applicable over the range: $0.5 \leq \eta_f \leq 1.0$ and $D/d_o \leq 8$.

For fins with tapered tips, Zukauskas, (1981) suggests multiplying the fin efficiency values with:

$$\xi = 1 + \left(0.125 - 0.125\sqrt{\frac{t_{f1}}{t_{f2}}}\right)mh_f \qquad\qquad .5$$

t_{f1} refers to the thickness at the tip and t_{f2} *is the thickness at the root*

To evaluate the fin surface effectiveness,

$$E_f = 1 - \frac{A_{fo}}{A_T}\left(1 - F_f\,\xi\,\eta_f\right) \qquad\qquad .6$$

F_f – Accounts for non-uniform heat transfer and takes the value of 1 for air-cooled heat exchangers and $(0.97 - 0.056\,mh_f)$ for heat recovery units.

2.1.1 Tube-In-Plate or Plate Fin-And-Tube Heat Exchangers:

Owing to their lightweight and low manufacturing costs, tube-in-plate heat exchangers are becoming commonly used in heat transfer equipment such areas as vehicle radiators, internal cooling of diesel engines and general air-conditioning (Lin, Lin, Liu and Wang, 2015). These heat exchangers are made by mechanically or hydraulically expanding tubes in a parallel continuous fin arrangement i.e. tubes tend to share the same fin. In order to further improve the overall performance of the tube-in-plate heat exchanger, several modifications of the plain flat fin have been generated and studied with varying results. Examples of these modifications include: wavy or corrugated fin, Louvered fin, offset strip fin and the perforated fin.

Plain fin tube-in-plate heat exchangers consist of plates to which no further modification has been carried out. Kays and London (1984), conducted extensive experiments on plain fins and provides thermal and flow performance data on heat exchangers with plain fins. Experimental data by Chang, Hsieh, Lin and Wang (1996), suggests that the pitch and thickness of the plain fins has an almost insignificant effect on the heat transfer and friction characteristics of the heat exchanger. Rich (1973), also concluded from his experimental results that the heat transfer coefficient is hardly affected by fin spacing. Further research by the same author Rich (1975), concludes that pressure drop per row across the heat exchanger was independent of the number of rows in the unit. Chang, Jang and Wu, (1996), further studied the performance of staggered and inline plain fin heat

exchangers and concluded that the heat transfer coefficient for staggered tube arrangements, surpassed that for inline tube arrangement by as much as 15 − 27% while the pressure drop of the former exceeding that of the latter by as much as 20 − 25%. Their observations also showed that beyond four rows, the heat exchanger had very little improvement in terms of the heat transfer coefficient. Abu Madi, Heikal and Johns (1998), studied the effects of flat and corrugated fins along with variations in number of tube rows, fin pitch and fin thickness on a heat exchangers. Their results showed that number of rows had an insignificant effect on the heat exchanger friction factor and that the Colburn factor (j) increased with a decrease in fin thickness. They also found that the thickness of the fin had very little effect on the friction factor of the heat exchanger. In a bid to further improve the efficiency of the plain fin, Jacobi and Joardar (2006), studied the effect of using winglet type vortex generators on plain fins in an inline heat exchanger bundle. They found that by using 3 vortex generators on alternating tube rows, the Colburn factor (j) in the inline heat exchanger improved by as much as 74% but however caused an increase in the pressure drop of about 41%. Jacobi and Joardar (2008) also analysed the same effect under dry conditions for single and three-row heat exchangers. Observations showed that for the single row unit, heat transfer coefficient improved from 16.5% to 44%, with a pressure drop of less than 12%. For the three-row unit, heat transfer improved from 29.9% to 68.8%; however a penalty was paid in the increase in pressure drop observed that rose from 26% to 87.5%. ElSherbini, and Jacobi (2011), studied the impact of vortex generators for a conventional refrigerator evaporator. They omitted punching the vortex generators on the first row of the heat exchanger. Results showed that the Colburn factor improved by up to 31% without any serious pressure drop consequences.
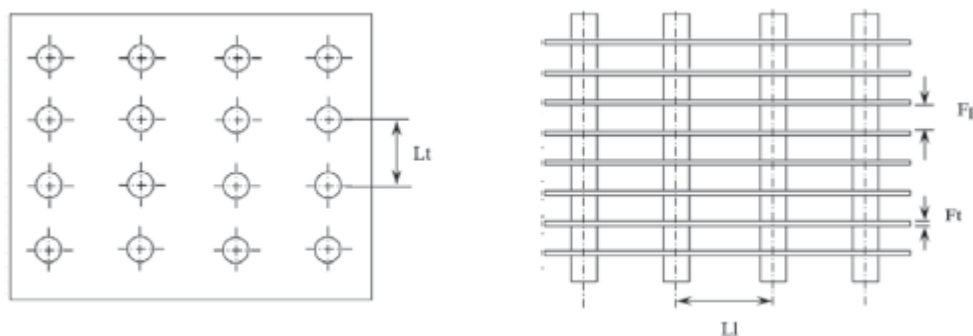
Figure 7: Plain fin tube heat exchanger (Source: Bhuiyan & Islam, 2016)

Heat transfer performance is improved in wavy-finned tube-in-plate heat exchangers as a result of the wavy nature of the fins, which constantly causes a disruption in the boundary layer of flow on the gas side Chang, Fu and Wang (1997), studied this effect for both inline and staggered tube heat exchanger arrangements. They reported that for Re<2000, Colburn factor (j) was found to be inversely proportional to an increase in number of tube rows. When Re>2000, Colburn factor was found to be independent of the number of rows. However, in the staggered arrangement, Colburn

factor (j) only reduced slightly when Re<900 and number of tube rows was increased. When Re>900, (j) increased rapidly with every increase in number of tube rows. To explain this phenomenon, they state that at low Reynold numbers, the thermal boundary layer formed along the wavy fin, tends to grow and deter heat transfer. However, at much higher Reynold numbers, a disruption in the boundary layer occurs which enhances the process of heat transferred. Factors which affect the heat transfer performance of wavy fins tend to be mostly geometrical and include the wave pitch, corrugation angle and the fin spacing. Chang, Du, Tao and Wang (1999), studied the extent of effect these parameters have on frictional factors and the Colburn factor (j) for herringbone wavy finned heat exchangers under wet conditions. Results showed that the frictional factor decreased as the fin pitch increased and got stronger as tube rows increased. Colburn factor (j) was found to increase as fin pitch and row number increased.
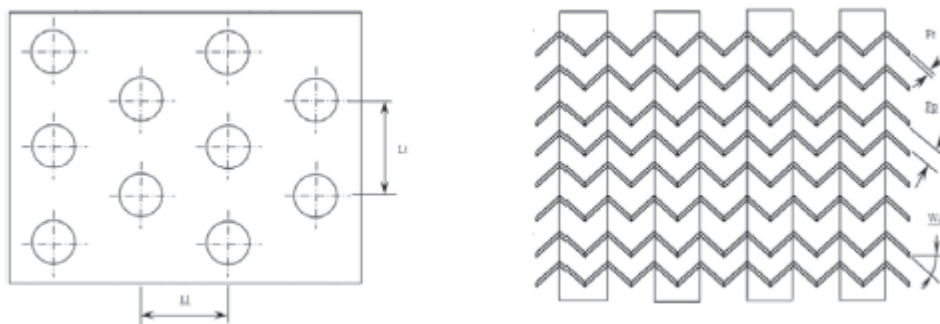
Figure 8: Wavy fin tube heat exchanger (Source: Bhuiyan & Islam, 2016)

In the offset strip tube-in-plate heat exchangers, improvement in heat transfer performance is achieved as a result of the boundary layers formed along the length of the offset strips. These boundary layers are then further disrupted as they pass between the gaps in the strips. In experimental data provided by Kays and London (1984), the thermal and flow performance of wavy finned tube-in-plate heat exchangers, is found to be very similar to that of the offset strip tube-in-plate heat exchanger. In comparison to the plain fin, the offset strip fins were found to have a Colburn factor, j, with a value 2.5 times greater. Their research data also showed that heat transfer increased by 150% and friction by 83% when offset strip fins were compared to plain fins.
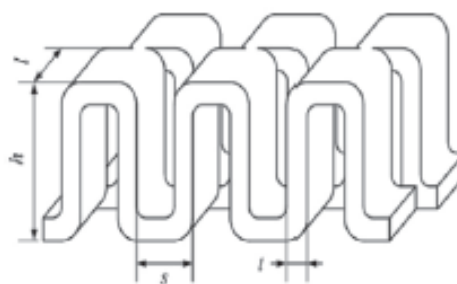
Figure 9: Offset strip fin tube heat exchanger (Source: Bhuiyan & Islam, 2016)

Louver-fins bear a similarity in terms of manufacture to the offset-fins. The only difference being that the slit fins are not offset like the offset strips; they are rather rotated 20-45^0 relative to the direction of air flow. Sheen and Yan (2000) observed that at the same Reynolds number, the Louver-fin had a higher Colburn factor (j) and frictional factor (f) when compared with the plain fin tube-in-plate heat exchanger.

Perforated fins are made by perforating even spaced slots or holes in a plain fin. The punched fins are then folded to a V-shape to create flow channels. Improvement in heat transfer performance is thus achieved by the boundary layer disturbance caused by the punched holes. Shah (1975) showed that the heat transfer performance of these fins were less than that of the offset-strip fins. Shah (1975) also suggests that this factor, combined with high levels of material waste generated during manufacture has made these fins unpopular with heat exchanger manufacturers.

Chapter 3

Convective Heat Transfer Coefficient for Forced Convection Heat Transfer

3.1   Introduction:

This chapter is a summary of the literature review conducted to determine correlations to use in evaluating the convective heat transfer coefficient for both the gas-side and the tube-side of the heat exchanger. The review covered the types of heat exchangers under consideration: Circular-fin, Tube-in Plate and Plain tube exchangers.

A summary of correlations used to evaluate the geometrical properties of the heat exchanger is also presented. The correlations reviewed and presented, also cover the circular-fin, tube-in-plate and plain tube heat exchangers.

3.2   Empirical evaluation of the heat transfer coefficient:

In the preceding chapters, the convective heat transfer coefficient *'h'* was identified as the most important factor in the convection heat transfer equation as it defines the process through which heat is conveyed by the motion of the fluid. However, due to its dependency on characteristics such as geometry, fluid thermal properties and process conditions, no single value or constant can be assigned to define it.

Holman (1992) provides the analytical process through which *'h'* can be evaluated. Unfortunately, due to the time consuming efforts required and the constantly changing conditions experienced in fluid flow, the use of these analytical methods in the design of heat exchangers will not always be practical. Therefore, the designer is forced to resort to the use of experimental data expressed in the form of empirical equations or graphical charts. These equations are usually evaluated at the bulk temperature of the fluid and are found to give a good level of accuracy if used within the parameters they were developed from.

The Nusselt number (Nu) defined as the ratio of convective heat transfer to conduction heat transfer is expressed in the equation below and is used to evaluate the convective heat transfer coefficient.

$$Nu = \frac{h}{k/d_h} \qquad\qquad .7$$

Depending on flow conditions, the relationship of the Nusselt number to fluid flow condition varies. In laminar flow, it is found to be strongly reliant on both the geometry of the flow passage and the thermal boundary formed by the fluid. However, Sekulić and Shah (2003) indicate that for fully developed turbulent flow, it is found to depend on the Reynolds and Prandtl number of the fluid. Several forms of the Nusselt number – Reynolds & Prandtl number relationship exist for both internal and external fluid flow. Some of these relationships are described below.

3.1.0   Heat transfer coefficient in fully developed turbulent flow in circular tubes:

Holman (1992) has attempted to describe the relationship between Nusselt number, Reynolds and Prandtl number. He justifies this by recognising the reliance of the heat transfer on the state of fluid flow (Reynolds number). He points out that the rate of heat and momentum diffusion, are linked by the Prandtl number of the fluid. These two parameters (Prandtl number and Reynolds number) he stated are thus expected to feature significantly in the derivation of the convective heat transfer coefficient. The difficulty then arises in determining the appropriate functional relationship of these two parameters. Using the Nusselt number equation below, Holman makes an attempt at determining the values of these constants:

$$Nu_d = C\,Re_d^m Pr^n \qquad .8$$

In the equation, *C, m, and n* are constants he suggests can be determined via experimental data. He suggested conducting a series of experiments where the rate of heat transfer under different temperature conditions during turbulent flow is measured. He further suggests varying the tube diameter in order to ensure that the Reynolds numbers are never constant. Using the first values obtained for one fluid, the log-log plot of Nu_d vs. Re_d is plotted in order to find an approximate value for 'm'. This is done at constant temperature to minimise the influence of the Prandtl number. Using the first obtained value for 'm', values for the remaining fluids are plotted as $log\left(\frac{Nu_d}{Re_d^m}\right) vs.\,log\,Pr$, which then determines the values 'n'. Using the value of the newly determined 'n', data is once again plotted for $log\left(\frac{Nu_d}{Pr^n}\right) vs.\,log\,Re_d$, which produces a value for 'm' and the component 'C'. Holman (1992), states that this correlation or process is within an accuracy of ±25 percent.

However, Boelter and Dittus (1930), provide values for *'C', 'm' and 'n'* which are valid where differences in temperature between the tube wall and fluid bulk are negligible. Fluid flow must also be fully developed, turbulent and have a Prandtl number between 0.6 and 100.

$$Nu_d = 0.023Re_d^{0.8}Pr^n \qquad .9$$

$$n = 0.4\,(if\,fluid\,is\,heated)\,and\,0.3(if\,fluid\,is\,cooled)$$

If fluid bulk temperatures are found to vary so widely as to introduce differences in fluid properties throughout the fluid, Sieder and Tate (1936) suggest using the equation:

$$Nu_d = 0.027Re_d^{0.8}Pr^{1/3}(\mu/\mu_w)^{0.14} \quad .10$$

Like the other equations, fluid properties are evaluated at the fluid bulk temperature except μ_w, which is determined at the temperature of the tube wall.

Petukov (1970) suggests using the equation below, valid for $4000 \le Re \le 5\times10^5$ and $0.6 \le Pr \le 60$.

$$Nu = \frac{(f/2)\,RePr}{1.07 + 12.7(f/2)^{1/2}(Pr^{2/3} - 1)} \qquad .11$$

$$f = \frac{1}{4(1.82\log_{10}Re - 1.64)^2} \qquad .12$$

The above equation is further refined to cover a wider range of data valid for $5 \times 10^5 \le Re \le 5 \times 10^6$ and $60 \le Pr \le 2000$ and exists in the form:

$$Nu = \frac{(f/2)\,RePr}{K_1 + K_2(f/2)^{1/2}(Pr^{2/3} - 1)} \qquad .13$$

$$f = \frac{1}{4(1.82\log_{10}Re - 1.64)^2} \qquad .14$$

$$K_1 = 1 + 13.6f \qquad .15$$

$$K_2 = 11.7 + 1.8Pr^{-1/3} \qquad .16$$

Gnielinski (1976) proposed using equation 17, which is an adaptation of the Petukov correlation. However, it has shown less accuracy for Re < 10,000 as highlighted by ESDU, 86022 (1988).

$$Nu = \frac{f/2\,(Re - 1000)Pr}{1 + 12.7(f/2)^{1/2}(Pr^{2/3} - 1)} \qquad .17$$

Churchill (1977) is valid for $0 < Pr < 10^6$ and $10 < Re \le 10^6$

$$(Nu)^{10} = (Nu_l)^{10} + \left\{ \frac{e^{2200 - Re/365}}{(Nu_l)^2} + \frac{1}{(Nu_t)^2} \right\}^{-5} \qquad .18$$

$$Nu_t = Nu_0 + \frac{0.079\,(f/2)^{1/2}RePr}{(1 + Pr^{4/5})^{5/6}} \qquad .19$$

$$Nu_0 = 4.8 \; for \; UWT \; and \; 6.3 \; for \; UHF$$
$$Nu_l = 3.657 \; for \; UWT \; and \; 4.364 \; for \; UHF$$

ESDU 92003 (1993), proposed using:

$$Nu = 0.037\big(Re^{0.75} - 180\big)Pr^{0.42}\big[1 + (x/D)^{2/3}\big] \qquad .20$$

$$\big[1 + (x/D)^{2/3}\big] - accounts \; for \; thermal \; entrance \; effects$$

3.3   Evaluating the heat transfer coefficient across cylindrical tube banks:

3.2.1   Principle of Flow across Curved Surfaces:

To predict the rate of heat transfer across the surface of a cylinder, Holman (1992) suggests considering the condition of the boundary layer created by the fluid bulk stream as it encounters the surface of the cylindrical tube. The formation of a pressure gradient leads to the separation of flow seen at the rear end of the cylindrical tube when the bulk stream velocity is high. To explain this flow separation phenomenon, it is assumed that pressure is constant in the boundary layer formed at any position defined x, which is measured from the first contact of the bulk stream with the cylinder. As

the fluid bulk continues to flow across the curved surface of the cylinder, this pressure is found to decrease and then increase once again as it approaches the back end of the cylinder.
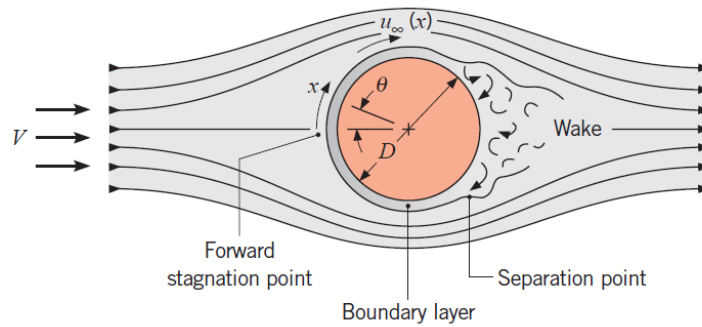
Figure 10: Depiction of fluid flow across the surface of a smooth cylinder

This transition creates an increase in the bulk stream velocity at the front side of the tube and a decrease at the opposite side of the tube. The transverse velocity, usually denoted as u_ϕ, which exists at the outside edge of the boundary gradually drops to zero at the surface of the cylinder. As the bulk stream continues along the cylinder surface to the back end, the sudden increase in pressure creates a reduction in overall velocity through the bulk stream as well as through the boundary layer. The relationship between pressure increase and decrease in velocity is explained using the Bernoulli equation for a streamline:

$$\frac{dp}{\rho} = -d\left(\frac{u^2}{2}\right)$$ .21

With the assumption that pressure is constant through the boundary layer, reverse flow is observed to begin at the boundary layer near the cylinder surface. This phenomenon he explains is caused by the poor fluid layer momentum at the cylinder surface, not being high enough to overcome the pressure increase. Separation point hence occurs when the velocity gradient drops completely to zero. . This flow separation is sometimes accompanied by fluid flow reversal and eventually becomes random and turbulent.
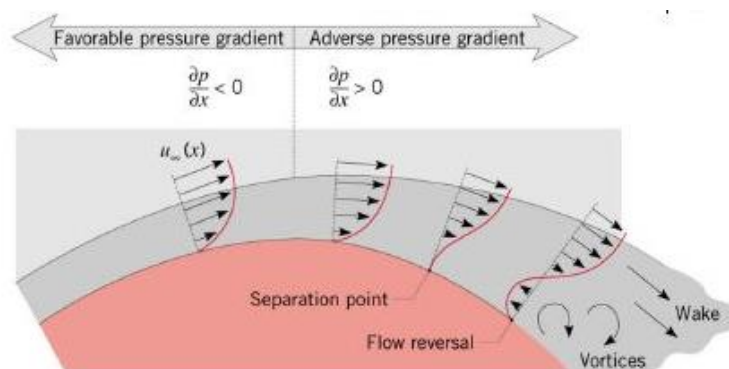
Figure 11: Depiction of flow separation across the surface of a smooth cylinder

24

The consequences of flow separation and flow reversal will clearly influence the rate of convective heat transfer between the cylindrical surface and the bulk stream as a result of the turbulence created. The extent of this influence was studied by Giedt (1949) for heat transferred from a heated tube to free air. His results showed that minimum values for the heat transfer coefficient occurred at Reynolds numbers between 70,800 and 101,300, which corresponded to the point at which flow separation occurred. At the opposite end of the tube, an increase in the heat transfer coefficient occurred as a result of the flow turbulence created. At even higher Reynolds numbers, he recorded 2 minimum values. The first occurring when flow transited from laminar to turbulent in the boundary layer and the second minimum was record at the point when the turbulent boundary layer separated. Heat transfer was found to increase rapidly when the boundary layer became turbulent and also when eddy motion occurred during flow separation.

Due to the complexity of the flow phenomenon described earlier, it is somewhat difficult and complicated to analytically evaluate the heat transfer coefficient for cases of flow over cylindrical surfaces. However, as also stated earlier, correlations of experimental data exist which can be applied with acceptable levels of success. For example, Drake and Eckert (1972) developed the equations below to evaluate the heat transfer coefficient in cross-flow from a heated tube to air:

$$Nu = \left(0.43 + 0.50 Re^{0.5}\right) Pr^{0.38} \left(\frac{Pr_f}{Pr_w}\right)^{0.25} \text{ applicable over the range } 1 < Re < 10^3 \qquad .22$$

$$Nu = \left(0.25 \, Re^{0.6} Pr^{0.38}\right) \left(\frac{Pr_f}{Pr_w}\right)^{0.25} \text{ applicable over the range } 10^3 < Re < 2 \, x 10^5 \qquad .23$$

Bernstein and Churchill (1977) also produced a correlation applicable over a large range of data:

$$Nu_{df} = 0.3 + \frac{0.62 \, Re_f^{1/2} Pr_f^{1/3}}{\left[1 + \left(\frac{0.4}{Pr_f}\right)^{2/3}\right]^{1/4}} \left[1 + \left(\frac{Re_f}{282,000}\right)^{5/8}\right]^{4/5} \text{ for } 10^2 < Re_d < 10^7; \, Pe_d > 0.2 \qquad .24$$

This equation was further modified to produce better accuracy and cover a larger range of data:

$$Nu_{df} = 0.3 + \frac{0.62 \, Re_d^{1/2} Pr_f^{1/3}}{\left[1 + \left(\frac{0.4}{Pr_f}\right)^{2/3}\right]^{1/4}} \left[1 + \left(\frac{Re_d}{282,000}\right)^{1/2}\right] \, 20,000 < Re_d < 400,000; \, Pe_d > 0.2 \qquad .25$$

Nakai and Okazaki (1975), proposed using:

$$Nu_{df} = \left[0.8237 - ln\left(Pe_d^{1/2}\right)\right]^{-1} Pe_d > 0.2 \qquad .26$$

Fluid properties in the equations above are evaluated at the film temperature and $Pe_d = 0.2$.

3.4 Heat transfer coefficient across tube banks:

3.4.1 Plain tube bank heat exchangers:

For this project, consideration was given to both the inline and staggered heat exchanger arrangements with plain tubes. To evaluate the Nusselt number, ESDU 73031 (1974), suggests using the equation below:

$$\overline{Nu} = Nu_r \; x \; F_1 x F_2 x F_3 \qquad\qquad .27$$

In the equation Nu_r is the average Nusselt number evaluated on the reference conditions:

- Constant fluid properties in the bulk fluid
- Tube row bank with 10 tube rows and at least 6 tubes per row
- Tube banks normal to advancing gas-side fluid flow
- (Tube length/Tube Diameter) > 5

F_1, F_2 and F_3 , account for departures from these reference conditions.

- F_1: Accounts for variations in fluid properties due to temperature differences in the tube wall and the bulk fluid (T_w and T_b).

$$F_1 = \left[\frac{Pr_b}{Pr_w}\right]^{0.26} \qquad\qquad .28$$

- F_2: Accounts for heat exchanger designs where the number of rows in the heat exchanger is not equal to 10. Values for C_0, C_1, C_2 and C_3 can be selected from Table 1 below.

$$F_2 = C_0 + \; C_1/N - \; C_2/N^2 + C_3/N^3 - values \; for : 4 \le N \le 20 \qquad .29$$

Arrangement	$(X_l - 1)/(X_t - 1)$	Re_b range	C_0	C_1	C_2	C_3
In – line	> 0.2	> 0.2 x 10^3	0.990	0.873	9.60	18.6
In – line	0.5 – 2	10^2 to 10^3	1.055	0.548	14.7	37.3
Staggered		> 10^2	1.025	0.093	4.06	6.60

Table 1: Values for C_0, C_1, C_2 and C_3

- F_3: Accounts for designs where the heat exchanger has inclined tubes.

$$F_3 = (sin \; \theta)^{0.6} \qquad\qquad .30$$

- Nu_r can be evaluated using the equation

$$Nu_r = aRe_b^m Pr_b^{034} \qquad\qquad .31$$

In this equation, Re_b and Pr_b refer to bulk fluid condition, while *'a' and 'm'* can be selected from the Table 2 or Table 3 below.

3.4.1.1 Inline Tube Arrangement:

Range of Re_b	X_t	X_l	X_t/X_l	a	m
$10 - 3$ x 10^2			1.0	0.742	0.431
3 x 10^2 - 2 x 10^5	1.2 – 4	≥ 1.15	1.0	0.211	0.651
2 x $10^5 - 2$ x 10^6			1.0	0.116	0.700

$2 \times 10^2 - 2 \times 10^5$	≥ 1.2		$0.4 - 0.5$	0.291	0.609
	$1.05 - 1.1$		$0.35 - 0.55$	0.177	0.643
	$4 - 6$	$1.4 - 1.7$		0.223	0.626
	$2 - 3$	$1.1 - 1.15$		0.107	0.708
	$4 - 6$	$1.1 - 1.2$		0.0624	0.730
	1.1	1.0		0.206	0.639
	1.25	1.0		0.123	0.679
	1.5	1.0		0.0834	0.707
	2.0	1.0		0.0593	0.727
	$4 - 6$	1.0		0.0435	0.744

Table 2: Values for *'a' and 'm'* in an inline plain tube arrangement

3.4.1.2   Staggered Tube Arrangement:

Range of Re_b	X_t	X_l	a	m
$10 - 3 \times 10^2$			1.309	0.360
$3 \times 10^2 - 2 \times 10^5$	All values between 0.6 and 4		0.273	0.635
$2 \times 10^5 - 2 \times 10^6$			0.124	0.700

Table 3: Values for *'a' and 'm'* in a staggered plain tube arrangement

Gaddis & Gnieslinski (1985) proposed pressure drop correlations to account for both inline and staggered plain tube heat exchangers. This was further developed and altered by Martin (2002) to represent the Hagen number which can be used to evaluate the Nusselt number:

$$Hg_{staggered} = Hg_{lam}$$
$$+ \, Hg_{turb,st} \left[1 - exp \left(1 - \frac{Re_d + 200}{1000} \right) \right] \qquad .32$$

$$Hg_{inline} =$$
$$Hg_{lam} + \, Hg_{turb,in} \left[1 - exp \left(1 - \frac{Re_d + 200}{2000} \right) \right] \qquad .33$$

$$Hg_{lam}$$
$$= 140 Re_d \frac{\left(X_l^{*0.5} - 0.6 \right)^2 + 0.75}{X_t^{*1.6} (4 \, X_t^* X_l^* / \pi - 1)} \qquad .34$$

$$Hg_{turb,st} = \left\{ \left[1.25 + \frac{0.6}{(X_t^* - 0.85)^{1.08}} \right] + \, 0.2 \left(\frac{X_l^*}{X_t^*} - 1 \right)^3 - 0.005 \left(\frac{X_l^*}{X_t^*} \right)^3 \right\} x \, Re_d^{1.75}$$
$$+ \, \Phi_{t,n} Re_d^2 \qquad .35$$

$$Hg_{turb,in} = \left\{ \left[0.11 + \frac{0.6 \, (1 - \, 0.94/X_l^*)^{0.6}}{(X_t^* - 0.85)^{1.3}} \right] x \, 10^{0.47(X_l^*/X_t^* - 1.5)} \right.$$
$$\left. + \, 0.015 \, (X_t^* - 1)(X_l^* - 1) \right\} x \, Re_d^{2 - 0.1(X_l^*/X_t^*)} + \, \Phi_{t,n} Re_d^2 \qquad .36$$

$$\Phi_{t,n} = \frac{1}{2 X_t^{*2}} \left(\frac{1}{N_r} - \frac{1}{10} \right) \; valid \; over \; the \; range: 5 \leq N_r \leq 10 \; and \; X_l^*$$
$$\geq 0.5 \, (2 X_t^* + 1)^{\frac{1}{2}} \qquad .37$$

$$\Phi_{t,n} = 2\left[\frac{X_d^* - 1}{X_t^*(X_t^* - 1)}\right]^2 \left(\frac{1}{N_r} - \frac{1}{10}\right) \; valid \; over \; the \; range: 5 \leq N_r \leq 10 \; and \; X_l^*$$

$$< 0.5 \, (2X_t^* + 1)^{\frac{1}{2}} \quad .38$$

$$\Phi_{t,n} = 0 \; for \; N_r > 10 \qquad\qquad .39$$

The Hagen number (Hg_{lam}), is valid for inline as well as staggered tube bundles except $X_t^{*1.6}$ changes to $X_d^{*1.6}$ for staggered tube arrangements.

Both $Hg_{staggered}$ and Hg_{inline}, are valid over the ranges, 1≤Re_d≤300'000, 7.9≤d_0≤73mm & N_r≥5 (inline & staggered arrangement), 1.25≤X_t^*≤3.0, 0.6≤X_l^*≤3.0 & X_d^*≥1.25, for staggered layout and 1.25≤X_t^*≤3.0 & 1.2≤X_l^*≤3.0 for inline layout

$$Lq_{staggered} = 0.92 \, Hg \, Pr \left[\frac{(4X_t^*/\pi) - 1}{X_d^*}\right] \; valid \; for \; bundles \; with \; X_l^* \geq 1 \qquad .40$$

$$Lq_{staggered} = 0.92 \, Hg \, Pr \left[\frac{(4X_t^*X_l^*/\pi) - 1}{X_l^*X_d^*}\right] \; valid \; for \; bundles \; with \; X_l^* < 1 \qquad .41$$

$$Lq_{inline} = 1.18 \, Hg \, Pr \left[\frac{(4X_t^*/\pi) - 1}{X_l^*}\right] \qquad .42$$

$$Nu_{staggered} = 0.404 Lq^{1/3} \qquad .43$$

$$Nu_{inline} = 0.404 Lq^{\frac{1}{3}} \left(\frac{Re_d + 1}{Re_d + 1000}\right)^{0.1} \qquad .44$$

Nusselt number Nu is valid over the range:

1≤Re_d≤2'000'000, 0.7≤Pr≤700, 7.9≤d_0≤73mm, 1.02≤X_t^*≤3.0, 0.6≤X_l^*≤3.0 and 4≤N_r≤80 for staggered tube bundles with a 30^0, 45^0 or 60^0 tube layout arrangement. For inline tube bundles, it is valid over the range 2≤N_r≤15.

Using the Nusselt number Nu equation, prediction was within ±14% for staggered tube bundle.

To evaluate the pressure drop across the unit, the equation below is suggested by Sekulić and Shah (2003), which includes the Hagen number derived from equation 32:

$$\Delta P = \frac{\mu^2}{\rho g_c} \frac{N_r}{D_o^2} Hg \qquad .45$$

3.4.2 Circular finned tube bank heat exchangers:

Briggs and Young (1963) predicted that for individually finned tubes in a staggered arrangement, the Colburn factor j could be determined using:

$$j = 0.134 Re_d^{-0.319} \left(\frac{s}{l}\right)^{0.2} \left(\frac{s}{\delta}\right)^{0.11} \qquad .46$$

The equation was predicted to cover the ranges: 1100≤Re_d≤18,000; 0.13 ≤s/l ≤0.63; 1.01 ≤s/δ≤7.62; 0.09 ≤l/d_o≤7.62; 0.011 ≤δ/d_o≤0.15; 1.54≤X_t/d_o≤8.23; 11.1≤d_o≤40.9mm and 246≤N_f≤768fins/m.

28

Correlations were predicted from tube bundles arranged in an equilateral triangle pitch. A 5%deviation was recorded when compared to experimental values.

To predict frictional factor, Briggs and Robinson (1966), proposed:

$$f_{tb} = 9.465 Re_d^{-0.316} \left(\frac{X_t}{d_o}\right)^{-0.927} \left(\frac{X_t}{X_d}\right)^{0.515} \qquad .47$$

This was predicted for the ranges: $2,000 \leq Re_d \leq 50,000$; $0.15 \leq s/l \leq 0.19$; $3.75 \leq s/\delta \leq 6.03$; $0.35 \leq l/d_o \leq 0.56$; $0.011 \leq \delta/d_o \leq 0.025$; $1.86 \leq X_t/d_o \leq 4.60$; $18.6 \leq d_o \leq 40.9$mm and $311 \leq N_f \leq 431$fins/m.

ESDU 86022 (1998) suggests using:

$$Nu = \overline{Nu_c} \; x \; E_f \; x \; F_1 \; x \; F_2 \qquad .48$$

$$\overline{Nu_c} = 0.242 \, Re^{0.658} \, Pr^{1/3} \left(\frac{s}{h_f}\right)^{0.297} \left(\frac{X_t}{X_l}\right)^{-0.091} \qquad .49$$

To account for an equilateral triangle layout, $\overline{Nu_c}$ is written as:

$$\overline{Nu_c} = 0.239 \, Re^{0.658} \, Pr^{1/3} \left(\frac{s}{h_f}\right)^{0.297} \qquad .50$$

F_1 – Accounts for a possible variation in fluid properties. However it was advised that a value of 1 can be used for air-cooled heat exchangers while for heat recovery conditions, the possibility of applying a correction factor had to be assessed.

F_2 – Accounts for the number of tube rows across which flow occurs. In forced draft air cooled heat exchangers, the value of $F_2 = 1$ has been suggested. However where flow inlet turbulence levels are bound to be low, such as in induced draft units, F_2 should be selected form the Table 4 below:

N_r	1	2	3	4 or more
F_2	0.76	0.84	0.92	1.00

Table 4: Correction factors for F_2 based on number of tube rows

This correlation is valid over the range: $2000 < Re < 40,000$, $0.13 < s/h_f < 0.57$ and $1.15 < X_t/X_l < 1.72$

To evaluate pressure drop Kays and London (1984) suggests using the equation:

$$\Delta P = \frac{m^2}{2\rho_m g_c}\left[(1 + \sigma^2)\rho_m\left(\frac{1}{\rho_o} - \frac{1}{\rho_i}\right) + n_r K\right] \qquad .51$$

$$K = 4.567 Re^{-0.242} \varepsilon^{0.504} \left(\frac{X_t}{D_r}\right)^{-0.376} \left(\frac{X_l}{D_r}\right)^{-0.546} \qquad .52$$

The equation was predicted to cover the ranges: $5000 < Re < 50,000$, $5 < \varepsilon < 23$, $1.85 < P_t/D_r < 4.75$, $1.50 < P_l/D_r < 4.00$, $157 \leq N_f \leq 437$fins/m, 5.6mm$\leq l \leq 16.5$mm, 9.5mm$\leq d_o \leq 51$mm, and $1.4 \leq D_f/D_o \leq 2.4$. A 5%deviation was recorded when compared to experimental values.

3.4.3 Tube – in – plate fin heat exchanger tube banks:
To account for exchangers where the tubes share a common fin usually in the form of a thin flat plate, Chi and Wang (2000) proposed:

$$j = 0.108 Re_{dc}^{-0.29} \left(\frac{X_t}{X_l}\right)^{c_1} \left(\frac{p_f}{d_c}\right)^{-1.084} \left(\frac{p_f}{D_h}\right)^{-0.786} \left(\frac{p_f}{X_t}\right)^{c_2} \text{ for values } N_r = 1 \qquad .53$$

$$j = 0.86 Re_{dc}^{c_3} N_r^{c_4} \left(\frac{p_f}{d_c}\right)^{c_5} \left(\frac{p_f}{D_h}\right)^{-0.93} \left(\frac{p_f}{X_t}\right)^{c_6} \text{ for values } N_r \geq 2 \qquad .54$$

$$c_1 = 1.9 - 0.23 \, lnRe_{dc} \qquad .55$$

$$c_2 = -0.236 + 0.126 \, lnRe_{dc} \qquad .56$$

$$c_3 = -0.361 - \frac{0.042 N_r}{ln \, Re_{dc}} + 0.158 \, ln \left[N_r \left(\frac{p_f}{d_c}\right)^{0.41} \right] \qquad .57$$

$$c_4 = -1.224 - \frac{0.076 (X_l/D_h)^{1.42}}{ln \, Re_{dc}} \qquad .58$$

$$c_5 = -0.083 + \frac{0.058 N_r}{lnRe_{dc}} \qquad .59$$

$$C_6 = -5.735 + 1.21 lnRed_c N_r \qquad .60$$

To evaluate frictional factor, Ref. [12] also proposed:

$$f = 0.0267 Re_{dc}^{c_7} \left(\frac{X_t}{X_l}\right)^{c_8} \left(\frac{p_f}{d_c}\right)^{c_8} \qquad .61$$

$$c_7 = -0.764 + 0.739 \left(\frac{X_t}{X_l}\right) + 0.177 \left(\frac{p_f}{d_c}\right) - \frac{0.00758}{N_r} \qquad .62$$

$$c_8 = -15.689 + \frac{64.021}{ln \, Re_{dc}} \qquad .63$$

$$c_9 = 1.696 - \frac{15.695}{ln \, Re_{dc}} \qquad .64$$

The equations were predicted to cover the ranges $300 \leq Re_{dc} \leq 20{,}000$; $6.9 \leq d_c \leq 13.6mm$; $1.30 \leq D_h \leq 9.37mm$; $20.4 \leq X_t \leq 31.8mm$, $12.7 \leq X_l \leq 32mm$, $1.0 \leq p_f \leq 8.7mm$ and $1 \leq N_r \leq 6$.

Chang, Hsieh Lin and Wang (1996), proposed using the equation below under dry conditions:

$$j_4 = 0.14 \, Re_{d_c}^{-0.328} \left(\frac{X_t}{X_l}\right)^{-0.502} \left(\frac{P_f}{d_c}\right)^{0.0312} \qquad .65$$

$$\frac{j_N}{j_4} = 0.991 \left[2.24 Re_{d_c}^{-0.092} \left(\frac{N}{4}\right)^{-0.031} \right]^{0.607(4-N)} \qquad .66$$

This was predicted to cover the ranges: $Re_{dc} = 800 - 7500$, $D_o = 7 - 19.51mm$, $P_f = 1.07 - 8.51mm$, $N_r = 1 - 8$, $X_t = 20.35 - 50.73mm$, $X_l = 12.7 - 44.09mm$

To evaluate frictional factor, Chang, Hsieh Lin and Wang (1996), also proposed:

$$f = 1.039 Re_{d_c}^{-0.418} \left(\frac{\delta_f}{d_c}\right)^{-0.104} N^{-0.0935} \left(\frac{P_f}{d_c}\right)^{-0.197} \qquad .67$$

The equation was predicted to over the ranges: $Re_{dc} = 800 - 7500$, $D_o = 10.51mm$, $P_f = 1.77 - 3.21mm$, $N_r = 2 - 6$, $X_t = 25.4mm$, $X_l = 22mm$

Abu Madi, Heikal, and Johns (1998) also proposed using the equation

$$j_4 = Re^{-0.44}R_4^{-3.07}R_{5,1}^{0.37}R_7^{-6.14}R_9^{-2.13} \qquad\qquad .68$$

$$\frac{j_4}{j_N} = 0.87 + 0.0000143Re^{0.55}N^{-0.67}R_3^{-3.13}R_{5,1}^{4.95} \qquad\qquad .69$$

$$f = Re^{-0.25}R_4^{-1.43}R_{5,1}^{1.37}R_8^{1.65}R_9^{-3.05} \qquad\qquad .70$$

$$R_3 = \frac{D_o}{D_i}\left(1 - \frac{\delta_f}{F_p}\right) + 2\frac{X_t X_l}{\pi D_i P_f} - \frac{D_o^2}{2D_i P_f} + \frac{2\delta_f X_t}{\pi D_i P_f N} \qquad\qquad .71$$

$$R_4 = \frac{P_f X_t}{(X_t - D_o)(P_f - \delta_f)} \qquad\qquad .72$$

$$R_5 = \frac{\pi N D_o \left(1 - \frac{\delta_f}{P_f}\right)}{X_t} + \frac{N}{P_f}\left(2X_l - \frac{\pi D_o^2}{2X_t} + \frac{2\delta_f}{N}\right) \qquad\qquad .73$$

$$R_{5,1} = \frac{R_5}{N} \qquad\qquad .74$$

$$R_6 = \frac{4X_l N}{R_5} \qquad\qquad .75$$

$$R_7 = \cfrac{1}{1 + \cfrac{2\pi D_o(P_f - \delta_F)}{4X_t X_l - \pi D_o^2 + \cfrac{4X_t\delta_f}{N}}} \qquad\qquad .76$$

$$R_8 = \frac{P_f}{D_o} \qquad\qquad .77$$

$$R_9 = \frac{X_l}{D_o} \qquad\qquad .78$$

The equation was predicted to over the ranges: Re_{dh} = 200—6000, D_o = 9.956mm, δ_f= 0.12—0.13mm, P_f = 1.64 – 2.65mm, N_r = 1—4, X_t = 19—25.4mm, X_l = 16—22mm. R_3 = 7.26 – 19.3, R_4 = 1.77 – 2.25, $R_{5,1}$ = 11.0 – 21.8, R_7 = 0.86 – 0.95, R_8 = 0.16 – 0.27, R_9 = 1.60 – 2.21.

Hsieh, Lin and Wang (1997) proposed the equation below for use under dehumidifying conditions

$$j_4 = 0.29773Re_{dc}^{-0.364}\varepsilon^{-0.168} \qquad\qquad .79$$

$$j_N = 0.4Re_{dc}^{-0.468+0.04076N}\varepsilon^{0.159}N^{-1.261} \qquad\qquad .80$$

$$f = 28.209\,Re_{dc}^{-0.5653}\left(\frac{F_p}{D_c}\right)^{-1.3405}\varepsilon^{-1.3343} \qquad\qquad .81$$

$$\varepsilon = \frac{A_{tot}}{A_{tube}} \qquad\qquad .82$$

The equation was predicted to over the ranges: Re_{dc} = 400—5000, D_c = 10.23mm, δ_f= 0.13mm, F_p = 1.82 – 3.20mm, N_r = 2—6, X_t = 25.4mm, X_l = 22mm $T_{dry,in}$ = 27^{0}C, RH = 50 – 90%.
Uncertainties were recorded to be within 92% for Colburn Factor, j and 91% for frictional factor, f

3.5 Heat Exchanger Geometrical Characteristics

The importance of the physical characteristics of the heat exchanger in determining the convective heat transfer coefficient can be seen in all the equations outlined above. For a single straight tube, the physical parameters required for computing the convective heat transfer coefficient in the inside tube flow, can be obtained easily. However, for more complex geometries as seen in tube banks with plate fins and circular fins, computation of the outside flow convective heat transfer coefficient becomes more complex as a result of the presence of fins (tube-in-plate and circular) and tube arrangements (staggered and aligned). Since the presence of these modifications, plays a significant part in heat transfer, a heat exchanger designed outside the range of parameters of the heat transfer correlations can produce final results which will be significantly different from values obtained experimentally.

Some of these physical characteristics needed in computing the convective heat transfer coefficient are listed below:

- The primary surface area, which accounts for the area of the tubes.
- The secondary surface area, which accounts for the area of any extended surfaces.
- The minimum free-flow area where the mean axial velocity of flow occurs as the fluid moves across the heat exchanger
- Frontal area
- Hydraulic diameter and flow length

3.5.1 Plain tube Heat Exchangers
3.5.1.1 Inline Arrangement:
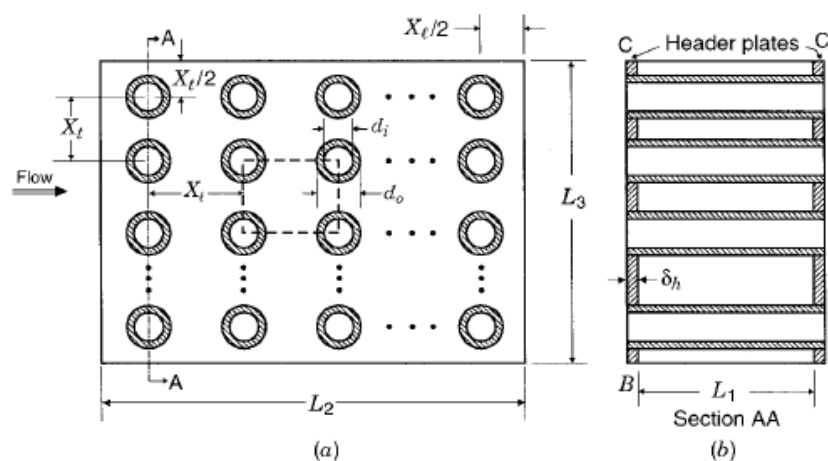
Figure 12: Inline arrangement for plain tube heat exchangers (Source: Shah, 1985)

Based on Fig. 12, the total heat area A includes the outside surface of the tubes and the outside surface of the top and bottom headers:

$$A = \pi d_0 L_1 N_t + 2 \left(L_2 L_3 - \frac{\pi d_0^2}{4} N_t \right) \qquad .83$$

Number of tubes in one row in the flow direction N'_t:

$$N'_t = \frac{L_3}{X_t} \qquad\qquad .84$$

The minimum free flow area A_o:

$$A_o = (X_t - D_o) N'_t L_1 \qquad\qquad .85$$

The frontal area A_{fr}:

$$A_{fr} = L_1 L_3 \qquad\qquad .86$$

Hydraulic Diameter D_h:

$$D_h = \frac{4 A_o L_2}{A} \qquad\qquad .87$$

Flow length = L_2

3.5.1.2   Staggered Arrangement:
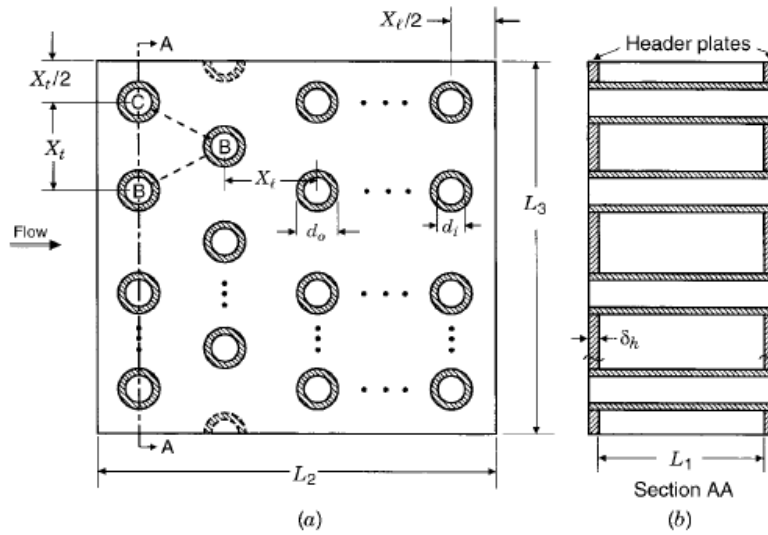
Figure 13: Staggered arrangement for plain tube heat exchangers (Source: Shah, 1985)

Total surface area A:

$$A = \pi d_0 L_1 N_t + 2\left(L_2 L_3 - \frac{\pi d_0^2}{4} N_t\right) \qquad\qquad .88$$

Number of tubes in one row in the flow direction N'_t:

$$N'_t = \frac{L_3}{X_t} \frac{L_2/X_l + 1}{2} + \left(\frac{L_3}{X_t} - 1\right) \frac{L_2/X_l - 1}{2} \qquad\qquad .89$$

The minimum free flow area A_o:

$$A_0 = \left[\left(\frac{L_3}{X_t} - 1\right) c' + (X_t - D_0)\right] L_1 \qquad\qquad .90$$

Where

$$c' = (X_t - D_0) - (X_t - D_0)\delta N_f \qquad\qquad .91$$

The frontal area A_{fr}:

$$A_{fr} = L_1 L_3 \qquad\qquad .92$$

Hydraulic Diameter D_h:

33

$$D_h = \frac{4A_o L_2}{A} \qquad\qquad .93$$

Flow length = L_2

3.5.2 Circular – Fin tube Heat Exchangers:
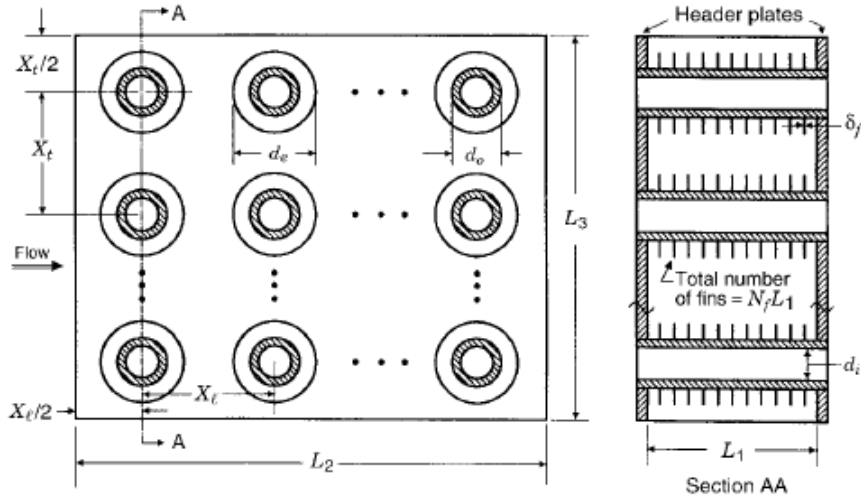
Figure 14: Arrangement for circular tube heat exchangers (Source: Shah, 1985)

To evaluate the primary surface area, the total surface area equation for a staggered or inline plain tube arrangement is used. However, the area covered by the fins, are deducted:

$$A_p = \pi d_0 (L_1 - \delta N_f L_1) N_t + 2 \left(L_2 L_3 - \frac{\pi d_0^2}{4} N_t \right) \qquad\qquad .94$$

The secondary surface area A_f:

$$A_f = \left[\frac{2\pi(d_e^2 - d_0^2)}{4} + \pi d_e \delta \right] N_f L_1 N_t \qquad\qquad .95$$

Therefore, total heat transfer surface area A:

$$A = A_p + A_f \qquad\qquad .96$$

The minimum free flow area A_o:

$$A_0 = \left[\left(\frac{L_3}{X_t} - 1 \right) c' + (X_t - d_0) - (d_e - d_0)\delta N_f \right] L_1 \qquad\qquad .97$$

$$where \; c' = (X_t - d_0) - (d_e - d_0)\delta N_f \qquad\qquad .98$$

The frontal area A_{fr}:

$$A_{fr} = L_1 L_3 \qquad\qquad .99$$

Hydraulic Diameter D_h:

$$D_h = \frac{4A_o L_2}{A} \qquad\qquad .100$$

Flow length = L_2

3.5.3   Tube – in – Plate Fin tube Heat Exchangers:
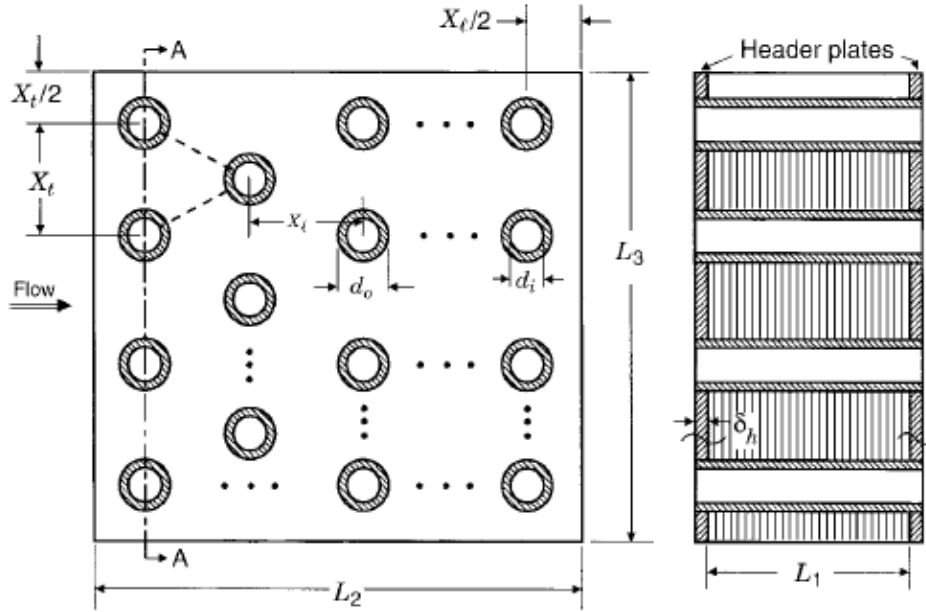
Figure 15: Staggered arrangement for circular tube heat exchangers (Source: Shah, 1985)

To evaluate the primary surface area A_p:

$$A_p = \pi d_0 (L_1 - \delta N_f L_1) N_t + 2 \left(L_2 L_3 - \frac{\pi d_0^2}{4} N_t \right) \qquad .101$$

The secondary surface area A_f:

$$A_f = 2 \left[L_2 L_3 - \left(\frac{\pi d_0^2}{4} \right) N_t \right] N_f L_1 + 2 L_3 \delta N_f L_1 \qquad .102$$

Therefore, total heat transfer surface area A:

$$A = A_p + A_f \qquad .103$$

The minimum free flow area A_o:

$$A_o = \left[\left(\frac{L_3}{X_t} - 1 \right) c' + (X_t - d_0) - (X_t - d_0) \delta N_f \right] L_1 \qquad .104$$

$$where\ c' = (X_t - d_0) - (X_t - d_0) \delta N_f \qquad .105$$

The frontal area A_{fr}:

$$A_{fr} = L_1 L_3 \qquad .106$$

Hydraulic Diameter D_h:

$$D_h = \frac{4 A_0 L_2}{A} \qquad .107$$

Flow length = L_2

Chapter 4

Validation of Heat Transfer Correlations

4.1   Introduction:

The first section of this chapter constitutes a description of the heat exchanger design software, ASPEN Exchanger Design and Rating (ASPEN EDR). The second section describes the research sources from where the gas-side heat transfer correlations used in ASPEN EDR have been derived to predict the heat transfer coefficient in circular fin, plain tube and tube-in-plate air-cooled heat exchangers. Finally, the validation process begins by using the log mean temperature design (LMTD) method and a set of pre-defined parameters to design and rate the plain, circular fin and tube-in-plate heat exchangers using heat transfer correlations obtained from open source literature. The results obtained are compared with results obtained for the same design carried out using the "Rating/Checking" function of the Aspen Air-cooled Exchanger (ACOL) software which is the air-cooled heat exchanger design tool for ASPEN EDR. The validation results are further discussed at the end of the chapter.

4.2   ASPEN Exchanger Design & Rating:

Possibly the most popular heat exchanger design software on the market, the Aspen – EDR offers a range of programs for the thermal and mechanical design of heat exchangers. The family of programs under Aspen – EDR include:

- Aspen Shell & Tube Exchanger: used in the thermal design of Shell & Tube Heat Exchangers.
- Aspen Shell & Tube Mechanical: used for the mechanical design, cost estimation and design drawings of Shell & Tube Heat Exchangers and pressure vessels.
- Aspen Air-cooled Exchanger: used for the thermal design of Air-Cooled Heat Exchangers
- Aspen Plate-Fin Exchanger: used for the thermal design of Plate-Fin Heat Exchangers
- Aspen Fired Heater: for the thermal design of Fired Heaters
- Aspen Plate Exchanger: for the thermal design of Plate Heat Exchangers.

The Aspen-EDR software is based on a combination of efforts from the Heat Transfer and Fluid-flow Service (HTFS) and the B-JAC company. The HTFS, a world renowned institution for experimental research in heat transfer and fluid flow in heat exchangers, provides the heat transfer correlations used to assess and design the heat exchangers, while the B-JAC company produce and sell the computer software needed for these assessments. These two organisations (HTFS and B-JAC) were at different times acquired by AspenTech and have since worked together to produce a design software used in several industries ranging from the chemical to the petroleum industries.

Aspen Air-cooled Exchanger (ACOL): is split into two sections which include the Input Section and the Result Section.

- Input Section: This section is provided for the input and definition of the design problem. Process conditions such as the fluid operating conditions (temperatures, pressures, mass flow rates etc.) and geometrical characteristics (tube outer diameters, wall thickness, tube layout, extended surface type, manufacturing material etc.) are defined within this section. The sub-sections listed below make up the Input Section.
  - Problem definition:
    - Headings/Remarks
    - Application options
    - Process Data
  - Physical property data
    - Stream Composition
    - Stream Properties
  - Exchanger Geometry
    - Geometry Summary
    - Unit Geometry
    - Tubes
    - Bundle
    - Headers & Nozzles
    - Fans
    - Structures/Walkways
  - Construction Specifications
    - Materials of Construction
    - Design Specifications
  - Program Options
    - Design options
    - Thermal Analysis
    - Methods/correlations
    - Outside Distribution
- Result Section: The Result section provides the analysis based on the values provided in the input section. The area ratio is the most important information provided because it tells the designer by how much he has either undersized or oversized the heat exchanger. Further analysis such as pressure drops, heat transfer coefficients, outlet temperatures, etc. are also provided.
  - Input Summary
    - Input summary
  - Result Summary
    - Warning & Messages
    - Optimization Path
    - Recap of Designs
    - API Sheet
    - Overall Summary
  - Thermal /Hydraulic Summary
    - Performance
    - Heat Transfer
    - Pressure Drop
  - Mechanical Summary
    - Exchanger Data
    - Setting Plan / Tubesheet Layout

- Cost/Weights
  - o Calculation Details
    - Interval Analysis – Outside Tubes
    - Interval Analysis – Tube Side
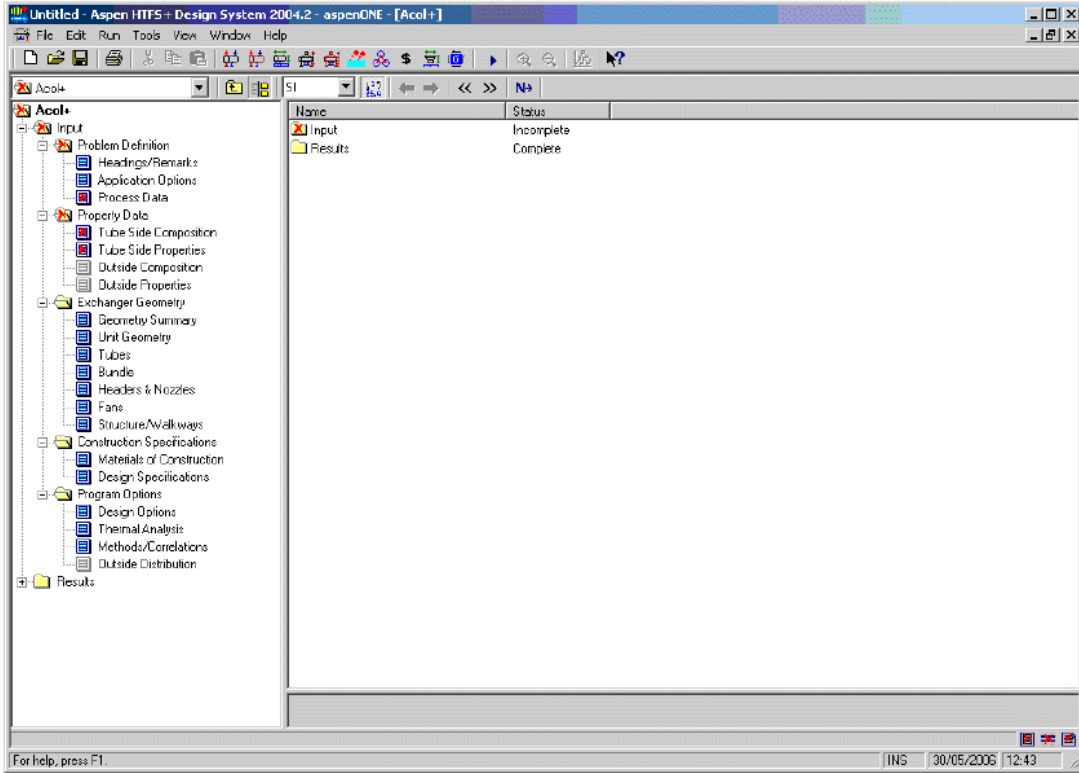
Figure 16: General outline of ASPEN – Air Cooled Exchanger (Input Section)
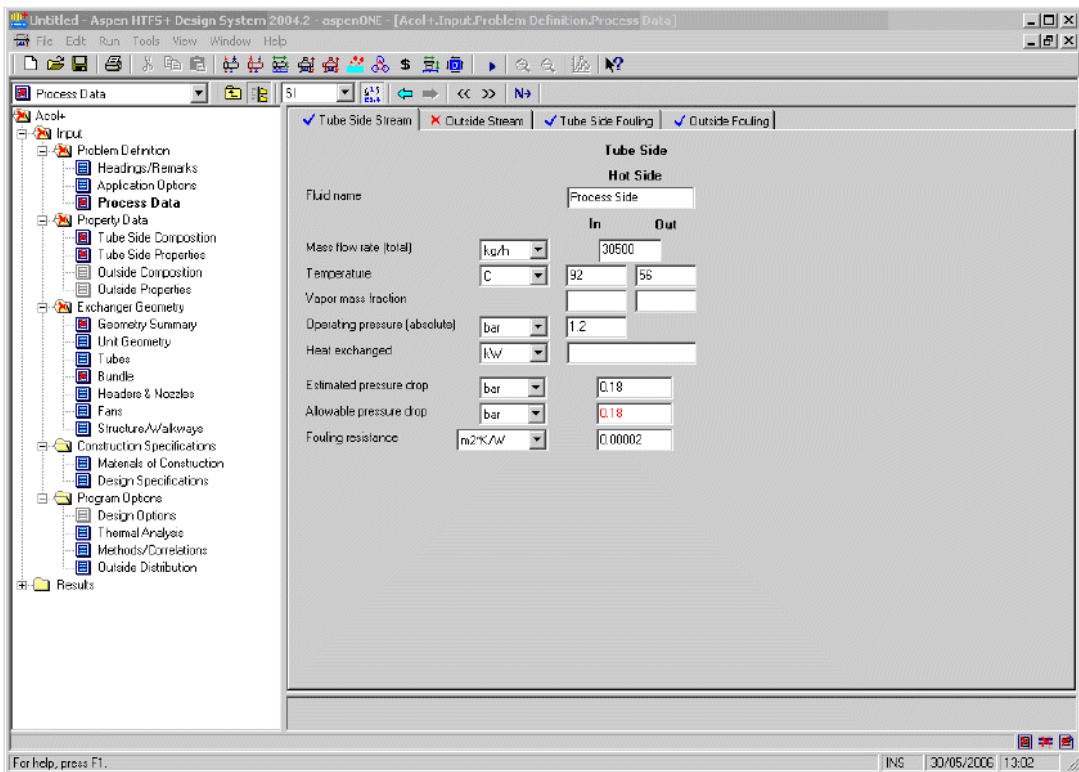
Figure 18: Selection of geometrical characteristics within ASPEN – Air Cooled Exchanger (Input Section)
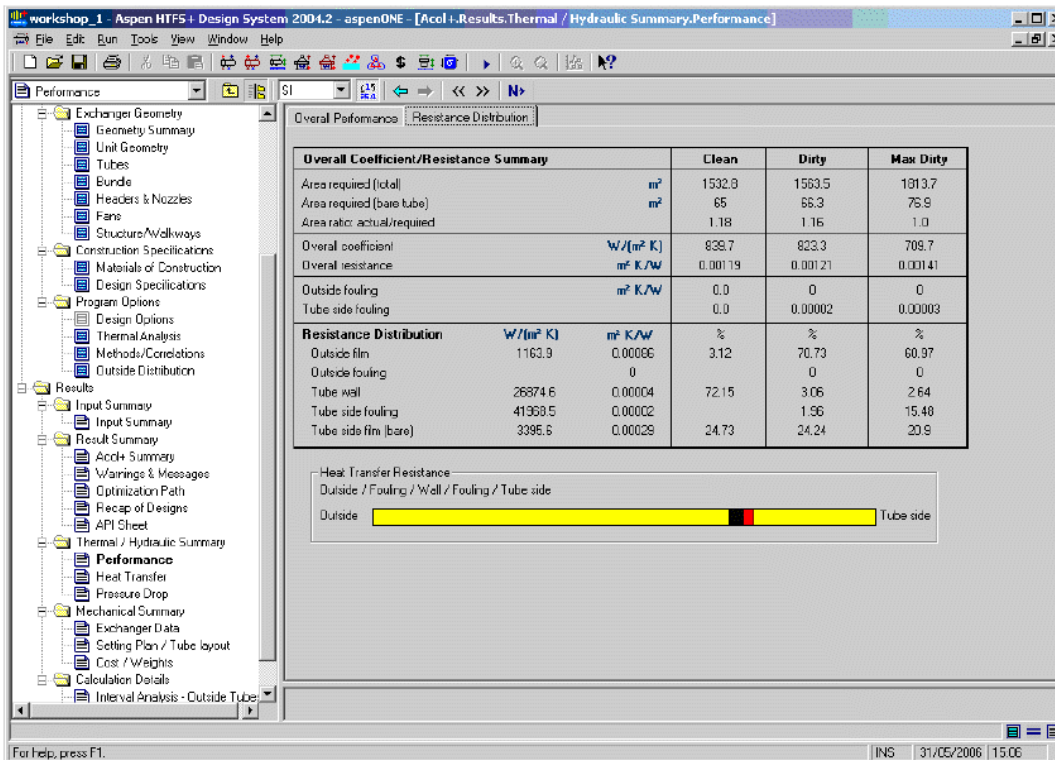
Figure 19: Results Section within ASPEN – Air Cooled Exchanger (input Section)

4.3 ASPEN EDR Methods and Correlations for Air Cooled Heat Exchangers

4.3.1   Circular – Fin Heat Exchangers:
4.3.1.1 Heat Transfer Coefficient Correlations:

The ASPEN ACOL heat transfer correlations for circular fin air-cooled heat exchanger design are derived from the research reported in PFR Part 1 (1976) and PFR Part 2, (1976). PFR Part 2, (1976) outlines the heat transfer and pressure drop characteristics of extended surface heat exchangers based on the theoretical and experimental analysis of compiled data reported in PFR Part 1, (1976). Analysis of this data was conducted to establish the effect geometrical variables have on the heat transfer and pressure drop characteristics of an extended surface heat exchanger. To ensure data accuracy, PFR Part 1, 1976 examined the experimental and data reduction methodology employed by these authors. In the experimental methodology, factors such as: data collection method (Steady State or Transient), heating medium, heating conditions, heat flux system and measurements (heat load, pressure drop, flowrate, and temperature measurement) were relied on to establish the accuracy of the compiled data. While in the data reduction method, PFR established data accuracy by studying the effect extended surfaces have on the true value of the gas-side heat transfer coefficient. Therefore, any research that factored in the effect of fins in heat transfer correlations was bound to have more accurate results than those reports which presented actual heat transfer coefficients. Error analysis was also used and it helped identify potential sources of error which include: errors as a result of deficiency in experimental procedures, errors from reading points on graphs, uncertainties in module dimensions and finally, errors caused by instrument uncertainty. By establishing criteria which must be fulfilled such as: use of logarithmic mean temperature in the heat transfer definition, heat balance check on both the tube and gas sides of the heat exchanger, etc. the probability of errors in the data reduction or analysis was significantly reduced.

At the end of the analysis, PFR 2 presents a correlation in the form of eqn. 108 below, for evaluating the gas-side heat transfer coefficient. This equation is based on a regression analysis of all the data derived from the geometrical variables analysis. The effect of geometrical variables on heat transfer was validated by studying experimental research data presented by the likes of Brauer (1961), Brauer (1961), Carnavos (1958), Jameson (1945), Mirkovic (1974), Robinson et. al. (1965), Ward et. al. (1959), Weirman et. al. (1975)

For round tube, helical round smooth fin heat exchangers, they found that only the fin tube variables, affect heat transfer. This was further verified by experiments using dry cooling towers. Therefore, the air-side heat transfer coefficient resembles the form:

$$h = 0.29\, Re_D^{-0.367}\, A_r^{-0.17}\, C_p\, \dot{m}_{max}\, Pr^{-2/3} \qquad .108$$

Experiments showed that PFR (1976) was accurate over the range of geometric dimensions indicated below, the equation predicted 80% of the data collected to within ±10% and 95% of the data collected to within ±18%.

1,000 ≤RE$_D$ ≤40,000, N$_r$≥2 and 4≤A$_r$≤34,

To predict pressure drop, PFR Part 2 (1976) suggests that consideration must be given to both the tube pitch and the finned tube variables. In addition to this, they state that the hydraulic diameter was better suited for the evaluation of pressure drop than the base diameter. The frictional factor therefore takes the form:

$$f = \left(150\, Re_h^{-1.0} + 1.8\, Re_h^{-0.2}\right) (P_l/d_h)^{0.35} (P_l/d_h)^{>4} \qquad .109$$

$$f = \frac{\Delta P/N_t}{\rho av\, G_{max}^2/2g_c} \qquad .110$$

The pressure drop correlation covers the range:

400 < Re$_h$ < 10,000 and 1.5 ≤ P$_l$/d$_r$ ≤ 3.8

If 1.5 ≤ P$_l$/d$_r$ ≥ 4.0, then frictional factor is evaluated using:

$$f = \left(13.6\, Re_h^{-0.3}\right) (P_l/d_h)^{0.35} (P_l/d_h)^{\leq4} \qquad .111$$

4.3.1.2 Pressure Drop Correlations:

For the prediction of pressure drop, ASPEN EDR has invested a lot of resources in an attempt to accurately predict the gas-side pressure drop of air cooled heat exchangers. This can be seen in the works of PFR (1976), HTFS1 (HTFS RS1016, 1997), HTFS2 (HTFS RS1036 1998), HTFS3 (HTFS RS1118, 2002) and HTFS3A. The most accurate of the lot, the HTFS3A method is based on experiments reported in HTFS RS1171 and HTFS RS1186. HTFS3A was conducted to illustrate the dependence of the gas-side pressure drop on the changing properties of the gas as it is heated on passing through the heat exchanger. This dependence was predicted to a degree by PFR (1976) and Weierman (1976) but not by the HTFS2 and HTFS3 methods. To illustrate this dependence, HTFS RS1171 measured pressure drop under isothermal conditions of 20°C and thermal conditions of mean bulk temperature 56°C while HTFS RS1186 measured pressure drop under isothermal conditions of 20°C, 45°C, 56°C and 75°C and thermal conditions of mean bulk temperature of 75°C. Results led them to develop a correction factor of 0.91 for mean air temperature at 20°C and 1.0 at an air inlet temperature of 56°C and above for the pressure drop correlation reported by HTFS3. These correction factors have been incorporated into ASPEN EDR. The HTFS3 correlations are outlined below.

$$\frac{\Delta P}{\rho} = 1.081 K_B u_0^{1.7} \qquad .112$$

Experimental results showed that the correlations predicted 98% of the data to within ±20% for air coolers. For open literature correlations, the HTFS3 predicts 79% of the data to within ±20%.

4.3.2   Plain – Tube Heat Exchangers:

4.3.2.1 Heat Transfer Coefficient Correlations:

To evaluate heat transfer coefficient, ASPEN EDR outlines a methodology in HTFS SM4 which is based on correlations adopted from ESDU 73031 (1973). The ESDU equations were developed for 10 tube rows or more, but have correction factors that allow for the same equations to be used for inline tube bundles and designs where the tube rows are less than 10 in number. These correction factors have been outlined and discussed earlier in Chapter 3. However, the heat transfer coefficient correlation takes the form:

$$\alpha_c = a \frac{\lambda_b}{D} Re_c^m Pr_b^{0.34} \qquad .113$$

4.3.2.2 Pressure Drop Correlations:

To evaluate pressure drop, a methodology is outlined in HTFS SM3, which uses ESDU (1980) to evaluate pressure drop without bypassing. The bypassing effect is accounted for, by using the Russell and Wills (1983) equation. The pressure drop equation is outlined below:

$$\Delta p_c = C \frac{L}{D} \rho_b \frac{u_s^2}{2} \varphi_1 \varphi_2 \qquad .114$$

$$\Delta p_B = 4 f N_R \rho_b \frac{u_B^2}{2} \ (for\ bypass\ pressure\ drop) \qquad .115$$

Where:
$\Delta p_c = crossflow\ pressure\ drop, Nm^{-2}$
$u_s = superficial\ velocity, ms^{-2}$
$\varphi_1 = viscosity\ correction\ factor, (-)$
$\varphi_2 = roughness\ correction\ factor, (-)$
$\Delta p_B = bypass\ pressure\ drop, Nm^{-2}$
$f = friction\ factor, (-)$
$N_R = number\ of\ tube\ rows\ crossed\ in\ direction\ of\ flow, (-)$
$u_B = bypass\ velocity, ms^{-2}$

4.3.3   Tube –in – Plate Fin Tube Heat Exchangers:

4.3.3.1 Heat Transfer Coefficient Correlations:

To evaluate heat transfer coefficient in tube-in-plate heat exchangers, ASPEN EDR outlines a methodology in HTFS ZM2 which is based on correlations adopted from PFR Part 2 (1976). PFR Part 2 (1976) carried out regression analysis on data provided by Rich (1973), Cox (27) and the Trane Company data presented by Kays and London (1) to represent the form:

$$h = 0.13 \ Re_D^{-0.33} \ C_p \ \dot{m}_{max} \ Pr^{-2/3} \qquad .116$$

Experiments showed that 80% of the data were predicted to within ±12% using the equation.

4.3.3.2 Pressure Drop Correlations:

To evaluate pressure drop, PFR Part 2 (1976) uses the equation;

$$f = \left(110\,Re_h^{-1.0} + 1.35\,Re_h^{-0.2}\right)\left(P_l/d_h\right)^{0.35} \qquad .117$$

4.4   Thermal Design Results and Comparison:

4.4.1   Plain tube heat exchanger:

From open source literature, ESDU 73031 (1974) was used to evaluate the convective heat transfer coefficient *'h'* of the gas-side fluid while Gaddis & Gnieslinski, (1985), was used to evaluate the pressure drop across the tube bank on the gas-side. For the tube-side, Boelter and Dittus (1930), was used to evaluate the convective heat transfer coefficient of the tube-side fluid.

The Aspen Air-cooled Exchanger software was set to the parameters below before running the calculation:

- **Program calculation mode:**   Rating/Checking function
- **Select geometry based on this dimensional standard:** SI
- **Tube-side application:**   Liquid, no phase change
- **Outside tube application:**   Dry Air
- **Equipment type:**   Air-cooled exchanger

4.4.1.1   Initial design data

Table 5: Process conditions and dimensions for plain tube heat exchanger

Gas-side volume flow rate	5m^3/s
Duct size	1.11m x 0.9m
Finned height of the exchanger	0.85m
Heat duty required	41kW
Tube-side fluid	Water
Tube-side inlet temperature	80^{0}C
Tube-side outlet temperature	60^{0}C
Gas-side fluid	Air
Gas-side inlet temperature	25^{0}C
Transverse pitch	0.055m
Longitudinal Pitch	0.05m
Tube Material	Copper
Tube Outer Diameter	0.0267m
Tube Inner Diameter	0.02096m
Tube Thickness	0.00287m
Tube Length	1m
Number of rows	8
Fluid velocity	0.1m/s
Fluid supply pressure	2
Number of tubes per row	15
Total number of tubes	120

The initial design parameters were checked to ensure they fell within the range of data for the equations defined by ESDU 73031 (1973), which was used to evaluate the convective heat transfer *'h'* for air flow across the heat exchanger. Table 6 and Table 7 show the design parameters assessed.

Table 6: Assessment of inline tube arrangement design parameters for plain tube heat exchangers

Inline Arrangement	
R_e	19,370
X_t^*	2.06
X_l^*	2.06
$(X_l^* - 1)/(X_t^* - 1)$	1
C_0	1.055
C_1	0.548
C_2	14.7
C_3	37.3
a	0.211
m	0.651
$4 \leq N_r \leq 10$	

Table 7: Assessment of staggered tube arrangement design parameters for plain tube heat exchangers

Staggered Arrangement	
R_e	19,370 (staggered)
X_t^*	2.06
X_l^*	1.87
$(X_l^* - 1)/(X_t^* - 1)$	0.82
C_0	1.025
C_1	0.093
C_2	4.06
C_3	6.60
a	0.2273
m	0.635
$4 \leq N_r \leq 10$	

The same parameters were also checked to ensure they fell within the range of data covered by the equations from Gaddis & Gnielinski (1985) which was used to evaluate the pressure drop across the heat exchanger. Table 8 and Table 9 show the design parameters assessed.

Table 8: Assessment of inline tube arrangement design parameters for plain tube heat exchangers

Inline Arrangement	
$N_r \geq 5$	8
$7.9 \leq D_0 \leq 73mm$	26.7mm
$1.25 \leq X_t/D_0 \leq 3.0$	2.1mm
$1.20 \leq X_l/D_0 \leq 3.0$	1.87mm

Table 9: Assessment of staggered tube arrangement design parameters for plain tube heat exchangers

Staggered Arrangement	
$N_r \geq 5$	8
$7.9 \leq D_0 \leq 73mm$	26.7mm
$1.25 \leq X_t/D_0 \leq 3.0$	2.1mm
$0.6 \leq X_l/D_0 \leq 3.0$	1.87mm
$(X_t^2 + X_l^2)^2/D_o \geq 1.25$	2.78

4.4.1.2 Results

Staggered Arrangement:

Comparisons of the results for the staggered tube arrangement are presented in Table 10 below.

Table 10: Plain tube staggered arrangement results

	Open Source Correlation Equations	Aspen Air-cooled Exchanger	% Deviation
Area ratio	1.14	1.06	7.5% over-prediction
Gas pressure drop, Pa	192	237	23% under-prediction
Total heat transfer surface area, m^2	10.75	9.3	15% over-prediction
Gas – outlet temperature	32	32	No deviation
Tube – side Reynolds number	5,078	4,877	4% over-prediction
Gas – side Reynolds number	19,370	21,798	13% under-prediction
Tube-side mass flow rate, kg/sec	0.4893	0.4893	No deviation
Gas mass flowrate, kg/sec.	5.92	5.92	No deviation
Number of passes	8	8	No deviation
Number of tubes per pass	15	15	No deviation
Average pressure drop of flow entering tubes, Pa	7	7.1	1% under-prediction
Average pressure drop of flow through tubes, Pa	9	9.7	7% under-prediction
Overall Heat Transfer Coefficient, w/m.K	107	113	6% under-prediction
LMTD	41	41.21	0.5% under-prediction
Face velocity, m/s	6.0	6.35	5.8% under-prediction
Heat transfer coefficient – gas side, W/m.K	135	124	8% over-prediction
Heat transfer coefficient – tube side, W/m.K	796	716	11% over-prediction

Inline Arrangement:

To represent an inline arrangement, the longitudinal dimension of the tube pitch was changed from 50mm to 55mm to match the transverse pitch. The same design routine was then repeated with the new inline tube arrangement and the results in Table 11 were obtained.

Table 11: Plain tube Inline arrangement results

	Correlation Equations	Aspen Air-cooled Exchanger	% Deviation
Area ratio	1.04	0.96	8% over-prediction
Gas pressure drop, Pa	144	184	27% under-prediction
Heat transfer coefficient – gas side, W/m.K	110	121.5	9.8% under-prediction
Heat transfer coefficient – tube side, W/m.K	796	718	11% over-prediction

4.4.1.3 Result discussion:

4.4.1.3.1 Staggered arrangement:

Area ratio: The area ratio is the most important value to the designer because it tells the designer by how much the heat exchanger unit has either been undersized or oversized compared to the operating requirements and the initial design data. Oversizing within reason, is common in the heat exchanger industry because operating conditions are not always as accurate as presented by the end-user. Therefore, to ensure that the heat exchanger unit continues to deliver the desired heat duty, an oversize of the unit "within reason", is necessary.

The open source design correlation predicts a heat exchanger oversize of 14% while ASPEN ACOL indicates an oversize of just 6% based on the initial design parameters. This represents an over prediction of 7.5% by the open source design correlations. To put this context, it means that 7.5%

more material will be used when the heat exchanger is manufactured using heat transfer correlations from open source literature.

Total heat transfer area: The total heat transfer area evaluated using open source literature (eqn.88 – eqn.93), showed that the heat exchanger will be 10.75m^2 overall. When this value is compared to the ASPEN ACOL result (9.3m^2), an over prediction of 15% is observed.

Overall heat transfer coefficient: The overall heat transfer coefficient is the summation of the resistance to heat transfer via conduction and convection on the tube and gas sides of the heat exchanger respectively. It constitutes a combination of heat transfer surface areas and heat transfer coefficients on both sides of the heat exchanger (fluid and gas sides). From Table 10 above, it is observed that the open source heat transfer correlations under-predicts the overall heat transfer coefficient by just 6% compared to the value obtained using ASPEN ACOL. The under-prediction is minute and will not affect the performance of the heat exchanger.

Gas – side pressure drop: The gas-side pressure drop result obtained using open source data shows a 23% under prediction from the ASPEN results. The consequence of the under prediction will manifest at the heat exchanger fan selection stage. Based on the results, fan pressure drop requirements will be under predicted and any fan selected based on these results, will deliver a duty less than required. Therefore, any pressure drop results obtained using the open source correlations for staggered plain tube heat exchangers will be treated as conservative and factored into any decision making regarding selection of heat exchanger components such as fans and transition ducts.

Tube – side pressure drop: Open source equations predict pressure drop to within 1% and 7% for fluid flow entering the tubes and through the tubes respectively when compared to the values obtained using ASPEN ACOL. The difference in both calculations is very small and within acceptable ranges of deviation.

Gas-side heat transfer coefficient: The open source heat transfer correlations over predict the gas-side heat transfer coefficient by 8% even though the two design methods (open source and ASPEN ACOL) use the same heat transfer correlations obtained from ESDU 73031. The over prediction is rather small and could be as a result of the more advanced computation power of ASPEN ACOL.

Tube-side heat transfer coefficient: The heat transfer coefficient on the tube-side of the heat exchanger is over predicted by 11% when open source heat transfer correlations are used. Although this represents a fairly high value, the controlling resistance is on the gas side of the heat exchanger and thus any over-prediction on the tube side will have very little effect on the overall design of the heat exchanger.

4.4.1.3.2   Inline arrangement:

Area ratio: The area ratio obtained using open source data over predicted the size of the unit required by 8% when compared to the result obtained with ASPEN ACOL. This result suggests that better prediction is obtained when the open source correlations are used for designing plain tube heat exchangers with staggered tube arrangement. In addition, the result clearly illustrates the advantage of a staggered heat exchanger tube arrangement over an inline arrangement.

Gas – side pressure drop: The gas-side pressure drop is under predicted by 27% and indicates that the open source pressure drop correlations will under predict the gas-side pressure drops in both the inline and staggered tube arrangements. The use of these correlations must be treated with caution in heat exchanger design.

Gas-side heat transfer coefficient: A reverse of the case seen in the staggered arrangement, the heat transfer coefficient is under predicted by the open source design method even though both methods depend on ESDU 73031 (1973) to predict the heat transfer coefficient on the gas-side of the heat exchanger.

Tube-side heat transfer coefficient: The prediction of the heat transfer coefficient on the tube side is also over by 11% which ideally should remain the same for both cases because the tube-side fluid is not affected by tube pitch arrangement.

4.4.1.4 Summary:

In the case of the staggered arrangement, the key design parameters such as gas-side heat transfer coefficient, area ratio, overall heat transfer coefficient gas-side, tube-side pressure drop etc., were all within acceptable ranges of deviation compared to the values obtained using ASPEN ACOL and could thus be used for developing the design toolkit. However, the gas-side pressure drop was considerably under predicted by the open source correlation equations and must be treated with caution when used in the design toolkit.

While in the case of the inline arrangement, the gas-side pressure drop is once again under predicted and thus must be treated with caution when used in the design toolkit. All other parameters are within acceptable ranges of deviation.

4.4.2   Circular-fin heat exchanger:

The Briggs and Young (1963) equation, was used to evaluate the Colburn Factor (j), which is used to evaluate the heat transfer coefficient of the gas-side fluid. Kays & London (1984) was used to evaluate the pressure drop across the tube bank on the gas-side. Finally, the Boelter and Dittus (1930) equation, was used to evaluate the heat transfer coefficient of the tube-side fluid.

In ASPEN EDR, the air cooled correlation equation, was set to HTFS3A which showed better accuracy in predicting air-side heat transfer coefficient and pressure drops than HTFS1, HTFS2, HTFS3 and PFR.

The Aspen Air-cooled Exchanger software was set to the parameters below before the results were run:

- **Program calculation mode:**   Rating/Checking function
- **Select geometry based on this dimensional standard:** SI
- **Tube-side application:**   Liquid, no phase change
- **Outside tube application:**   Dry Air
- **Equipment type:**   Air-cooled exchanger
- **Outside tube methods and correlations:**   HTFS3A

4.4.2.1   Initial Design Data

Table 12: Process conditions and dimensions for circular-fin heat exchanger

Gas-side volume flow rate	$5.5 m^3/s$
Duct size	1.11 x 1m
Finned height of the exchanger	0.9m
Heat duty required	100kW
Tube-side fluid	Water
Tube-side inlet temperature	80^0C
Tube-side outlet temperature	60^0C
Gas-side fluid	Air
Gas-side inlet temperature	30^0C
Transverse pitch	0.055m
Longitudinal Pitch	0.050m
Fin Material	Aluminium 1060
Tube Material	Carbon steel
Tube Outer Diameter	0.0267m
Tube Inner Diameter	0.02096m
Tube Thickness	0.00287m
Tube Length	1m
Number of rows	4
Number of fins/m	276 fins/m
Fluid velocity	0.22m/s
Fluid supply pressure	2bar
Fin thickness	0.0007m
Fin tip diameter	0.055m
Number of tubes per row	16
Total number of tubes	64

The initial design parameters were checked to ensure they fell within the range of data for Briggs and Young (1963). Table 13 below shows the results of the assessment.

Table 13: Assessment of design parameters for circular-fin tube heat exchanger

$0.13 \leq s/l \leq 0.63$	0.256
$1.01 \leq s/\delta \leq 7.62$	5.176
$0.09 \leq l/d_o \leq 7.62$	0.53mm
$0.011 \leq \delta/d_o \leq 0.15$	0.026m
$1.54 \leq X_t/d_o \leq 8.23$	2.1mm
$11.1 \leq d_o \leq 40.9mm$	26.7mm
$246 \leq N_f \leq 768 fins/m$	276 fins/m
Staggered tube layout	30^0

The initial design parameters were checked to ensure they fell within the range of data for Kays & London (1984). Table 14 below shows the results of the assessment.

Table 14: Assessment of design parameters for circular-fin tube heat exchanger

$5 \leq \varepsilon \leq 23$	13.21
$5.6mm \leq l \leq 16.5mm$	14.15mm
$1.85 \leq X_t/D_r \leq 4.75$	2.1mm
$1.50 \leq X_l/D_r \leq 4.00$	1.87mm
$1.50 \leq D_f/D_r \leq 4.00$	2.06mm
$9.5 \leq d_o \leq 51mm$	26.7mm
$157 \leq N_f \leq 437 fins/m$	276 fins/m

4.4.2.2   Results

Results from the assessment are presented in Table 15 and discussed in sub-section 4.3.2.3.

Table 15: Circular-fin staggered arrangement results

	Correlation Equations	Aspen Air-cooled Exchanger	% Deviation
Area ratio	1.12	1.05	6% over-prediction
Gas pressure drop, Pa	418	391	7% over-prediction
Total Heat Transfer area, m^2	71	67	5.63% over-prediction
Gas – outlet temperature	45.5	45.5	No deviation
Tube – side Reynolds number	11,172	11,160	0.1% over-prediction
Gas – side Reynolds number	23,507	26,084	11% under-prediction
Tube-side mass flow rate, kg/sec	1.19	1.19	No deviation
Gas mass flowrate, kg/sec.	6.4044	6.4044	No deviation
Number of passes	4	4	No deviation
Number of tubes per pass	16	16	No deviation
Average pressure drop of flow entering tubes	34	41	20% under-prediction
Average pressure drop of flow through tubes	34	37	9% under-prediction
Fin surface effectiveness	0.92	0.88	4.5% over-prediction
Overall Heat Transfer Coefficient, W/m.K	647	640	1.1% over-prediction
LMTD	32.2	32.16	0.12% over-prediction
Heat exchanger face velocity, m/s	6.1	6.38	5.8% under-prediction
Heat transfer coefficient – gas side, W/m.K	1215.36	1309	7.15% under-prediction
Heat transfer coefficient – tube side, W/m.K	1496.6	1338	12% over-prediction

4.4.2.3   Result discussion:

Area Ratio: Comparison between the results showed only a 6% over-prediction of the area ratio when open source heat transfer correlation data is used for design purposes. The extent of deviation is minute and suggests that the design method employed to develop the toolkit, is similar to the deign method used by ASPEN ACOL.

Total heat transfer area: The open source equations (eqn. 94 – eqn. 100) showed only a 5.63% deviation from ASPEN equations.

Overall heat transfer coefficient: The values obtained from the calculations, showed just a 1.1% deviation from the values obtained using ASPEN EDR. This shows a very good prediction of the heat transfer coefficients for both the gas-side and tube-side fluids using the heat transfer coefficient equations obtained from Briggs and Young (1963) and Dittus-Boelter (1930) respectively.

Gas – side pressure drop: using the Kays and London (1984) gas-side pressure drop equations, a 7% deviation was observed when compared to the results produced by ASPEN EDR. This showed a good prediction of the gas-side pressure drop considering that extra measures have been taken to improve the accuracy of the ASPEN correlations in HTFS3A.

Tube – side pressure drop: Open source equations under predict pressure drops by 18% and 9% for fluid flow entering the tubes and through the tubes respectively when compared to the values obtained using ASPEN ACOL. The same pressure drop equations and tube sizes were used in the plain tube validation exercise with smaller deviations observed. However, tube side velocity was less (0.1m/s) and suggests that larger tube side velocities could introduce larger deviations in the tube side pressure drop values.

Gas – side heat transfer coefficient: The Briggs and Young (1963) correlation closely predicted the same results as the PFR equations from ASPEN with only a 7.15% deviation.

Tube – side heat transfer coefficient: The heat transfer coefficient on the tube-side of the heat exchanger is over predicted by 12% when open source heat transfer correlations are used. This indicates almost the same deviation observed in the plain tube validation exercise which suggests that the ASPEN ACOL equations for the tube-side heat transfer coefficient, is used across all 3 types of air-cooled heat exchangers.

4.4.2.4 Summary:
The circular fin air-cooled heat exchanger validation exercise showed the most impressive results of all three types of air-cooled heat exchangers when compared to the ASPEN ACOL results. All the key design parameters such as gas-side heat transfer coefficient, gas-side pressure drop, area ratio, overall heat transfer coefficient gas-side, etc., were within acceptable ranges of deviation and strongly indicates that the equations available in the public domain, are the same as those used in ASPEN ACOL.

4.4.3   Tube-in-plate fin heat exchanger:
Wang and Chi (2000) was used to evaluate the Colburn Factor (j), which was eventually used to evaluate the heat transfer coefficient of the gas-side fluid. Wang and Chi (2000), was also used to evaluate the frictional factor needed for pressure drop calculations across the tube bank on the gas-side and Dittus and Boelter (1930), was used to evaluate the heat transfer coefficient of the tube-side fluid.

The Aspen Air-cooled Exchanger software was set to the parameters below before the results were run:

- **Program calculation mode:**   Rating/Checking function
- **Select geometry based on this dimensional standard:** SI
- **Tube-side application:**   Liquid, no phase change
- **Outside tube application:**   Dry Air
- **Equipment type:**   Air-cooled exchanger

4.4.3.1   Initial Design Data

Table 16: Process conditions and dimensions for tube-in-plate fin heat exchanger

Gas-side volume flow rate	1.22m^3/s
Finned height of the exchanger	0.46m
Tube-side fluid	Water
Tube-side inlet temperature	90^{0}C
Tube-side outlet temperature	70^{0}C
Gas-side fluid	Air
Gas-side inlet temperature	0^{0}C
Gas-side outlet temperature	48^{0}C
Transverse pitch	0.025m
Longitudinal Pitch	0.025m
Fin Material	Aluminium 1060
Tube Material	Copper
Tube Outer Diameter	0.010m
Tube Inner Diameter	0.008m
Tube Thickness	0.001m
Tube Length	0.45m
Number of rows	3
Number of fins/m	472 fins/m
Fluid velocity	1.05m/s
Fluid supply pressure	2bar
Fin thickness	0.0001m
Number of tubes per row	18
Total number of tubes	54

The initial design parameters were checked against Wang and Chi (2000) to ensure they fell within the range of data. Table 17 below shows the results of the assessment:

Table 17: Assessment of design parameters for tube-in-plate fin heat exchanger

300 $\leq Re_{dc} \leq$ 20,000	7,615
6.9 $\leq d_c \leq$ 13.6mm	12
1.30 $\leq D_h \leq$ 9.37mm	14.5
20.4$\leq X_t \leq$ 31.8mm	25mm
12.7$\leq X_l \leq$ 32mm	25mm
1.0$\leq p_f \leq$ 8.7mm	2.11
1$\leq N_r \leq$ 6	3

4.4.3.2   Results

Results from the assessment are presented in Table 18 and discussed in sub-section 4.3.3.3

Table 18: tube-in-plate fin staggered arrangement results

	Toolkit	Aspen Air-cooled Exchanger	% Deviation
Area ratio	0.87	0.76	14% over-prediction
Gas pressure drop, Pa	244	253	3.7% over-prediction
Total Heat Transfer area, m^2	14	12	16% over-prediction
Heat Duty, kW	76	75.4	0.7% over-prediction

Tube – side Reynolds number	23,055	22,556	2.2% over-prediction
Gas – side Reynolds number	7,615	8,866	16% over-prediction
Tube-side mass flow rate, kg/sec	0.9	0.9	No deviation
Gas mass flowrate, kg/sec.	1.6	1.6	No deviation
Number of passes	3	3	No deviation
Number of tubes per pass	18	18	No deviation
Average pressure drop of flow entering tubes	776	800	3.1% under-prediction
Average pressure drop of flow through tubes	760	874	15% under-prediction
Fin surface effectiveness	0.92	0.87	5.7% over-prediction
Overall Heat Transfer Coefficient	1,280	1,498	17% under-prediction
LMTD	55	55.6	1% under-prediction
Minimum free flow area, mm^2	0.1125	0.0990	14% over-prediction
Face velocity, m/s	6.0	6.59	10% under-prediction
Heat transfer coefficient – gas side, W/m.K	1235.32	1494.73	21% under-prediction
Heat transfer coefficient – tube side, W/m.K	6819	5987	13.9% over-prediction

4.4.3.3   Result discussion:

Area ratio: Both area ratio results indicate that the current heat exchanger geometry will not achieve the desired duty. However, the toolkit over predicts this deficiency by up to 14% when compared to the results of ASPEN ACOL.

Total heat transfer area: The toolkit over predicts the overall surface area of the heat exchanger by 16% when compared with the results of ASPEN ACOL. The extent of the disparity has not been tested on larger heat exchangers to determine if this value increases proportionally with the size of the heat exchanger. However, at this stage it can be said that the disparity is little and equations 101 – 103 could be deemed suitable for use in the toolkit.

Overall heat transfer coefficient: An under-prediction of 17% by the open source correlations indicates that either the gas-side or the tube-side heat transfer coefficient value will differ considerably with those of ASPEN ACOL. The size of the deviation is significant, considering that it a combination of both the gas-side and tube-side heat transfer coefficients.

Gas – side pressure drop: Open source correlations, under predicted the gas-side pressure drop by 3.7% compared to the ASPEN ACOL results. It indicates good predictability of Chi and Wang (2000) (eqn. 53) for the gas-side pressure drop in tube-in-plate heat exchangers.

Tube – side pressure drop: Open source equations under predict pressure drops by 3.1% and 15% for fluid flow entering the tubes and through the tubes respectively when compared to the values obtained using ASPEN ACOL. Results from the earlier exercises, had indicated that larger deviations are likely to occur as the velocity of flow increases.

Gas – side heat transfer coefficient: With an under-prediction of 21%, the Wang and Chi (20002) heat transfer correlations deviation showed the largest deviation of all the heat exchanger designs considered.

Tube – side heat transfer coefficient: The heat transfer coefficient on the tube-side of the heat exchanger was over predicted by 14% by the open source heat transfer correlations. Once again, it follows the trend observed earlier in both the plain tube and tube-in-plate heat exchangers.

4.4.3.4 Summary:

The tube-in-plate fin air-cooled heat exchanger validation exercise showed the largest deviations of all three types of air-cooled heat exchangers when compared with the ASPEN ACOL results. Although the gas-side pressure drop value was less than 4% off the value predicted by ASPEN ACOL, the more important gas-side heat transfer coefficient showed an under-prediction of as much as 21%. This under-prediction will ultimately affect the final value of the overall heat transfer coefficient and possibly lead to an oversized heat exchanger.

Chapter 5

Heat Exchanger Design Optimization

5.1   Introduction:

Due to the several possible combinations with design variables that include: number of tube rows, tube length, tube OD, tube pitch layout, fin pitch etc., the design and analysis stage of air cooled heat exchangers can become a time consuming and expensive process. Therefore to minimise time spent at this stage, the conventional method of design is applied. This method would involve keeping one constraining variable constant and iterating the other variables one-at-a-time until the design requirements are met. For example using the "Rating" design method, the tube diameter could be kept constant and other factors such as tube length, number of rows, number of fins, etc. varied and once the desired solution is reached, no further consideration is given to altering these variables to determine if the design requirements can be met using a different combination. This invariably means the rating design method could prove more expensive to the manufacturer based on the theory that the larger the overall surface area of the unit, the more manufacturing materials will be required to build it. This also means that the unit will take longer to manufacture thus leading to an increase in labour costs. A combination of these two costs (materials and labour) could easily price any small-to-medium scale enterprise (SME) out of the highly competitive heat exchanger market. Other factors which could increase the final cost of manufacturing include: material surface treatment (galvanizing or painting), type of manufacturing material (e.g. stainless steel), non-destructive testing (NDT) etc. Although these are special requirements specified by the consumer, they increase the final cost of the heat exchanger since they also increase proportionally to the size of the heat exchanger unit. However, in most cases, the consumer is willing to pay more for these "extras".

On-the-other hand, when using the optimization solution methods in the thermal design process, all independent design variables (tube length, tube OD etc.), are considered simultaneously in various combinations in order to deliver a solution that satisfies all design requirements even if one or more of the design variables has to be kept constant. An example of optimization in the design process is to aim to optimize the final overall heat transfer surface area of the heat exchanger while still ensuring the unit delivers the duty required. Optimization in this instance means that the final overall surface area matches exactly what will be required to deliver the required duty. This problem statement thus becomes the focal point of design unlike the conventional method where any size is deemed satisfactory as long as it satisfies the design requirements. Thus, the final solution in the optimization process not only ensures that all design requirements are met but also that the optimal configuration of the geometrical dimensions is used to achieve it. Ideally, optimization will eliminate the need to carry out several iterations of any particular variable which saves design time.

In an attempt to replicate the optimization design methods, a "Sizing" design option has been added to the heat exchanger design toolkit. The "Sizing" option will enable the designer specify minimum and maximum values of specific heat exchanger variables along with desired increments. The design process then involves running a combination of all the variables through the heat transfer equations, along with the increments as specified by the designer one step at a time. The final results will show the best combination of the design variables that will give the optimum heat exchanger surface area which will achieve the desired heat duty. In other to prevent a glut of unnecessary results, the toolkit has been designed to ensure that only thermal conductance ratio values less than 1.5 times the required thermal conductance are displayed.

$$UA_{required} \leq 1.5 \ x \ UA_{design}$$

The difference between the conventional and optimization methods of design can be seen the flow chart below:
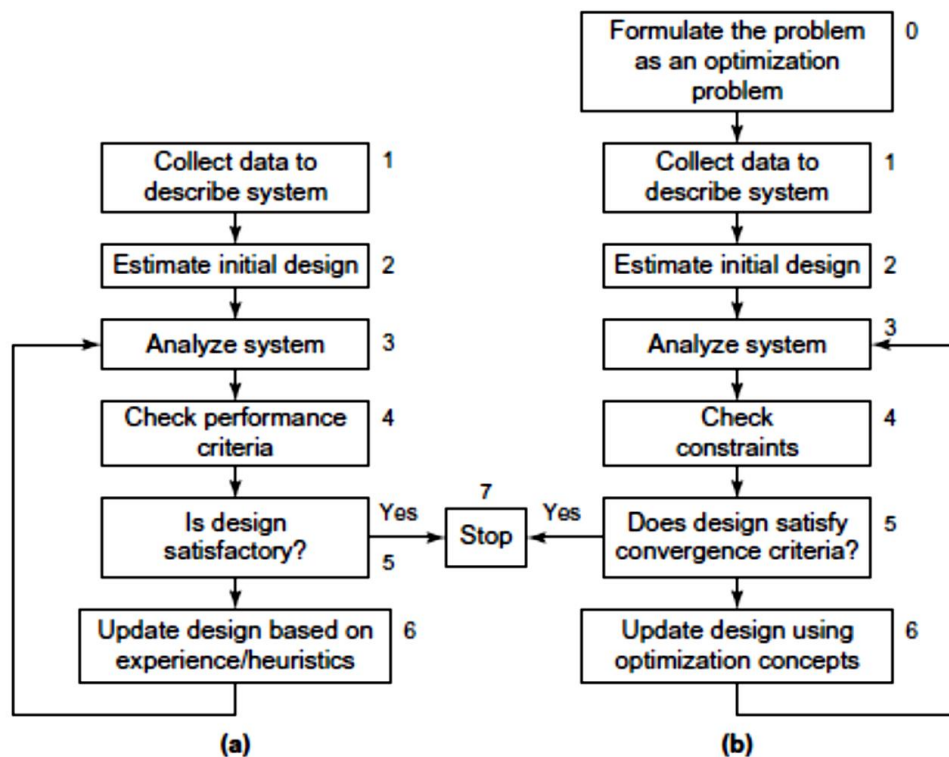
Figure 20: Comparison of (a) conventional design method and (b) optimum design method, Source: Introduction to Optimum Design, 2012

5.1.1 Aim:

The aim of this exercise is to validate the 'Sizing' design option which will be made available in the heat exchanger toolkit using the optimization tool 'GRG nonlinear Solver' available in Microsoft Excel. This exercise will determine the values of the design variables that will produce the optimum heat transfer surface area in the design of an air-cooled heat exchanger while still achieving the specified heat duty.

5.1.2 Methodology:

1. Select a heat exchanger type from either the circular-fin, tube-in-plate or plain tube type heat exchanger as case study.

2. Outline the operation conditions of the heat exchanger and use the LMTD design method to determine the thermal conductance required. The equation will be of the form:

$$\frac{Q}{\Delta T_{LMTD}} = UA_{required} \qquad .118$$

3. Use the conventional design method to determine the values of the design variables when the desired heat duty is achieved. The "Rating" option available in the design toolkit will be used to perform the conventional method of design. This calculation will establish the viability of the configuration to deliver the desired heat duty. This will involve altering each independent design variable one-at-a-time and observing the effect on the final result. Design satisfaction is achieved when:

$$UA_{required} = UA_{design}$$

4. Outline upper limits, lower limits and increments for the independent design variables which will be used in the optimization design process.

5. Establish the size of the heat exchanger by applying these design variables to the "Sizing" option available in the toolkit in order to determine the several possible combinations of the design variables when the thermal conductance is achieved.

6. Establish the size of the heat exchanger by applying the same upper and lower design variable limits to the optimization tool **GRG non-linear equation solver** available in Microsoft Excel to determine the values of the independent design variables when the thermal conductance is achieved.

7. If the optimization criterion is not met, the upper and lower limits of the design constraints outlined in Step 4 will be adjusted to include a larger field. The process will be repeated until the criterion in Step 3 is achieved.

8. Compare the results obtained from the "Sizing" option in the toolkit with the results from the GRG nonlinear solver.

5.2   Literature Review:

Optimization design of air cooled heat exchangers has been used by several researchers to achieve different objectives. For example, Doodman, Fesanghary and Hosseini (2009), used the Global Sensitivity Analysis (GSA) optimization method to determine the effect of geometrical parameters on the final cost of the heat exchanger. Then, they applied the harmony search (HS) optimization method to find the optimum configuration for an air-cooled condenser. They compared their

algorithm to the results of the more common Genetic Algorithm (GA) and found that although the HS algorithm converged to an optimum solution, the GA algorithm produced higher accuracy. Manassaldi, Mussati and Scenna (2014), developed a mathematical model for the optimal design of air-cooled heat exchangers using seven discrete decisions that included: type of finned tube, number of rows & number of tubes per row, number of tube passes, fins per tube length, fin thickness and fluid flow regime. The optimization problem was developed as a mixed-integer non-linear programming (MILP) problem, which was implemented in the general algebraic modelling system (GAMS) and then solved using the branch and bound method. As part of their study, they also determined the optimum equipment configuration in order to minimize the investment and operating costs of the ACHE. Bahrami and Salimpour (2011) approached the optimization problem differently. They attempted to optimize the air cooled heat exchanger by studying entropy generation caused by heat transfer and pressure losses on the tube and air sides of the ACHE. By varying geometry and flow parameters, they discovered that an increase in the tube-side Reynolds number was proportional to an increase in irreversibility as a result of an increase in pressure drop while entropy generation contributed little to the heat transfer process. On the air-side, they observed the same phenomenon but in this case, entropy generation augmented the heat transfer process. Their results enabled them develop a correlation to predict the optimum value for the Reynolds number of the tube-side fluid in order to reduce entropy generation. Aspelund, Shelton and Stewart (2005) developed a design model based on analytical and empirical correlations for condenser units used in air-conditioning system. Thereafter, they applied their model to the Simplex optimization algorithm, to determine the optimum design geometry for the condenser units with an objective function defined by maximizing the Coefficient of Performance (COP) of the unit. Their results showed that by reducing system entropy, a solution similar to maximizing the system COP could be achieved. Evenko (2002) conducted an optimization study of air cooled heat exchanger tube bundles by deriving a mathematical model to examine the effect of design variables on the performance of the heat exchanger. Aute, Qiao, Radermacher and Singh (2010), studied the optimization of air cooled heat exchanger by varying the fin density along the HX tubes on ACHE based on varying air flow velocity across the unit. Using the Genetic Algorithms (GA) optimization solution method, they observed that non-uniform fin density along the heat exchanger tubes under uniform air flow did not improve the thermal performance of the unit. Conversely, thermal performance was increased by up to 2% when the air flow was proportionally varied and between 1.5 – 2% when the air flow pattern was parabolic. Firstly, Cavazzuti and Corticelli (2008) used CFD to design a compact heat exchanger and then applied several optimization algorithms (Simplex, MOGT, MOGA-II and RDA analysis) in a multi-objective optimization process to maximize heat transfer while minimizing pressure loss for fluid flow within the transitional flow region (Reynolds = 1000, Pr = 0.74) in compact heat exchangers with enhanced surfaces. Sunden, Wang and Xie (2008), applied genetic

algorithm (GA) to determine the minimum weight and annual cost for a finned tube heat exchanger designed using the LMTD method. They concluded that the GA optimization method offered a much better option for the design of ACHE rather that the traditional trial and error method, which had the tendency to produce values which aren't optimal. They also concluded that the objective function of heat exchanger optimization could be defined in terms of minimum surface area, or the minimum cost. Janiga, Nobile, Ranut and Thevenin (2014), studied the internal and external flows for heat exchanger bundles in cross flow. They used a multi-objective function method, which aimed to maximise the rate of heat transfer on the air-side of the heat exchanger as well as reduce pressure drop for flows on both sides of the heat exchanger. The fluid flow in the heat exchanger was simulated using ANSYS CFX, and then optimization carried out using two different genetic algorithms, non-dominated sorting genetic algorithm-II (NSGA-II) and FMOGA-III. Janiga, Hilbert, Nobile and Thevenin (2006), also demonstrated that CFD could be coupled to the optimization process, when they applied parallel genetic algorithm in an attempt to optimise the shape of an extended surface (blade) for a heat exchanger in order to maximise the heat transfer rate while minimizing the pressure loss across it.

'Overall' optimization has also been researched and has mostly been directed at the reduction of the total annual running costs for the ACHE. This form of optimization has been at the forefront of research and several correlations have been derived to identify the relationship between the several factors that make up the annual running cost equation. The analysis and optimization of any derived equation has been consistently considered in widely available literature and the reason for this, is obviously the cost saving benefits it provides to the consumer. Kashani, Hajabdollah, and Maddahi (2013), produced such an equation where the total annual running cost was expressed in the form below:

$$Co_{Tot} = \alpha Co_{INV} + Co_{OPE} + Co_{MAI} \qquad .119$$

$$\alpha = \frac{ir}{1 - (1 + ir)^{-y}}, ir \text{ and } y \text{ are interest rates and depreciation time}$$

Co_{INV} includes the investment cost for the HX bundle (Co_{HE}) and the fan operating system parts (Co_{FS}). Co_{MAI} is defined in terms of the annual maintenance costs associated with both the heat exchanger ($Co_{HE, MAI}$) and the fan ($Co_{FS, MAI}$). Finally, the HX operations cost (Co_{OPE}), is defined as the cost of energy required to induce a draft across the HX unit. The objective of their research was to simultaneously minimize two conflicting values, the temperature approach ($\Delta T_{approach} = T_{out, tube} - T_{in, air}$) of the two interacting fluids and the total annual running costs of the heat exchanger, whilst considering such decision variables as the tube ID & OD, tube length, number of tubes per row, etc. They recognised that the closer $\Delta T_{approach}$ got to a minimal value, the larger the ACHE required would become which then caused the final cost of the unit to rise. Results rightly predicted that tube

length, number of tubes per row, fin height, fin density, air velocity, fin thickness and tube ID & OD, caused the conflict between the objective functions. Using the non-dominated sorting genetic algorithm (NSGA) optimization technique, they were able to minimize these two constraints and obtain an optimum solution. Martin (1999) considered deriving a cost based equation of the form below, to predict the capital costs (C) associated with the ACHE:

$$C = C_1 + C_0 \qquad .120$$

C_1 accounts for the capital costs and C_o accounting for operations costs. He achieved his aim, by deriving the optimal value for the Reynolds number of fluid flow across the heat exchanger. He chose to optimize the Reynolds number because he discovered that the fluid flow velocity was proportional to the annual cost of investment (C_1, associated with the overall surface area of the ACHE) and the operating costs (C_0, associated with pumping fluid through the exchanger). Buys and Kroger, (1989) used the optimization technique, to determine the optimal dimensions for a finned tube bundle that would be installed in an existing cooling system using a cost structure of the form:

$$C_{ft} = \left[C_{wf}(C_t + C_f) + C_{fix} \right] L_t n_{tb} n_b \qquad .121$$

C_{wf} is defined as the weighting factor, C_t as cost per unit length of core tube, C_f as cost of fin material per unit length of tube, C_{fix} as the fixed cost per unit length of tube, L as tube length, n_{tb} as number of tubes in bundle and finally n_b as number of tube bundles. Caputo, Pelagagge and Salini (2016), developed a mathematical model for the cost estimation of shell and tube heat exchangers, based on the HXs geometrical features and manufacturing procedures for the subassembly parts that make up the heat exchanger.

The cost equation is of the form:

$$C_E = \sum_x \left(Cmat_x + \sum_{k=1}^{Nop} Cop_x \right) \qquad .122$$

$Cmat_x$, is defined as the cost estimate for the x-th subassembly material and $\sum_{k=1}^{Nop} Cop_x$, is defined as the cost estimate for the k-th manufacturing procedure needed for the x-th subassembly part. Hewitt and Pugh (2007), reviewed and presented work that had been conducted by ESDU 94043 (1994), for the costing of heat exchangers. They presented "data items" for the quick selection, sizing and costing for different heat exchangers at the initial stage of design. The costing method they examined, was for two-stream heat exchangers and is based on the use of a 'C' value, which is defined by $Q/\Delta T_m$. They explain that the use of the 'C' method provides a quick comparison between different heat exchangers without consideration for the total area of the unit 'A' and overall heat transfer coefficient 'U', two values which are directly linked and can prove quite difficult most times

to evaluate. ESDU 94043 (1994), provides a quick method for roughly estimating the cost of an ACHE based on the model:

$$C = C_t + C_M + C_L \quad .123$$

Where C_L accounts for labour costs, C_m accounts for acquiring/manufacturing items such as fans, structures, etc. and C_t refers to cost associated with acquiring heat exchanger tubes.

Unfortunately, the ESDU cost model and all the other cost models mentioned are hardly realistic in the real world. To support this argument, we examine the ESDU model; the C_L values used in the equation are based on labour costing codes proprietary to the company selected for the study. With the possibility of manufacturing cheaply abroad now available, labour costs will vary widely when compared across companies. Even when compared locally, costs will be seen to vary across the spectrum. Therefore, applying the C_L values provided will produce inaccurate results for another company. The model for C_t was based on a fixed set of design variables for the heat exchanger tube. The first variable was a 25.4mmOD with a fin pitch of 433 fins per meter and a fin OD of 57mm. The second design variable was based on a 19mm OD tube with a fin pitch of 430 fins per meter and fin OD of 38mm. Unfortunately, experience has shown that in certain cases, tubes can be pitched transversely from as low as 45mm, fin heights can range from 14mm to 16mm and fins per tube metre can range from 118 to 433, depending on the unit design. Certain SMEs sometimes go as far as 'gilling' their own heat exchanger tubes, which is the process of tension winding a metal strip around a tube, to form a spiral fin. The evaluation of C_t model has also been based on a constant heat exchanger tube length of 12.2m and a bare tube surface area of 25m^2 and above. Manufacturing experience has shown that handling difficulties can be experienced when heat exchanger tubes are longer than 6m. To solve this problem, designers would reduce the length of tube used, inadvertently increasing number of rows required in the heat exchanger. This means that the total surface area can sometimes be less or more than the 25m^2 used in the ESDU cost model. To be fair, ESDU, tested the effect of varying the tube type (extruded, & L-fin), tube length (1.65m, 3.05m, 6.1m, 9.1m and 15m) and noise reduction (75dBA) on the costing model. Unfortunately, they omitted testing the effect of varying the number of rows, as well as the tube fin pitch, both factors which add considerably to the final cost of an ACHE. Finally, the C_M model used in the model was also developed by a company selected for the study, so hardly applicable to other companies.

Overall, it was observed that the level of research into minimizing the costs associated with manufacturing (which will be of immense benefit to the manufacturer) has not been at the same level as that associated with minimizing the annual running costs of the heat exchanger (beneficial to only the end user/ client). When examined, the difference between the two cost structures is that for the end-user/client, the equation for the annual running costs of the ACHE will resemble the forms

detailed above and include such factors as the operating costs, investment costs, replacement costs etc. On-the-other hand for the small-to-medium scale (SME) designer/manufacturer, the cost equation will ultimately resemble the equation below:

$$C_{Total} = C_{Materials} + C_{Manufacturing} \qquad .124$$

$$C_{Manufacturing} = C_{Time} \; x \; C_{£/manpower \; (labour \; cost)}$$

Even if the cost models in the literature review could be proven to be beneficial to the SME designer/manufacturer, implementation in the design process can be far too complex for an SME with little or no experience in the use/ownership of the software upon which these cost models were developed. Hence the reason why this present study is being simulated using the GRG Non-Linear Solver available in Microsoft Excel. The Generalised Reduced Gradient (GRG) Non-Linear solution methods are examined in Appendix C.

5.4   Optimization Exercise:

1. **Project/Problem Description:** The project aim is to determine the optimum values for the design variables used in the thermal sizing of a circular-fin air-cooled heat exchanger (ACHE). These optimum values must be able to achieve all design requirements for the heat exchanger.

2. **Data and Information Collection**: Based on the overall heat transfer equation,

$$UA_{Total} = \frac{Q}{\Delta T_{LMTD}}$$

    The total heat transfer surface area of the heat exchanger A_{Total} is evaluated using the essential equations which comprise of the primary surface area, A_p (accounting for the surface area of the heat exchanger tubes) and the secondary surface area, A_f (accounting for the surface area of the fins). These two sub-equations (A_p & A_f) consist of design variables such as tube OD, fin OD, number of rows, fin thickness, transverse pitch, longitudinal pitch, etc. that directly influence the final size of the heat exchanger.

    The overall heat transfer coefficient, U, is evaluated using secondary equations which include the heat transfer correlation equations (gas and tube side), Reynolds number evaluation equations etc.

3. **Definition of Design Variables**: The design variables also referred to as the optimization variables, are a set of variables used to describe the geometrical characteristics of the heat exchanger. The design variables are split into two categories; **the independent and dependent variables**. Variables are described as "independent" when any initial numerical

value can be used to define them while on-the-other-hand, the value of a "dependent" variable is determined by a combination of two or more independent variables. Therefore, the values of the independent variables usually decide the final size of any designed heat exchanger unit. With respect to heat exchangers, the independent variables include: tube outer diameter, d_o, tube length, L_1, number of tube rows, N_r, Number of fins/metre, N_f, Transverse Pitch, X_t, Fin thickness, δ, stack height L_3 and Tube thickness, δ_t. While the dependent variables include: Longitudinal Pitch, X_l, Fin tip diameter d_f, Gas flow length or length of header L_2, etc.

Since the overall heat transfer surface area of the circular-fin type heat exchanger is a combination of the surface area of the fins and the surface area of the heat exchanger tubes, it is made up of both dependent and independent variables. In order to eliminate the influence of the dependent variables, the overall heat transfer surface equation has been reduced to its simplest form and the relationship between the independent and dependent variables established. The independent variables were then used to replace the dependent variables in the total surface area equation.

For a circular fin heat exchanger, the total surface area consists of the heat exchanger tubes & header plates (both making up the primary surface, A_p) and the fins (referred to as the secondary surface, A_f):

$$A_{Total} = A_p + A_f \quad .125$$

$$A_f = \left[\frac{2\pi(d_f^2 - d_0^2)}{4} + \pi d_f \delta\right] N_f L_1 N_t \quad .126$$

$$A_p = \pi d_0(L_1 - \delta N_f L_1)N_t + 2\left(L_2 L_3 - \frac{\pi d_0^2}{4} N_t\right) \quad .127$$

However,

$$d_f = (2h_f) + d_o \quad .128$$

$$X_l = 0.866 X_t \; (based \; on \; an \; equilateral \; tube \; pitch)$$

$$L_2 = (N_r \; x \; X_l) or \; (N_r \; x \; 0.866 X_t) \quad .129$$

$$N_t = \left[\frac{L_3}{X_t}\frac{L_2/X_l + 1}{2} + \left(\frac{L_3}{X_t} - 1\right)\frac{L_2/X_l - 1}{2}\right] or$$

$$\left[\left\{\frac{L_3}{X_t}\frac{((N_r \; x \; 0.866X_t)/0.866X_t) + 1}{2}\right\} + \left\{\left(\frac{L_3}{X_t} - 1\right)\frac{((N_r \; x \; 0.866X_t)/0.866X_l) - 1}{2}\right\}\right] or$$

$$\left[\left\{\frac{L_3}{X_t} x \frac{N_r + 1}{2}\right\} + \left\{\left(\frac{L_3}{X_t} - 1\right) x \frac{N_r - 1}{2}\right\}\right] or \; \frac{2L_3 N_r - N_r X_t + X_t}{2X_t} \quad .130$$

Therefore $A_f \; and \; A_p$ can be re-written to contain only the independent variables in the form:

62

$$A_f$$

$$= \frac{\left(8\pi h_f^2 N_r N_f L_3 L_1 + 8\pi h_f d_o N_f N_r L_3 L_1 + 8\pi \delta h_f N_f N_r L_3 L_1 + 4\pi \delta d_o N_f N_r L_3 L_1 - 4\pi h_f^2 N_f N_r L_1 X_t - 4\pi h_f d_o N_f N_r L_1 X_t - 4\pi \delta h_f N_f N_r L_1 X_t - 2\pi \delta d_o N_f N_r L_1 X_t + 4\pi h_f^2 N_f L_1 X_t + 4\pi h_f d_o N_f L_1 X_t + 4\pi \delta h_f N_f L_1 X_t + 2\pi \delta d_o N_f L_1 X_t\right)}{4X_t}$$

$$A_p = \frac{4\pi N_r d_o L_1 L_3 - 4\pi N_r \delta N_f L_1 L_3 d_o - 2\pi N_r X_t d_o L_1 + 2\pi d_o N_f N_r X_t \, \delta L_1 + 2\pi X_t d_o L_1 - 2\pi d_o X_t \delta N_f L_1 + 6.928 X_t^2 N_r L_3 - 2\pi d_o^2 N_r L_3 - \pi d_o^2 N_r X_t + \pi d_o^2 X_t}{4X_t} \qquad .132$$

4. **Optimization Criterion:** At this stage, we define the optimization criterion for the design, which ideally should be the objective of the whole process. The object function must be influenced directly or indirectly by the independent design variables stated at Step 3. Since the aim is to optimize the size of the heat exchanger, the objective in this instance would be the optimization of the total heat transfer surface area of the circular-fin heat exchanger. This must be achieved along with ensuring that the thermal conductance based on the operating conditions is at least equal to the thermal conductance achieved by a combination of the design variables.

$$UA_{required} = UA_{optimization}$$

5. **Operating conditions:** The same operating conditions used in the validation of the heat transfer correlations (refer to Chapter 4) for the circular fin heat exchanger, will be used to test the optimization process.

6. **Formulation of constraints**: Based on the operating conditions outlined in Step 5, the constraints placed on the objective function are defined and have to be satisfied by the optimization process. These constraints are tied in directly with the design variables outlined earlier in the overall heat transfer equation. These constraints are outlined below:

$$118 \leq N_f \leq 433$$
$$0.040m \leq X_t \leq 0.055m$$
$$0.9 \leq L_1 \leq 1m$$
$$2 \leq N_r \leq 6$$
$$0.014m \leq h_f \leq 0.016m$$
$$L_3 = 0.9m$$
$$\delta = 0.0007m$$
$$d_o = 26.7mm$$
$$UA = 3105$$

Results:

The optimization exercise began by running the GRG nonlinear solver within the boundaries outlined in section 6 above. Thereafter, the lower boundary constraint for the "number of fins" was shifted upwards to lessen the group size. The latter exercise was used to study the influence of boundary values or initialization variables on the results produced by the solver as well as compare any results with those produced by the "Sizing" option in the toolkit.

For each boundary, GRG non-linear solver found a solution for the overall heat transfer surface area equation to satisfy the thermal conductance requirement. The results obtained and presented in Table 20 – Table 24 shows that the "Sizing" design option in the toolkit accurately predicted the same results

as the GRG nonlinear solver. The tables show that the lower boundary of the number of fins per metre used in each calculation was increased from 118 fins per metre to 276 fins per metre, while the upper boundary was kept stable at 433 fins per metre. The largest deviation in total surface area was seen when the lower boundary was set at 197 fins per metre (Table 22). The deviation at this boundary peaked at 1.6% for the overall heat transfer surface area and 3% for the pressure drop. Thereafter it dropped to 1.5% (236 fins per metre) and 1.3% (276 fins per metre) respectively for the total heat transfer surface area. The pressure drops also dropped to 2.15% (236 fins per metre) and 1.6% (276 fins per metre) respectively afterwards.

Table 25 – Table 28 shows results for calculations when the lower boundary for the number of tube rows was moved from 2 to 4, while the upper boundary remained at 6 rows. For these calculations, the lower boundary for the number of fins per metre was also moved from 118 fins per metre to 276 fins per metre. The results again show that the "Sizing" toolkit accurately predicted the same results as the GRG non-linear solver. In this instance, the maximum deviation is seen when the lower boundary for the number of fins is 118 fins per meter where the "Sizing" results over-predict the overall heat transfer surface area and pressure drop by 1.9% and 1.72% respectively. Thereafter, the extent of deviation falls to as low as 1.6% and 0.5% for the overall heat transfer surface area and pressure drop respectively, when the number of fins per meter is 236 fins per meter.

Table 19: Conventional design results

Area ratio	1.12
Total Heat Transfer area, m^2	71
Number of rows	4
Number of fins/m	276
Tube length, m	1
Transverse pitch, m	0.055
Longitudinal pitch, m	0.05
Number of tubes	60
Heat duty, kW	100
Gas pressure drop, Pa	418

Table 20: Lower boundary: 118 fins/m

	GRG Non-linear solver	Toolkit Sizing
Area ratio	1.00	1.01
Total Heat Transfer area, m^2	33.84m^2	34.25 (1.2%)
Gas pressure drop, Pa	570	578.5 (1.5%)
Number of rows	3	3
Tube length, m	1	1
Transverse pitch, m	0.0405	0.0405
Longitudinal pitch, m	0.035	0.035
Number of tubes	66	66

Table 21: Lower boundary: 157 fins/m

	GRG Non-linear solver	Toolkit Sizing
Area ratio	1.00	1.01
Total Heat Transfer area, m^2	40.7	41.25 (1.3%)
Gas pressure drop, Pa	532	543 (2%)
Number of rows	3	3
Tube length, m	1	1
Transverse pitch, m	0.0429	0.43
Longitudinal pitch, m	0.037	0.037
Number of tubes	62	62
Heat duty, kW	100	100

Table 22: Lower boundary: 197 fins/m

	GRG Non-linear solver	Toolkit Sizing
Area ratio	1.00	1.01
Total Heat Transfer area, m^2	47.25	48 (1.6%)
Gas pressure drop, Pa	511	527 (3%)
Number of rows	3	3
Tube length, m	1	1
Transverse pitch, m	0.045	0.045
Longitudinal pitch, m	0.039	0.039
Number of tubes	60	60
Heat duty, kW	100	100

Table 23: Lower boundary: 236 fins/m

	GRG Non-linear solver	Toolkit Sizing
Area ratio	1.00	1.00
Total Heat Transfer area, m^2	53.3	54.1 (1.5%)
Gas pressure drop, Pa	501	512 (2.15%)
Number of rows	3	3
Tube length, m	1	1
Transverse pitch, m	0.047	0.047
Longitudinal pitch, m	0.041	0.041
Number of tubes	56	56
Heat duty, kW	100	100

Table 24: Lower boundary: 276 fins/m

	GRG Non-linear solver	Toolkit Sizing
Area ratio	1.00	1.01
Total Heat Transfer area, m^2	59.25	60 (1.3%)
Gas pressure drop, Pa	499	507 (1.6%)
Number of rows	3	3
Tube length, m	1	1
Transverse pitch, m	0.0489	0.0489
Longitudinal pitch, m	0.042	0.042
Number of tubes	54	54
Heat duty, kW	100	100

Table 25 – Table 29 show results for shifting the lower boundary for the number of tube rows from 2 – 4.

Table 25: Lower boundary: 118 fins/m

	GRG Non-linear solver	Toolkit Sizing
Area ratio	1.00	1.01
Total Heat Transfer area, m^2	38.26	39 (1.9%)
Gas pressure drop, Pa	371.5	378 (1.72%)
Number of rows	4	4
Tube length, m	1	1
Transverse pitch, m	0.0476	0.0476
Longitudinal pitch, m	0.041	0.041
Number of tubes	74	74
Heat duty, kW	100	100

Table 26: Lower boundary: 157 fins/m

	GRG Non-linear solver	Toolkit Sizing
Area ratio	1.00	1.01
Total Heat Transfer area, m^2	45.5	46.1 (1.3%)
Gas pressure drop, Pa	353	358 (1.4%)
Number of rows	4	4
Tube length, m	1	1
Transverse pitch, m	0.051	0.051
Longitudinal pitch, m	0.044	0.044
Number of tubes	69	69
Heat duty, kW	100	100

Table 27: Lower boundary: 197 fins/m

	GRG Non-linear solver	Toolkit Sizing
Area ratio	1.00	1.01
Total Heat Transfer area, m^2	52.49	53.16 (1.26%)
Gas pressure drop, Pa	343.67	347 (1%)
Number of rows	4	4
Tube length, m	1	1
Transverse pitch, m	0.054	0.054
Longitudinal pitch, m	0.047	0.047
Number of tubes	65	65
Heat duty, kW	100	100

Table 28: Lower boundary: 236 fins/m

	GRG Non-linear solver	Toolkit Sizing
Area ratio	1.00	1.01
Total Heat Transfer area, m^2	56.82	57.73 (1.6%)
Gas pressure drop, Pa	416.4	418.5 (0.5%)
Number of rows	4	4
Tube length, m	0.94	0.94
Transverse pitch, m	0.055	0.055
Longitudinal pitch, m	0.048	0.048
Number of tubes	65	64
Heat duty, kW	100	100

5.4   Conclusion:

The exercise conducted showed that both the GRG non-linear solver and the "Sizing" option in the toolkit could be used as cost saving tools in the design of heat exchangers. This cost saving is achieved by optimizing the initial geometrical design variables such that the final overall size of the heat exchanger matches the required thermal conductance.

The results from the GRG non-linear solver showed a higher degree of accuracy when the initialization variables were selected from within the upper and lower boundary limits. These results only differed from the "Sizing" option results by only as much as 1.6% for the overall surface area and 3% for the gas side pressure drop (197 fins per metre and 3 tube rows) and 1.9% for the overall surface area and 1.72% for the gas side pressure drop (118 fins per metre and 4 tube rows).

Unfortunately, although the GRG non-linear solver still converged when the initialization values were randomised or selected from outside the limit boundaries or design constraints, the results proved too inconsistent to be relied upon. As noted by Manassaldi et. al. (2013), the initialization values in any optimization problem, plays an important role in both convergence and accuracy of obtained results. They found this to be very important where the model size was large and included several non-linear constraints. The inconsistency of the GRG non-linear solver results with random initial values showed the solver cannot be relied on for day-to-day heat exchanger design.

On-the-other hand, the accuracy and consistency of the "Sizing" option in the toolkit in predicting the same results as the GRG non-linear solver when the initial values were within the boundary limits, demonstrates its reliability for day-to-day heat exchanger design.

Chapter 6

Conclusion and Recommendations

6.1   Introduction:

The final chapter provides inferences drawn from the entire toolkit development process, right from heat transfer correlation selection to the GUI development of the toolkit. Recommendations are also given that will increase the potential of the heat exchanger design toolkit.

6.2   Conclusion:

The aim of this project has been the development of a toolkit specifically for the design of air-cooled heat exchangers. The types of air-cooled heat exchangers considered were the circular fin, tube-in-plate and the plain tube heat exchanger. In order to perform these designs, heat transfer correlations for both the gas and tube side fluids had to be obtained from research data available in the public domain. Comparison of design results produced with these correlations showed various degrees of deviation from those produced with the industry standard software ASPEN-EDR. Aspects of the design results which were compared include: total heat transfer surface area, gas heat transfer coefficient, area ratio, tube side heat transfer coefficient, pressure drops, etc. The largest deviation was recorded in the design of the tube-in-plate heat exchanger, with a 14% over-prediction of the area ratio by the toolkit results compared to the ASPEN results. The least deviation was seen in the circular-fin where only a 6% over prediction was recorded. The results from the design of the plain tube heat exchanger, recorded a 7.5% and 8% over prediction by the toolkit for the staggered and inline arrangement respectively. The conclusion drawn from these results was that for any heat exchanger design where the geometrical characteristics and operating conditions stayed within the range specified in the publicly available heat transfer correlations, the final results were more likely to be accurate. Unfortunately, the extent of inaccuracy was not explored for conditions where the geometrical characteristics and operating conditions of the heat exchanger strayed outside the defined parameters.

In addition to the validation exercise described above, an attempt was made to incorporate overall heat transfer surface area optimization as part of the design capability of the toolkit. This design capability was referred to as "Sizing" and could be selected as a design option in the toolkit. When this option is selected, the designer is able to specify the minimum and maximum values along with desired increments for specific characteristics of the heat exchanger. Thereafter, the optimised solution produced by the toolkit will be based on a permutation and combination of these characteristics. In order to validate this functionality, an exercise was conducted which compared the results produced by Excel GRG nonlinear equation solver with those obtained from the toolkit. The results recorded showed that when the log mean temperature difference (LMTD) design method is used, the overall heat transfer surface area could be optimised to suit the required thermal conductance. The first validation exercise

showed the largest deviations recorded were 1.6% for the overall heat transfer surface area and 3% for the pressure drop at 197 fins per metre. While in the second exercise, the largest deviations recorded at 197f fins per meter, were 1.9% and 1.72% for the overall heat transfer surface and pressure drops respectively.

Development of the toolkit involved considering several programming languages such as C+, C++, Excel VBA and Java in terms of ease of use and accessibility. Excel Visual Basic for Applications (VBA) was finally selected because it could incorporate a graphic user interface (GUI) and also gave the developer, the freedom to modify the toolkit to suit the changing needs. Another reason for the selection of Excel VBA was that the Microsoft Office package which contains the Excel package is easily accessible and could be installed simultaneously on several computer systems. During its development, the toolkit went through several modifications before a final version was settled on. One such modification was the inclusion of heat transfer fluids such as Ethylene glycol, Transcal N, etc. in the list of available fluids.

6.3   Recommendations:

To determine the convective heat transfer coefficients, correlations were used which covered only a certain range of data. This in itself presents a problem which must be resolved if a high level of result accuracy is desired for any thermal design where the initial parameters lie outside of the specified range. Consideration should be given to developing heat transfer correlations that are adaptable to any geometrical dimensions and operating conditions.

The design toolkit is currently only capable of rating and sizing air-cooled heat exchangers. Its further development is encouraged to the point where it is capable of producing CAD drawings of the heat exchanger as well as complete material and labour costs needed to manufacture the heat exchanger. These additional features will save the time devoted to these separate activities as well as give the designer a feel for how the heat exchanger will look after manufacture and also what final costs will most likely be, especially if he is working on a tight budget

The capability of the design toolkit should be extended to sizing and rating other types of heat exchangers such as shell & tube, Plate, serpentine coils etc. This capability, will give the designer greater freedom to choose the best kind of heat exchanger that suits his process conditions.

The design toolkit has been developed using Excel Visual Basic for Applications (VBA), which is a widely available Microsoft based software package. However, not all computers run on the Microsoft Operating System. This means that any potential user of the toolkit must have a system running on the Microsoft OS. It is recommended that the toolkit is developed as a stand-alone version. This means that afterwards, the toolkit can be installed on virtually any computer system.

References

1. M. S. Bhatti and R. K. Shah, 1987, Turbulent and transition convective heat transfer in ducts, in Handbook of Single-Phase Convective Heat Transfer, S. Kakaç, R. K Shah, and W. Aung, eds., Wiley, New York, Chap. 4.

2. D. E. Briggs and E. H. Young, 1963, Convection heat transfer and pressure drop of air flowing across triangular pitch banks of finned tubes, Chem. Eng. Prog. Symp. Ser. 41, Vol. 59, pp. 1-10.

3. A. P. Colburn,1933, A method of correlating forced convection heat transfer data and a comparison with fluid friction, Trans. Am. Inst. Chem. Eng., Vol. 29, pp. 174 – 210; reprinted in Int. J. Heat Mass Transfer , Vol. 7, pp. 1359 – 1358, 1964

4. F. W. Dittus, and L.M.K Boelter, 1930, Heat transfer in automobile radiators of tubular type, University of Calif. Publications in Engineering, Vol. 2, pp. 443 – 461

5. Engineering Services Data Unit (ESDU, 86022), 1988, High-fin staggered tube banks: heat transfer and pressure drop for turbulent single phase gas flow.

6. S. G. Kandilikar, 1991, development of a flow boiling map for sub-cooled and saturated flow boiling of different fluids in circular tubes, ASME J. Heat Transfer, Vol. 113, pp. 190 – 200

7. S. G. Kandilikar, M. Shoji, and V. K. Dhir, eds., 1999, Handbook of Phase Change: Boiling and Condensation, Taylor & Francis, New York

8. W. Kays and, A.L. London, 1984, Compact heat exchangers. 3rd edition, McGraw-Hill.

9. H. Martin, 2002, The generalized Lévêque equation and its practical use for the prediction of heat and mass transfer rates from pressure drop, Chem. Eng. Sci., Vol. 57, pp. 3217 – 3223.

10. K. K. Robinson and D. E. Briggs, 1966, Pressure drop of air flowing across triangular pitch banks of finned tubes, Chem. Eng. Prog. Symp. Series 64, Vol. 62, pp. 177 – 184.

11. M. M. Shah, 197S.E7, a general correlation for heat transfer during sub-cooled boiling in pipes and annuli, ASHRAE Trans., Vol. 83, No. 1, pp. 205 – 215; also, M. M. Shah, 1982, Chart correlation for saturated boiling heat transfer: equations and further study, ASHRAE Trans., Vol. 88, No. 1, pp. 85 – 196.

12. C. C. Wang, and K. U. Chi, 2000, Heat transfer and friction characteristics of plain fin-and-tube heat exchangers; Part 2; Correlation, Int. J. Heat Mass Transfer, Vol. 43, pp. 2692 – 2700.

13. A. Žukauskas, 1987, Convective heat transfer in cross flow, Handbook of Single-Phase Convective Heat Transfer, S. Kakac¸, R. K. Shah, and W. Aung, eds., Wiley, New York, Chap. 6.

14. S.W. Robert, G. T. Lestina, Air-Cooled Heat Exchangers, 2014, Process Heat Transfer (Second Edition), Academic Press, pp. 509 – 553.

15. A.D. Kraus, A. Aziz and J. Welty, 2001, Extended Surface Heat Transfer. New York: Wiley.

16. A. E. Bergles, 1998, Handbook of Heat Transfer, 3rd edition, 1998. McGraw-Hill, New York, NY, USA

17. A. E. Bergles, 2001, "The implications and challenges of enhanced heat transfer for the chemical process industries," Chemical Engineering Research and Design, Vol. 79, no. 4, pp. 437 – 444.

18. E. I. Nesis, A. F. Shatalov, and N. P. Karmatskii, 1994 "Dependence of the heat transfer coefficient on the vibration amplitude and frequency of a vertical thin heater," Journal of Engineering Physics and Thermophysics, vol. 67, no. 1-2, pp. 696–698.

19. J. K. Hagge and G. H. Junkhan, 1975, "Experimental study of a method of mechanical augmentation of convective heat transfer in air," Tech. Rep. HTL3, ISU-ERI-Ames-74158, Iowa State University, Amsterdam, The Netherlands.

20. M. Siddique, A.R.A. Khaled, N. I. Abdulhafiz, and A.Y. Boukhary, 2010, International Journal of Chemical Engineering, Vol. 2010, pp. 1-28. Hindawi Publishin Corporation.

21. J. C. Choi and S. D. Kim, 1992 "Heat-transfer characteristics of a latent heat storage system using MgCl2· 6H2O," *Energy*, vol. 17, no. 12, pp. 1153–1164.

22. B. Horbaniuc, G. Dumitrascu, and A. Popescu , 1999, "Mathematical models for the study of solidification within a longitudinally finned heat pipe latent heat thermal storage system," Energy Conversion and Management, vol. 40, no. 15, pp. 1765–1774.

23. Y. Zhang and A. Faghri, 1996, "Heat transfer enhancement in latent heat thermal energy storage system by using the internally finned tube," International Journal of Heat and Mass Transfer, vol. 39, no. 15, pp. 3165–3173.

24. F. Agyenim, P. Eames, and M. Smyth, 2009, "A comparison of heat transfer enhancement in a medium temperature thermal energy storage heat exchanger using fins," *Solar Energy*, vol. 83, no. 9, pp. 1509–1520.

25. K. J. Bell and A. C. Mueller, 2001. Wolverine Engineering Data Book II. Wolverine Tube, Inc; www.wlv.com.

26. Minton PE. Heat exchanger design, 1991. In: McKetta JJ, editor. Heat Transfer Design Methods. New York: Marcel Dekker.

27. H. Hamakawa, K. Nakashima, T. Kudo, E. Nishida, T. Fukano, (2008), Vortex shedding from a circular cylinder with spiral fin, J. Fluid Sci. Technol. 3 (6) 787–795.

28. E. Naess, 2010, Experimental investigation of heat transfer and pressure drop in serrated-fin tube bundles with staggered tube layouts, Appl. Therm. Eng. 30 1531–1537.

29. A. Nuntaphan, T. Kiatsiriroat, C.C. Wang, 2005, Air side performance at low Reynolds number of cross-flow heat exchanger using crimped spiral fins, Int. Commun. Heat Mass Transfer 32 (1–2) 151–165.

30. L.H. Tang, M. Zeng, Q.W. Wang, 2009, Experimental and numerical investigation on air-side performance of fin-and-tube heat exchangers with various fin patterns, Exp. Therm. Fluid Sci. 33 818–827.

31. P. Pongsoi, S. Pikulkajorn, S. Wongwises, 2012, Experimental study on the air-side performance of a multipass parallel and counter cross-flow L-footed spiral fin-and-tube heat exchanger, Heat Transfer Eng. 33 (15) 1–13.

32. P. Pongsoi, P. Promoppatum, S. Pikulkajorn, S. Wongwises, 2013, Effect of fin pitches on the air-side performance of L-footed spiral fin-and-tube heat exchangers, Int. J. Heat Mass Transfer 59 75–82

33. P. Kiatpachai, S. Pikulkajorn, S. Wongwises, 2015, Air-side performance of serrated welded spiral fin-and-tube heat exchangers, Int. J of Heat and Mass Transfer, Vol. 89. Pp. 724-732

34. B. Anoop, C. Balaji, K. Velusamy, 2015, A characteristic correlation for heat transfer over serrated finned tubes, Annals of Nuclear Energy Vol. 85, pp. 1052 – 1065

35. D.H. Lee, J.M Jung, J.H Ha, Y.I.Cho, 2012, Improvement of heat transfer with perforated circular holes in finned tubes of air-cooled heat exchanger, Int. communications in heat and mass transfer, vol. 39, issue 2, pp. 161 – 166

36. M. Lee, T. Kang, Y. Joo, Y. Kim, (2011), Heat transfer characteristics of spirally-coiled circular fin-tube heat exchangers operating under frosting conditions, Int. J of Refrigeration, Vol. 34, issue 1, pp. 328 – 336

37. F. McQuiston, D.R. Tree, Optimum space envelopes of the finned tube heat transfer surface, 1972, ASHRE Trans., Vol. 78, Part II, pp. 144 – 152.

38. A. Zukauskas, 1981, Air-cooled heat exchangers. In Heat exchangers: thermal-hydraulic fundamentals and design, eds. S.Kakac, A.E.Bergels and F.Mayinger, McGraw-Hill, 1981

39. Z. Lin, C. Liu, M. Lin, L. Wang, 2015, Numerical study of flow and heat transfer of circular tube bank fin heat exchanger with curved delta-winglet vortex generators, Applied thermal engineering, 88, pp. 198 – 210

40. C.C. Wang, Y.J Chang, Y.C. Hsieh, Y.T. Lin, 1996, Sensible heat and friction characteristics of plate fin-and-tube heat exchangers having plane fins, Int. J. Refrig. Vol. 19, No. 4, pp. 223 – 230

41. D.G. Rich, 1973, The effect of fin spacing on the heat transfer and friction performance of multi-row plate fin-and-tube heat exchangers, ASHRAE Trans. Vol. 79(2), pp.137 – 145

42. D.G. Rich, 1975, The effect of number of tube rows on heat transfer performance of smooth plate fin-and-tube heat, ASHRAE Trans, 81(1), pp. 307 - 317

43. J. Jang, M. Wu, W. Chang, 1996, Numerical and experimental studies of three-dimensional plate-fin and tube heat exchangers, Int. J. Heat Mass Transfer, Vol. 39, No. 14, pp 3057 – 3066

44. M. Abu Madi, R.A. Johns, M.R. Heikal, 1998, Performance characteristics correlation's for round tube and plate finned heat exchangers, Int. J. of Refrigeration, Vol. 21, Issue 7, pp. 507 – 517

45. A. Joardar and A.M. Jacobi, 2006, A numerical study of flow and heat transfer enhancement using an array of delta-winglet vortex generators in a fin-and-tube heat exchanger, J. Heat Transfer 129(9), pp. 1156 – 1167

46. A. Joadar and A.M. Jacobi, 2008, Heat transfer enhancement by winglet-type vortex generator arrays in compact plain-fin-and-tube heat exchangers. Int. J. of Refrigeration Vol. 31, Issue 1, pp. 87 – 97

47. A.I. ElSherbini, A.M. Jacobi, 2011, The thermal-hydraulic impact of delta-wing vortex generators on the performance of a plain fin-and-tube heat exchanger. HVAC & R Research, Volume 8, Issue 4.

48. C.C. Wang, W.L. Fu, C.T. Chang, 1997, Heat transfer and friction characteristics of typical wavy fin-and-tube heat exchangers, Exp. Thermal Fluid Sci., Vol. 14(2), pp. 174 – 186

49. C.C. Wang, Y.J. Du, Y.J. Chang, W.H. Tao, 1999, Airside performance of herringbone fin-and-tube heat exchangers in wet conditions, Canadian J. Chemical Engineering, Vol. 77 (6), pp. 1225 – 1230

50. W.M. Yan, P. J. Sheen, 2000, Heat transfer and friction characteristics of fin-and-tube heat exchangers, Int. J. Heat Mass Transfer, Vol. 43, pp. 1651-1659

51. R. Shah, (1975), Perforated heat exchanger surfaces, Part 2 – Heat transfer and flow friction characteristics, ASME Paper 75

52. J.P.Holman, 1992, Heat Transfer, 7th Edition, McGraw-Hill International (UK) Limited.

53. E.N. Sieder, C.E. Tate, 1936, Heat transfer and pressure drop of liquids in tubes, Ind. Eng. Chem., vol. 28, p. 1426.

54. B.S. Petukhov, 1970, Heat transfer and friction in turbulent pipe flow with variable physical properties. Advances in Heat Transfer, Academic Press, vol. 6, pp. 503-564.

55. V. Gnielinski, 1976. New equations for heat and mass transfer in turbulent pipe and channel flow. Int. Chem. Eng., vol. 16, No. 2, pp. 359-366.

56. S.W. Churchill, 1977. Comprehensive correlating equation for heat, mass and momentum transfer in fully developed flow in smooth tubes. Ind. Eng. Chem. Fundam., vol. 16, No. 1, pp. 109-116.

57. R.K. Shah, M.S. Bhatti, 1987, Handbook of single phase convective heat transfer, Chapter 4, John Wiley.

58. W.H. Giedt, 1949, Investigation of variation of point unit-heat-transfer coefficient around a cylinder normal to an air stream, Trans ASME, VOL. 71, PP. 375-381.

59. E.R.G. Eckert, R.M. Drake, 1972, Analysis of Heat and Mass Transfer, McGraw-Hill Book Company, New York.

60. S.W. Churchill, M. Bernstein, 1977. A correlating equation for forced convection from gases and liquids to a circular cylinder in cross flow, J, Heat Transfer, vol. 99, pp. 300-306.

61. S. Nakai, T. Okazaki, 1975, Heat transfer from a horizontal circular wire at small Reynolds and Grashof numbers – 1 pure convection, Int. J. Heat Mass Transfer, vol. 18, pp. 387.

62. C.C. Wang, Y.C. Hsieh, Y.T. Lin, 1997, Performance of Plate Finned Tube Heat Exchangers under Dehumidifying Conditions, J. Heat Transfer. Vol. 119, pp. 109 – 117

63. E.S. Gaddis, V. Gnielinski, 1985, Pressure drop in cross flow across tube bundles, Int. Chem. Eng., Vol. 25, pp. 1 – 15.

64. Engineering Services Data Unit (ESDU, 73031), 1973, Convective heat transfer during crossflow of fluids over plain tube banks.

65. R.K. Shah, D.P. Sekulic, 2003, Fundamentals of Heat Exchanger Design. John Wiley & Sons Inc. Hoboken, New Jersey. USA.

66. R.J Goldstein, W.E. Ibele, S.V Patantar, T.W Simon, T.H. Kuehn, P.J.Strykowski, K.K. Tamma, J.V.R. Heberlein, J.H. Davidson, J.Bischof, F.A. Kulacki, U. Kortshagen, S. Garrick, V. Srininvasan, 2006, Heat Transfer – A review of 2003 Literature, Int. J of Heat and Mass Transfer, Vol. 49, Issue 3 – 4, pp. 451 – 534.

67. R.J Goldstein, W.E. Ibele, S.V Patantar, T.W Simon, T.H. Kuehn, P.J.Strykowski, K.K. Tamma, J.V.R. Heberlein, J.H. Davidson, J.Bischof, F.A. Kulacki, U. Kortshagen, S. Garrick, V. Srininvasan, K. Ghosh, R. Mittal, 2010, Heat Transfer – A review of 2005 Literature, Int. J of Heat and Mass Transfer, Vol. 53, Issue 21 – 22, pp. 4397 – 4447.

68. R.J Goldstein, W.E. Ibele, S.V Patantar, T.W Simon, T.H. Kuehn, P.J.Strykowski, K.K. Tamma, J.V.R. Heberlein, J.H. Davidson, J.Bischof, F.A. Kulacki, U. Kortshagen, S. Garrick, V. Srininvasan, 2005, Heat Transfer – A review of 2002 Literature, Int. J of Heat and Mass Transfer, Vol. 48, Issue 5, pp. 819 – 927.

69. R.J Goldstein, E.R.G. Eckert, S.V Patantar, T.W Simon, T.H. Kuehn, P.J.Strykowski, K.K. Tamma, J.V.R. Heberlein, J.H. Davidson, J.Bischof, F.A. Kulacki, U. Kortshagen, S. Garrick, 2003, Heat Transfer – A review of 2001 Literature, Int. J of Heat and Mass Transfer, Vol. 46, Issue 11, pp. 1887 – 1992.

70. R.J Goldstein, E.R.G. Eckert, S.V Patantar, T.W Simon, T.H. Kuehn, P.J.Strykowski, K.K. Tamma, A. Bar-Cohen, W.E.Ibele, J.V.R. Heberlein, J.H. Davidson, J.Bischof, F.A. Kulacki, U. Kortshagen, S. Garrick, 2001, Heat Transfer – A review of 1999 Literature, Int. J of Heat and Mass Transfer, Vol. 44, Issue 19, pp. 3579 – 3699.

71. R.J Goldstein, E.R.G. Eckert, S.V Patantar, T.W Simon, T.H. Kuehn, P.J.Strykowski, K.K. Tamma, A. Bar-Cohen, W.E. Ibele, J.V.R. Heberlein, J.H. Davidson, J.Bischof, F.A. Kulacki, U. Kortshagen, 1999, Heat Transfer – A review of 1995 Literature, Int. J of Heat and Mass Transfer, Vol. 42, Issue 15, pp. 2717 – 2797.

72. R.J Goldstein, E.R.G. Eckert, S.V Patantar, T.W Simon, T.H. Kuehn, P.J.Strykowski, K.K. Tamma, A. Bar-Cohen, W.E.Ibele, J.V.R. Heberlein, J.H. Davidson, J.Bischof, F.A. Kulacki, U. Kortshagen, D.L. Hofeldt, K.A. Stelson, 1996, Heat Transfer – A review of 1993 Literature, Int. J of Heat and Mass Transfer, Vol. 39, Issue 5, pp. 885 – 963.

73. R.J Goldstein, E.R.G. Eckert, S.V Patantar, T.W Simon, T.H. Kuehn, P.J.Strykowski, K.K. Tamma, A. Bar-Cohen, W.E.Ibele, J.V.R. Heberlein, J.H. Davidson, J.Bischof, F.A. Kulacki, U. Kortshagen, S.

Garrick, 2001, Heat Transfer – A review of 1998 Literature, Int. J of Heat and Mass Transfer, Vol. 44, Issue 2, pp. 253 – 366.

74. R.J Goldstein, E.R.G. Eckert, S.V Patantar, T.W Simon, T.H. Kuehn, P.J.Strykowski, K.K. Tamma, A. Bar-Cohen, W.E.Ibele, J.V.R. Heberlein, J.H. Davidson, J.Bischof, F.A. Kulacki, U. Kortshagen, S. Garrick, 2000, Heat Transfer – A review of 1997 Literature, Int. J of Heat and Mass Transfer, Vol. 43, Issue 14, pp. 2431 – 2528.

75. R.J Goldstein, E.R.G. Eckert, S.V Patantar, T.W Simon, T.H. Kuehn, P.J.Strykowski, K.K. Tamma, A. Bar-Cohen, W.E.Ibele, J.V.R. Heberlein, J.H. Davidson, J.Bischof, F.A. Kulacki, U. Kortshagen, S. Garrick, 2000, Heat Transfer – A review of 1996 Literature, Int. J of Heat and Mass Transfer, Vol. 43, Issue 8, pp. 1273 – 1371.

76. R.J Goldstein, E.R.G. Eckert, S.V Patantar, T.W Simon, T.H. Kuehn, P.J.Strykowski, K.K. Tamma, A. Bar-Cohen, W.E.Ibele, J.V.R. Heberlein, J.H. Davidson, J.Bischof, F.A. Kulacki, U. Kortshagen, D.L. Hofeldt, 1997, Heat Transfer – A review of 1994 Literature, Int. J of Heat and Mass Transfer, Vol. 40, Issue 16, pp. 3729 – 3804.

77. R.J Goldstein, E.R.G. Eckert, S.V Patantar, T.W Simon, T.H. Kuehn, E. Pfender, H.O. Lee, S.L. Girshick, W.E.Ibele, 1987, Heat Transfer – A review of 1986 Literature, Int. J of Heat and Mass Transfer, Vol. 30, Issue 12, pp. 2449 – 2523.

78. R.J Goldstein, E.R.G. Eckert, S.V Patantar, T.W Simon, T.H. Kuehn, P.J.Strykowski, K.K. Tamma, A. Bar-Cohen, W.E.Ibele, J.V.R. Heberlein, J.H. Davidson, K.A. Stelson, D.L. Hofeldt, 1994, Heat Transfer – A review of 1992 Literature, Int. J of Heat and Mass Transfer, Vol. 37, Issue 9, pp. 1285 – 1375.

79. R.J Goldstein, E.R.G. Eckert, S.V Patantar, T.W Simon, T.H. Kuehn, E. Pfender, N. Decker, D.L. Hofeldt, 1984, Heat Transfer – A review of 1983 Literature, Int. J of Heat and Mass Transfer, Vol. 27, Issue 12, pp. 2179 – 2214.

80. H.A. Ibrahim, 2012, Fouling in Heat Exchangers, MATLAB – A Fundamental Tool for Scientific Computing and Engineering Applications, Vol. 3, Prof. Vasilios Katsikis (Ed.), InTech.

81. BCS Incorporated, 2008, Waste Heat Recovery: Technology and Opportunities in U.S. Industry, U.S Department of Energy Industrial Technologies Program.

82. The Future of Heating: A strategic framework for low carbon heat in the UK, 2012, Department of Energy & Climate Change.

83. MCP – 1159: Heat exchangers: A Global Strategic Business Report
http://www.strategyr.com/pressMCP-1159.asp

84. D.W. Green, R.H. Perry, 2008, Perry's Chemical Engineer's Handbook. 8th Edition. McGraw-Hill New York. USA.

85. A.A Bhuiyan, A.K.M. Sadrul Islam, 2016, Thermal and hydraulic performance of finned-tube heat exchnagers under different flow ranges: A review of modelling and experiment. Int. J of Heat and Mass Transfer, 101, pp. 38 – 59.

86. R.K.Shah, 1985, Compact heat exchangers, in Handbook of Heat Transfer Application, 2nd ed. W.M. Rohsenow, J.P. Hartnett, and E.N. Ganic, eds., McGraw-Hill, New York., pp. 4 – 174 to 4 – 311.

87. Engineering Services Data Unit (ESDU, 92003), 1993, Forced convection heat transfer in straight pipes. Part 1: turbulent flow.

88. Engineering Services Data Unit (ESDU, 98003), 1998, Design and performance evaluation of heat exchangers: The effectiveness – NTU method. Part 1: Introduction

89. A.R Doodman, M. Fesanghary and R. Hosseini, 2009, A robust stochastic approach for design optimization of air cooled heat exchangers. Applied Energy 86, pp. 1240 – 1245.

90. J.I. Manassaldi, N.J. Scenna and S.F. Mussati, 2014, Optimization mathematical model for the detailed design of air cooled heat exchangers. Energy 64, pp. 734 – 746.

91. M.R. Salimpour, Z. Bahrami, 2011, Thermodynamic analysis and optimization of air cooled heat exchangers. Heat Mass Transfer 47, pp. 35 – 44.

92. S.W. Stewart, S.V. Shelton and K.A. Aspelund, 2005, Finned tube heat exchanger optimization methodology. Heat Transfer Engineering 26(7) pp. 22 – 28.

93. V.I. Evenko, 2002, Optimizing air cooled heat exchanger tube bundle parameters Vol. 38, Nos. 1–2.

94. H. Qiao, V. Singh, V. Aute and R. Radermacher, 2010, Optimization of fin density for air cooled heat exchanger. International Refrigeration and air conditioning conference, 2313 pp. 1 – 8.

95. M. Cavazzuti, M.A. Corticelli, 2008, Optimization of heat exchanger enhanced surfaces through multi-objective genetic algorithms. Numerical Heat Transfer, Part A, 54, pp. 603 – 624.

96. G. Xie, Q. Wang and B. Sunden, 2008, Application of a genetic algorithm for thermal design of fin-and-tube heat exchangers. Heat Transfer Engineering 29(7) pp. 597 – 607.

97. P. Ranut, G. Janiga, E. Nobile and D. Thevenin, 2014, Multi-objective shape optimization of a tube-bundle in cross-flow. International Journal of Heat and Mass Transfer Engineering 68 pp. 585 – 598.

98. R. Hilbert, G. Janiga, E. Nobile and D. Thevenin, 2006, Multi-objective shape optimization of a heat exchanger using parallel genetic algorithms. International Journal of Heat and Mass Transfer Engineering 49 pp. 2567 – 2577.

99. A.H.A. Kashani, A. Maddahi, and H. Hajabdollahi, 2013, Thermal-economic optimization of an air-cooled heat exchanger unit. Applied Thermal Engineering 54 pp. 43 – 55.

100. H. Martin, 1999, Economic optimization of compact heat exchangers. EF-Conference on compact heat exchangers and enhancement technology for the process industries, Banff, Canada, July 18-23, 1999.

101. J.D. Buys, D.G. Kroger, 1989, Dimensioning heat exchangers for existing dry cooling towers. Energy Conversion Management Vol. 29, No. 1, pp. 63 – 71.

102. A.C Caputo, P.M. Pelagagge and P. Salini, 2016, Manufacturing cost model for heat exchangers optimization. Applied Thermal Engineering 94, pp. 513 – 533.

103. M. Cavazzuti, M.A. Corticelli, 2008, Optimization of heat exchanger enhanced surfaces through multi-objective genetic algorithms. Numerical Heat Transfer, Part A, 54, pp. 603 – 624.

104. G.F. Hewitt, S.J.Pugh, 2007, Approximate design and costing methods for heat exchangers. Heat Transfer Engineering, 28(2), pp. 76 – 86.

105. Engineering Services Data Unit (ESDU, 94043), 1994, Selection and costing of heat exchangers, Air-cooled type.

106. D.G., Rich, June 24 – 28, 1973, paper presented at the ASHRAE Annual Meeting, Louisville, Kentucky, USA.

107. HTFS – ZM1, 1980, Pressure drop of air through tube-in-plate heat exchangers.

108. HTFS – ZM2, 1979, Convective heat transfer of air through tube-in-plate heat exchangers.

109. B., Cox, 1973, Performance of compact heat transfer surfaces – finned & bare tube banks. Union Carbide Corporation, Nuclear Division, Oak Ridge Gaseous Diffusion Plant, Oak Ridge, Tennessee USA.

110.   M.A., RUSSELL, and M.J.N., WILLS, 1983, "The development of a friction factor relationship for crossflow bypass", AERE-R 11154

111.   PFR Engineering Systems, Inc., 1976, "Heat transfer and pressure drop characteristics of dry tower extended surfaces. Part II: Data analysis and correlations." BNWL-PFR-7-102, PFR Inc., Marina del Rey, California, USA

112.   HTFS – SM3, 1984, Friction Pressure Drop for plain tube banks in crossflow with or without bypassing.

113.   HTFS – SM4, 1992, Crossflow heat transfer on a bank of tubes. First published January, 1985

114.   Engineering Sciences Data Unit, 1980, Crossflow pressure loss over banks of plain tubes in square and triangular arrays including effects of flow direction.

115.   H., Brauer, 1961, Chemie-Ing-Tech, 33, Part II, 431 – 438

116.   H., Brauer, 1961, Kaltetchnik, 13 Jahrgang, Heft 8, 274 – 279

117.   T.C., Carnavos, 1958, U.S. Department of Commerce Clearing House, Report No. AECU-3970

118.   S.L., Jameson, 1945, Trans. ASME, No. 67, 633 – 642,

119.   Z., Mirkovic, (1974), "Heat Exchangers: Design and Theory Source Book". By Afgan and Schlunder, McGraw-Hilll Book Co. Chapter 20.

120.   K.K., Robinson, and D.E., Briggs, 1965, AIChE, Eighth National Heat Transfer Conference

121.   C., Weirman, J., Taborek, and W.J., Marner, 1975 paper presented at the 15th National Heat Transfer Conference, San Francisco.

122.   D.J., Ward, and E.H., Young, 1959, CEP Symposium, Series No. 29, Vol. 55, 37.

123.   A., Kenbar, 2005, Performance characteristics of staggered finned-tube bundles with small fin tip gap, RS1171.

124.   S.R., Mcilwain, A., Kenbar, and T., Brisbane, 2002, HTFS3: Improvements to HTFS2 method for heat transfer and pressure drop in staggered arrangement of plain high finned tubes, RS1118.

125.   T., Ralston, R. K., Byskov, P. E., Farrant, C. M., Chu, 1997, 'HTFS Models for Heat transfer and pressure drop applied to staggered arrangements of tubes with plain helical fins', HTFS RS1016

126.   T., Ralston, C. M., Chu, 1998, 'HTFS2: Improved models for heat transfer and pressure drop applied to staggered arrangements of tubes with plain helical fins', HTFS RS1036.

127.   C., Weierman, 1976, Correlations ease the selection of finned tubes, Oil and Gas Journal, September, 1976.

Appendix A

Heat Exchanger Design

Introduction:

The aim of this chapter is to describe the process of heat exchanger design. It begins by introducing the concept of heat transfer and how it occurs. It further describes the 3 main modes through which most heat transfer process occurs and the equations which govern the transfer process. It goes on to give a description of the broken down methodology for complete heat exchanger design. The thermal and hydraulic section under the design methodology is then further expanded to describe the thermal design process using the Log Mean Temperature Difference (LMTD) and ε-NTU methods for heat transfer analysis in heat exchangers. The types of fluid flow arrangement and their impact on the heat transfer process is discussed and the final section is dedicated to describing the meaning of thermal conductance (UA) and how it can be adapted to simplify the heat exchanger design process.

Modes of Heat Transfer:

Heat being a form of energy, means it can be transferred from one location to the other as long as a temperature gradient exists. The main modes through which this transfer occurs are listed and described below:

○ **Conduction:**

Conduction heat transfer is prevalent within a solid body in which a temperature gradient already exists. This allows the heat energy travel from a high temperature region to a lower temperature region, mostly with negligible movement of the particles making up the body. This form of heat transfer is described by Fourier's law; which states that the rate of heat flow is directly proportional to the temperature gradient in that direction and to the area normal to the flow.

$$Q = -kA\frac{\partial T}{\partial x} \ or \ q = -k\frac{\partial T}{\partial x} \quad .133$$
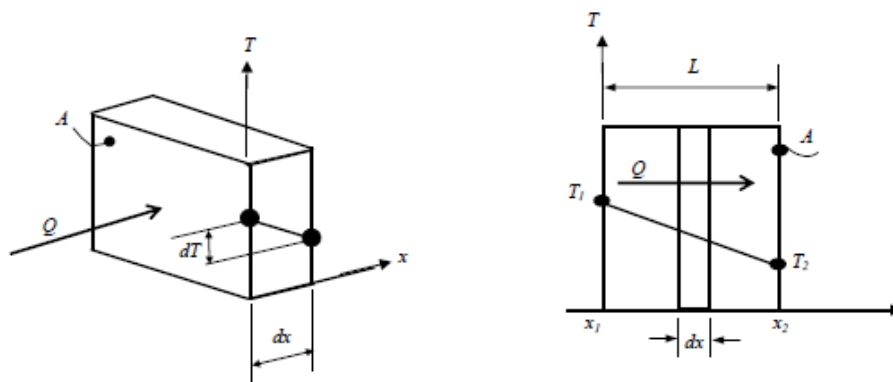

Figure 21: Conduction heat transfer through a plane wall

Q or q in the equation represents the heat transfer rate, $\frac{\partial T}{\partial x}$ represent the temperature gradient in the direction of heat flow; k represents the thermal conductivity of the body/material and the negative sign indicates that the second law of thermodynamics which states that heat is transferred in the direction of decreasing temperature, is satisfied. It is assumed that the transfer process happens under steady state conditions, which means that the temperature at each point in the body is invariant with time; hence; $\frac{\partial T}{\partial x} = 0$. It is also assumed that the heat travels in one-dimension and temperature is uniform in directions perpendicular to this direction; $\frac{\partial T}{\partial y} = \frac{\partial T}{\partial z} = 0$.

When heat travels in the x direction, $T = T(x)$ and Fourier's equation becomes:

$$Q = -kA \frac{dT}{dx} \qquad .134$$

Considering a plane wall of thickness L, and elemental thickness; dx,

$$q = -k \frac{dT}{dx} \ or \ qdx = -kdT \quad .135$$

When integrated between the limits of x and T, the equation takes on the form,

$$q(x_2 - x_1) = \int_{T_2}^{T_1} k \ dT \quad .136$$

Assume the thermal conductivity; k is constant across the material,

$$qL = k(T_1 - T_2) \ or \ q = \frac{k(T_1 - T_2)}{L} \quad .137$$

$$Q = \frac{kA \ (T_1 - T_2)}{L} \quad .138$$

For a multi-layered wall,

$$Q = \frac{k_1 A \ (T_1 - T_2)}{L_1} = \frac{k_2 A \ (T_2 - T_3)}{L_2} = \frac{k_3 A \ (T_3 - T_4)}{L_3} \quad .139$$

Where $k_1, k_2 \ and \ k_3$ represent the thermal conductivities of the wall layers. Rearranging the equation yields:

$$\frac{QL_1}{k_1 A} = T_1 - T_2 \quad .140$$

$$\frac{QL_2}{k_2 A} = T_2 - T_3 \quad .141$$

$$\frac{QL_3}{k_3 A} = T_3 - T_4 \quad .142$$

If these are added and T_2, T_3 are eliminated:

$$T_1 - T_4 = Q\left(\frac{L_1}{k_1 A} + \frac{L_2}{k_2 A} + \frac{L_3}{k_3 A}\right) \qquad .143$$

$$Q = \frac{T_1 - T_4}{\Sigma L / kA} = \frac{T_1 - T_4}{\Sigma R} \qquad .144$$

Where ΣR represents the sum of the resistances: $L_{1,2\,\&\,3}/k_{1,2\&3}A$

For a cylinder or pipe, where $Area = 2\pi r L$:

$$Q = -k\,(2\pi r L)\frac{dT}{dr} \qquad .145$$

Integrating between the limits,

$$Q\,ln\frac{r_2}{r_1} = 2\pi kL(T_1 - T_2) \qquad .146$$

With respect to thermal resistance;

$$R = \frac{ln\frac{r_2}{r_1}}{2\pi kL}\frac{K}{W} \qquad .147$$

o **Convection:**

Convection heat transfer is used to describe the heat transferred between a fluid in motion and any surface it is in contact with it as long as they at different temperatures. A boundary layer is formed between the surfaces with temperature and velocity varying within the boundary, in comparison to that in the bulk of the fluid. Any resistance to heat transfer therefore, will be due to conditions generated in this boundary layer. In turbulent flow, two further sub-layers are formed across the bounding surface.

Figure 22: Boundary layer formed by fluid flow over a flat smooth surface
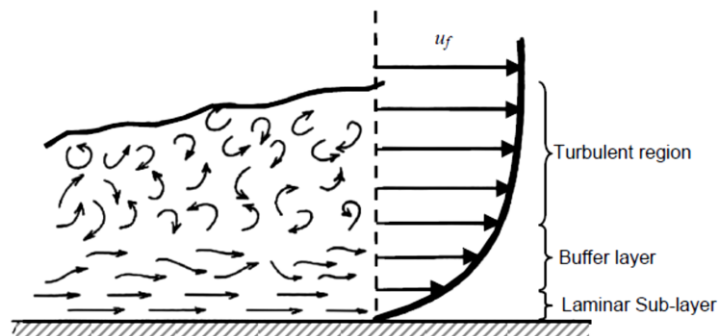
The first layer referred to as the laminar layer, sits at the bottom of the two layers; this layer is usually in direct contact with the bounding surface. The next layer is the buffer layer, across which the nature of flow changes from laminar to turbulent. Heat transfer occurs via conduction from the fully turbulent layer to the interacting surface through

the buffer and laminar layers. It then follows that turbulence or the disruption within these layers, greatly enhances the ease with which heat is transferred.

Convection heat transfer is categorized based on the nature of flow of the fluid moving across the interacting surface. In natural convection heat transfer, the nature of this flow is governed by density differences caused by temperature variations in the bulk of the fluid. While in the forced convection heat transfer, an external mechanical means such as a fan or pump is used to generate turbulence in the fluid.

To evaluate the heat transferred in convection, Newton's law of cooling equation is used.

$$Q = hA(T_s - T_f) \qquad .148$$

Where h refers to the convection heat transfer coefficient. This value (convection heat transfer coefficient) $'h'$ is evaluated from the factors which affect the extent to which heat is transferred. Based on the condition of flow (natural or forced), these factors will vary.

In forced convection heat transfer, these factors include: surface geometry or dimension $'l'$, flow velocity $'v'$, fluid viscosity $'\mu'$, fluid thermal conductivity $'k'$, fluid specific heat capacity $'Cp'$, and fluid density $'\rho'$. Using dimensional analysis to derive a relationship between these factors,

$$h = \phi l^b v^a k^c \mu^i Cp^j \rho^n \qquad .149$$

Where $'\phi'$ represents the dimensionless factor and $'a''b''c'' i'' j'$ and $'n'$ represent the dimensionless exponents. Solving the equation using the primary dimensions: mass (M), length (L), time (t), temperature (T) and heat (H), gives:

$$\frac{hl}{k} = \phi\left(\frac{\rho vl}{\mu}\right)^n \left(\frac{\mu Cp}{k}\right)^j \qquad .150$$

If a function $'f'$ is used,

$$\frac{hl}{k} = f\left(\frac{\rho vl}{\mu}, \frac{\mu Cp}{k}\right) \qquad .151$$

$$Nu = f(Re, Pr) \qquad .152$$

Where:

$$Nusselt\ number, Nu = \frac{hl}{k} \qquad .153$$

$$Reynolds\ number, Re = \frac{\rho vl}{\mu} \qquad .154$$

$$Prandtl\ number, Pr = \frac{\mu Cp}{k} \qquad .155$$

Experimental data for forced convection heat transfer $'h'$ is thus expressed in the form of these parameters.

For natural convection heat transfer, velocity is excluded from equation above, as flow is dependent on the buoyancy forces acting within the fluid. To account for the buoyancy forces acting per unit volume, the temperature difference between a warm fluid with density ρ and an undisturbed cold fluid ρ_f is used and often designated as ΔT.

$$g(\rho_g - \rho) = \rho\beta g\Delta T \qquad .156$$

$$coefficient\ of\ cubical\ expansion, \beta = \frac{\rho_f - \rho}{\rho(T - T_f)} \qquad .157$$

Therefore, the dimensional relations for natural heat transfer convection can be written as:

$$h = \phi\Delta T^a l^b k^c \mu^i Cp^j \rho^n (\rho\beta)^p \qquad .158$$

Solution of the equation, using the primary dimensions: mass (M), length (L), time (t), temperature (T), and heat (H) yields:

$$\frac{hl}{k} = \phi\left(\frac{\beta g\Delta T l^3 \rho^2}{\mu^2}\right)^p \left(\frac{\mu Cp}{k}\right)^j \qquad .159$$

Where the function f is used,

$$\frac{hl}{k} = f\left(\frac{\beta g\Delta T l^3 \rho^2}{\mu^2}, \frac{\mu Cp}{k}\right) \qquad .160$$

$$Nu = f(Gr, Pr) \qquad .161$$

Where:

$$Nusselt\ number, Nu = \frac{hl}{k} \qquad .162$$

$$Grashof\ number, Gr = \frac{\beta g(T_s - T_f)l^3 \rho^2}{\mu} \qquad .163$$

$$Prandtl\ number, Pr = \frac{\mu Cp}{k} \qquad .164$$

Experimental data for natural convection heat transfer $'h'$ is expressed in the form of these parameters.

o **Radiation**

Also referred to as thermal radiation, is the form of heat transfer that occurs via electromagnetic waves when a temperature difference occurs within a vacuum. The

rate of emission from such a body referred to as a "Black-body", is described in the equation below, and referred to as the Stefan-Boltzmann law of thermal radiation:

$$q_{emitted} = \sigma A T^4 \qquad .165$$

Where σ is a constant of proportionality and referred to as the Stefan-Boltzmann constant with a value equivalent to 5.669 x 10^{-8} W/m^{2}K^4. This equation applies only to black-bodies, which are described as perfect radiation absorbers and emitters.

For the heat transmitted and exchanged between two bodies:

$$\frac{q_{net\ exchange}}{A} \propto \sigma\left(T_1^4 - T_2^4\right) \qquad .166$$

Considering that not all bodies are entirely 'black', a factor referred to as the emissivity factor is introduced. Consideration must also then be given to the fact that emitted radiation can be lost to the environment during transmission. Therefore, the final heat transfer equation thus becomes:

$$q = F_\epsilon F_G \sigma A\left(T_1^4 - T_2^4\right) \qquad .167$$

Where F_ϵ is the emissivity function and F_G is the geometric view factor function. These two values differ across body configurations and must thus be determined before an accurate value for radiation heat transfer can be determined.

Heat Exchanger Design Methodology:

Heat exchanger design is based on an iterative process due to the several operational conditions which must all be satisfied before assurance is given that the exchanger will do the required duty. Kays and London (1984) [8] broke the steps required for the optimum design of heat exchangers into the following based on the figure below:
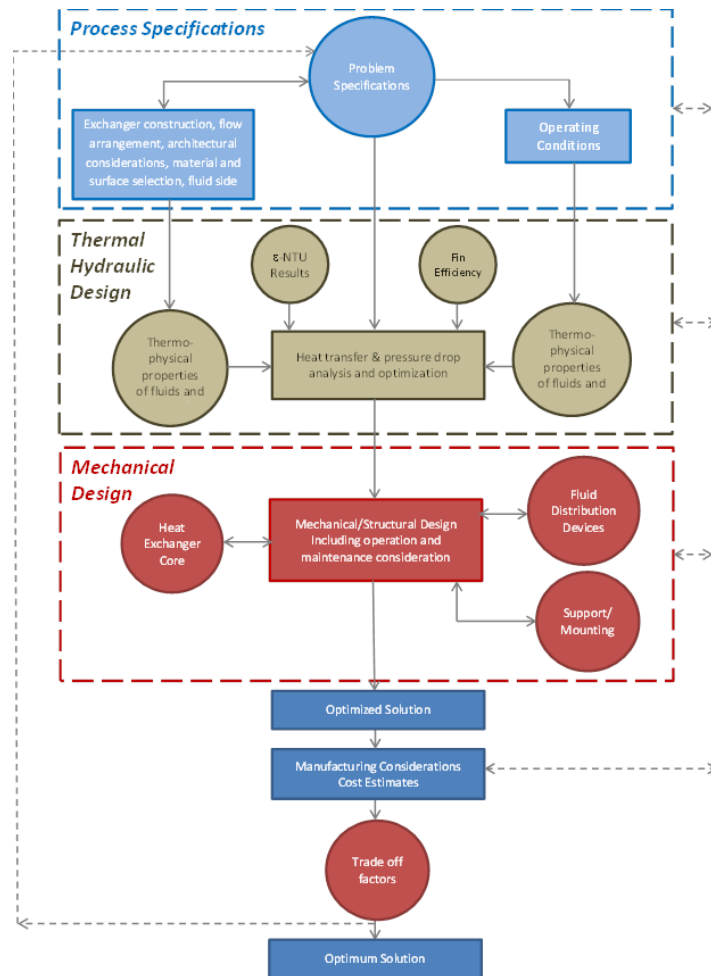
Figure 23: Heat exchanger design methodology (Shah & Sekulić, 2003)

o **Process and Design specification**: this stage accounts for all the initial information/process conditions which will enable the thermal engineer gain a good understanding of the requirements of the heat exchanger yet to be designed. Process specifications usually include mass flow rates of the interacting fluids, temperatures, pressure drops, supply pressures, allowable pressure drops, corrosiveness and fouling characteristics of interacting fluids, etc. This information will enable the engineer decide the heat exchanger best suited for the process (shell & tube, plate, extended surface etc.), flow arrangements, materials etc.

o **Thermal and hydraulic design:** involves using either of the two equations below to evaluate the heat duty requirements of the heat exchanger.

$$q = m_{1 \ or \ 2} \ x \ \Delta h_{1 \ or \ 2} \qquad .168$$

$$q = UA\Delta T_m \qquad .169$$

Equation 168, referred to as the enthalpy rate equation evaluates heat duty based on change in enthalpy of a bulk fluid moving through the heat exchanger under isobaric conditions. If the fluid is in its single phase, the heat duty is computed using:

84

$$q = mC_{p_{1\ or\ 2}}\Delta T_{1\ or\ 2,\ inlet\ \&\ outlet} \qquad \cdot 170$$

Equation 169, evaluates heat transfer based on the different heat transfer modes (conduction, convection and radiation) prevalent in the heat exchanger. The heat transferred, is seen to be directly proportional to the area, A, and mean temperature difference of the interacting fluids ΔT_m. The mean temperature difference in this case, refers to the mean temperature difference of the interacting fluids, based on their entry and exit temperatures. The factor 'U' is defined as the overall heat transfer coefficient which accounts for the different heat transfer methods occurring in the heat exchanger. Within the thermal and hydraulic design block, several subsets of design parameters are required to produce an appropriate design solution. These subsets include: surface heat transfer and flow friction characteristics, geometrical properties and thermophysical properties of the fluids.

o **Mechanical design:** Mechanical design of heat exchangers ensures that the units are structurally stable under specified operational conditions. These conditions include: steady-state, start-up, shutdown or even earthquake conditions. Each section of the heat exchanger undergoes a mechanical assessment to determine its behaviour under these conditions. For example, the thermal stress developed in the heat exchanger as a result of the changes in temperature of the interacting fluids, will be determined as part of the mechanical design process to ensure that the tubes, nozzles and headers can bear the thermal stress developed. If mechanical bonding techniques such as brazing or welding are used, the joints under question must be assessed to ensure they can bear the loads generated in the heat exchanger to avoid failure during operation. Several international codes and standards such as the ASME pressure vessel codes, Specification for unfired fusion welded pressure vessels (PD5500) are available solely for this purpose.

o **Manufacturing considerations and cost:** During design, consideration must be given to method of manufacture. Design complexity will determine if new tools are needed, all which must be available before manufacturing can begin. Lead times, quality control and availability of workshop staff are lumped into factors which must be considered in this phase. Costs associated with a heat exchanger must also be considered. These costs include: capital, installation, operating and in some cases, disposal.

o **Trade-off factors and system-based optimization:** As a result of the iterative process involved in heat exchanger design, trade-offs are inevitable at the design stage. An example is where a heat transfer fluid such as Ethylene Glycol is added to water as anti-freeze. This process ensures the frost protection of pipes but however reduces the heat

transfer capability of the fluid and also adds to the pumping requirements of the system. Another example is the use of stainless steel for the manufacture of heat exchangers meant for use in corrosive operating environments. Stainless steel will always be the preferred construction material to mild steel even though it is more expensive and has lesser heat conducting capabilities than mild steel.

An optimized heat exchanger design therefore constitutes a balance of all the quantitative and qualitative factors mentioned above.

Thermal & Hydraulic Design:

Flow arrangements:

The arrangement/alignment of flow of the interacting fluids plays a vital role in the heat transferred across the heat exchanger as research has shown that certain arrangements have more merits than other arrangements. Flow arrangement therefore plays a role in the design of heat exchangers and must be considered and agreed on before design commences. Arrangements include:

-   Counter-current or Counter-flow: this arrangement sees the interacting fluids flow past each other in parallel but opposite directions. If temperature variation is assumed to occur entirely in one dimension, then counter-current flow is considered the most efficient in transferring heat across interacting fluids when compared to all other flow arrangements [Ref. (65)]. They also describe this arrangement as one where the least thermal stress is produced in the tube wall when compared to other flow arrangements. The figure below shows the direction heat flow occurs for such flow arrangements:

Figure 24: Temperature flow in single-phase counterflow arrangement heat exchanger with no boiling or condensation (Shah & Sekulić, 2003).

-   Parallel or Co-current flow: in this flow arrangement, the interacting fluids are introduced into the heat exchanger from the same direction and also tend to exit the heat exchanger in the same direction. Figure 25 shows how heat is transferred in a heat exchanger with such a fluid flow arrangement. This flow arrangement is described as the flow arrangement with the poorest effectiveness amongst single

86

pass heat exchangers for all considered cases of overall thermal conductance, heat capacity rates and flow inlet temperatures [Ref. 65]. It further explains that even lower effectiveness is experienced in multi-pass heat exchangers with parallel or concurrent flow. Another disadvantage is that a large temperature gradient exists at the tube inlet between the hot and cold fluids, and thus has the high potential of introducing thermal stresses at the location. However, despite its poor qualities, the parallel flow arrangement has advantages that make it useful for certain heat transfer applications. They include:

- o For nucleate boiling applications, they are able to initiate the boiling process a lot quicker than other arrangements.

- o Maximum wall temperatures produced in this arrangement is lower than that produced in the counter-current flow arrangement for the same number of transfer units (NTUs), thermal capacity ratio and flow inlet temperatures. This thus eliminates the possibilities of fouling or fluid decomposition.

- o Parallel flow arrangements allow for a more even temperature distribution along the tube wall. This advantage has found usefulness in the design of heat exchangers with temperature sensitive materials or extremely viscous liquids.

- o Minimum wall temperatures produced, is still higher than that produced by other flow arrangements for the same number of transfer units (NTUs), thermal capacity ratio and flow inlet temperatures even though its overall heat exchanger effectiveness is low. This arrangement therefore minimises the possibility of condensation if the fluid is composed of corrosive vapours or where it is possible that the warmer fluid might lose so much heat as to freeze.
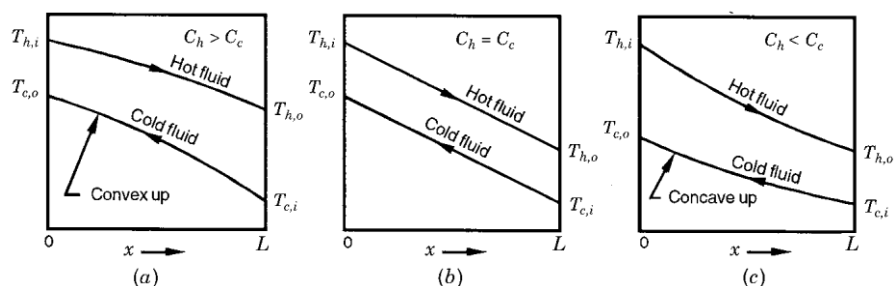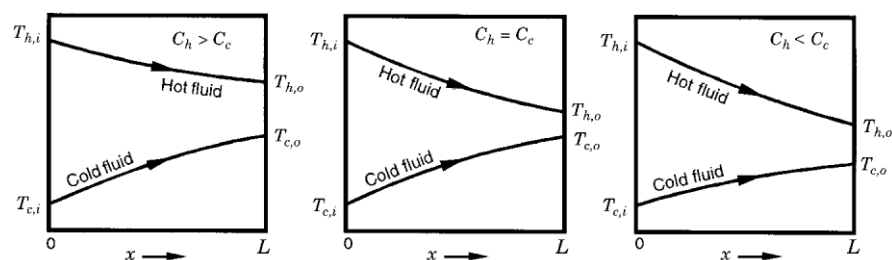

Figure 25: Temperature flow in a single-phase parallel flow arrangement heat exchanger with no boiling or condensation (Shah & Sekulić, 2003).

- Cross flow: in this heat exchanger flow arrangement, the interacting fluids flow perpendicular to each other. The thermal effectiveness of this type of arrangement is described as being between that of the parallel and counter-current flow arrangements [65]. The cross flow arrangement is the most common arrangement for extended surface heat exchangers because

headers can be used as the inlet and outlet of the tube-side fluid, while the second fluid referred to as the gas-side fluid flows across the tubes.
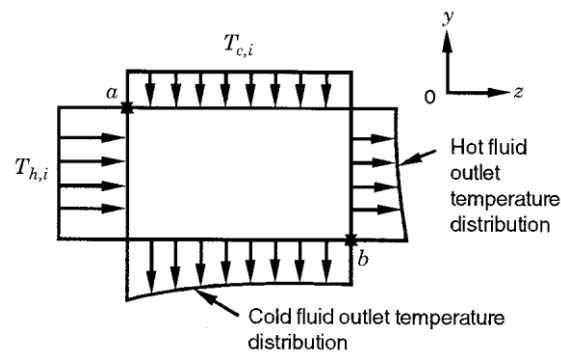
Figure 26: Temperature flow at the inlet and outlet of an unmixed-unmixed crossflow arrangement heat exchanger (Shah & Sekulić, 2003).

The cross flow arrangement further introduces the concept of mixed or unmixed flows for both fluid streams. The tube-side or gas-side fluid is considered completely mixed when a temperature gradient ceases to exist within the fluid. When either fluid is unmixed, there exists a temperature gradient in at least one direction perpendicular to the flow of the fluid. In the case of multiple row heat exchangers, the tube-side fluid is completely mixed in the headers. However, when they split and flow into individual tubes, they are considered to be unmixed. The presence of extended surfaces can also introduce an unmixed flow arrangement for the gas-side fluid especially where plates are used for extended surface purposes. Several other fluid combinations exist: unmixed – mixed, both fluids mixed, both fluids unmixed, partially unmixed – partially mixed and mixed – partially mixed.
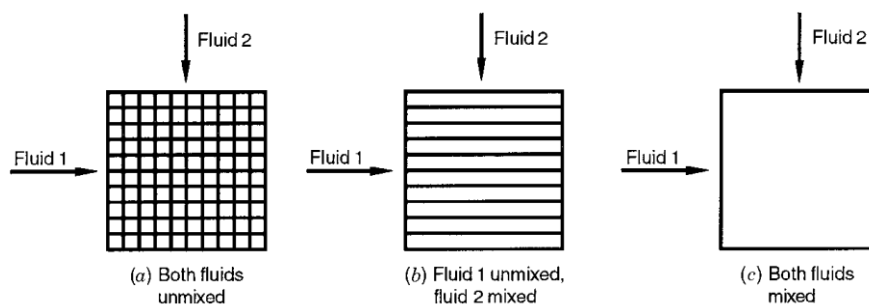
Figure 27: Types of mixing in crossflow heat exchanger (Shah & Sekulić, 2003).

Other flow arrangements exist which include; Divided-flow TEMA J Shell, Split-Flow TEMA G Shell. However, these are common to shell and tube heat exchangers and will thus not be considered.

Design theories:

Several thermal design theories are available for the design of heat exchangers, e.g. the ε-NTU method, the P-NTU method, the LMTD method, the $P_1 - P_2$ method and the $\psi - P$ method [Ref. 65]. However, only the first three methods listed were studied during the design stage of the toolkit. Each of these

theories comes with its own merits and demerits. Only the LMTD method and the ε-NTU method will be discussed due to their specific application to the design of extended surface heat exchangers.

The validity of the ε-NTU and the LMTD method theories are based on a number of assumptions which are outlined below:

- o The heat exchanger operates solely under steady-state conditions. Flow rates and fluid temperatures are constant and are independent of time.

- o There are no heat energy sources or sinks in either the interacting fluids or the heat exchanger walls.

- o Heat loss to surroundings is negligible.

- o Fluid temperatures are uniform across the heat exchanger cross-section in both counterflow and parallel flow conditions. This means that within the heat exchanger, there is prefect transverse mixing and no temperature gradient normal to the direction of flow.

- o Thermal resistances in the tube walls are distributed uniformly in the heat exchanger.

- o Phase change does not occur in any of the fluids. If it does occur, it does under constant temperature conditions, same as a single-component fluid at constant pressure.

- o Longitudinal heat conduction both in the fluids and heat exchanger walls are negligible.

- o Overall heat transfer coefficients are constant throughout the heat exchanger. Independent of temperature, position or time. This requirement also applies to phase-changing fluids.

- o The specific heat capacity for each fluid is constant through the heat exchanger.

- o For extended surfaces, the surface efficiency of the extended surface is constant and uniform.

- o The heat transfer surface area A of the heat exchanger is distributed uniformly on each fluid side regardless of single or multi-pass arrangements.

- o Fluid velocities and temperatures at entry on each fluid side, is uniform across the heat exchanger cross-section. Uneven fluid distribution does not occur.

- o Rate of fluid flow is distributed uniformly in the heat exchanger for each fluid. No flow bypassing, leaks or flow stratification occurs in the unit. Flow conditions are characterized by mean or bulk velocities at any cross-section.

However, It must be stated that in cases where the fluids on both sides of heat exchanger walls are in two-phase states, then these assumptions are rendered invalid as a result of the mass transfer that occurs which will invariably change the thermal properties, flow rates and heat transfer coefficients of the interacting fluids.

1. **Log Mean Temperature Difference (LMTD):**

Considering the energy equation of Eqn. 169, the temperature difference between the interacting fluids will vary between the inlet and the outlet of the heat exchanger. Therefore an average value must be used for calculation purposes. Using the parallel flow heat exchanger as an example, the heat transfer equation for an elemental section can be represented in a form similar to Eqn. 38 as:

$$d_q = -m_h c_h dT_h = m_c c_c dT_c \qquad .171$$

$$dT_h = -\frac{dq}{m_h c_h} \qquad .172$$

$$dT_c = \frac{dq}{m_c c_c} \qquad .173$$

$$dT_h - dT_c = d(T_h - T_c) = -dq\left(\frac{1}{m_h c_h} + \frac{1}{m_c c_c}\right) \qquad .174$$

Solving for dq and substiuting the equation above,

$$\frac{d(T_h - T_c)}{(T_h - T_c)} = -U\left(\frac{1}{m_h c_h} + \frac{1}{m_c c_c}\right)dA \qquad .175$$

Integrating between the two conditions,

$$ln\frac{T_{h2} - T_{c2}}{T_{h1} - T_{c1}} = -UA\left(\frac{1}{m_h c_h} + \frac{1}{m_c c_c}\right) \qquad .176,$$

Further expressing $m_h c_h$ & $m_c c_c$ in the form of heat transferred,

$$m_c c_c = \frac{q}{T_{h1} - T_{h2}} \ or \ m_h c_h = \frac{q}{T_{c2} - T_{c1}}, \qquad .177$$

Substituing in equation 37,

$$\frac{q}{UA} = \frac{(T_{h2} - T_{c2}) - (T_{h1} - T_{c1})}{ln((T_{h2} - T_{c2}/(T_{h1} - T_{c1}))} \qquad .178$$

The RHS of Eqn. 178 can also be re-written in the form of Eqn. 179 and is referred to as the Log Mean Temperature Difference (LMTD).

$$\Delta T_{LMTD} = \frac{\Delta T_2 - \Delta T_1}{ln\frac{\Delta T_2}{\Delta T_1}} \qquad .179$$

The values ΔT_2 and ΔT_1 represent the temperature difference of the interacting fluids at each end of the heat exchanger in either parallel or counter current flow conditions.

For counter current flow:

$$\Delta T_2 = T_{h,i} - T_{c,o} \qquad .180$$

$$\Delta T_1 = T_{h,o} - T_{c,i} \qquad .181$$

For parallel or co-current flow:

$$\Delta T_2 = T_{h,i} - T_{c,I} \qquad .182$$

$$\Delta T_1 = T_{h,o} - T_{c,o} \qquad .183$$

The LMTD method assumes as stated above, that the overall heat transfer coefficient is constant along the flow length of the heat exchanger and that the specific heat capacities of the fluids does not change with temperature. To apply the LMTD method in the design of all other flow arrangements, the counter current flow equation for temperature difference is used because it provides the designer with the maximum temperature change possible in the heat exchanger. The log mean correction factor 'F' is then applied to account for deviations from the pure counter current flow arrangement. This works by comparing the ratio of heat transfer in the given heat exchanger to the heat transferred in a pure counter current flow arrangement with the same thermal capacity ratios and fluid exit temperatures. When the 'F' value is close to 1, it does not mean that the exchanger is highly effective (a counter current exchanger gives the maximum heat transferable in the unit), it simply means that its performance is close to the performance of a pure counter current exchanger operating under the same conditions:

$$Q = FUA\Delta T_{LMTD} \ or \ F = \frac{Q}{UA\Delta T_{LMTD}} \qquad .184$$

The correction factor 'F' is dimensionless, and is dependent on the heat capacity ratio 'C*$_{1\ or\ 2}$(R)', flow arrangement and the temperature effectiveness 'R$_{1\ or\ 2}$ (P)' of the heat exchanger. The equations below describe its relationship to these three factors:

$$F = f_1\big(C_{1,}^* R_1\big) = f_1\big(C_{2,}^* R_2\big) - for \ stream \ symmetric \ heat \ exchnager \qquad .185$$

$$F = f_1\big(C_{1,}^* R_1\big) = f_2\big(C_{2,}^* R_2\big) - for \ stream \ asymmetric \ heat \ exchnager \qquad .186$$

As a result of these dependent factors, 'F' is found to vary widely for even the same heat exchanger manufactured under different process conditions.

Table 29 below gives explicit equations for evaluating 'F' based on the flow arrangement, temperature effectiveness 'R$_{1\ or\ 2}$ (P)' and the heat capacity ratio 'C*$_{1\ or\ 2}$(R)'

Table 29:

Flow arrangement	Equation
Counter current flow	F = 1
Parallel or co-current flow	F = 1

Cross flow (single-pass):	
- Hot fluid unmixed, cold fluid mixed, with stream asymmetric	$$F = \frac{ln[(1 - C_1^*P_1)/(1 - P_1)]}{(C_1^* - 1)\ ln[1 + (1/C_1^*)\ ln(1 - C_1^*P_1)]}$$ $$= \frac{ln[(1 - C_1^*P_2)/(1 - P_2)]}{(1 - 1/C_2^*)\ ln[1 + C_2^* ln(1 - P_2)]}$$
- Hot fluid mixed, cold fluid unmixed, with stream asymmetric	$$F = \frac{ln[(1 - C_2^*P_2)/(1 - P_2)]}{(C_2^* - 1)\ ln[1 + (1/C_2^*)\ ln(1 - C_2^*P_2)]}$$ $$= \frac{ln[(1 - C_1^*P_1)/(1 - P_1)]}{(1 - 1/C_1^*)\ ln[1 + C_1^* ln(1 - P_1)]}$$

Where explicit equations are not available, graphs are provided, and Fig. 28 [84] below gives an example of such a graph provided for the selection of the appropriate correction factor, *'F'*.
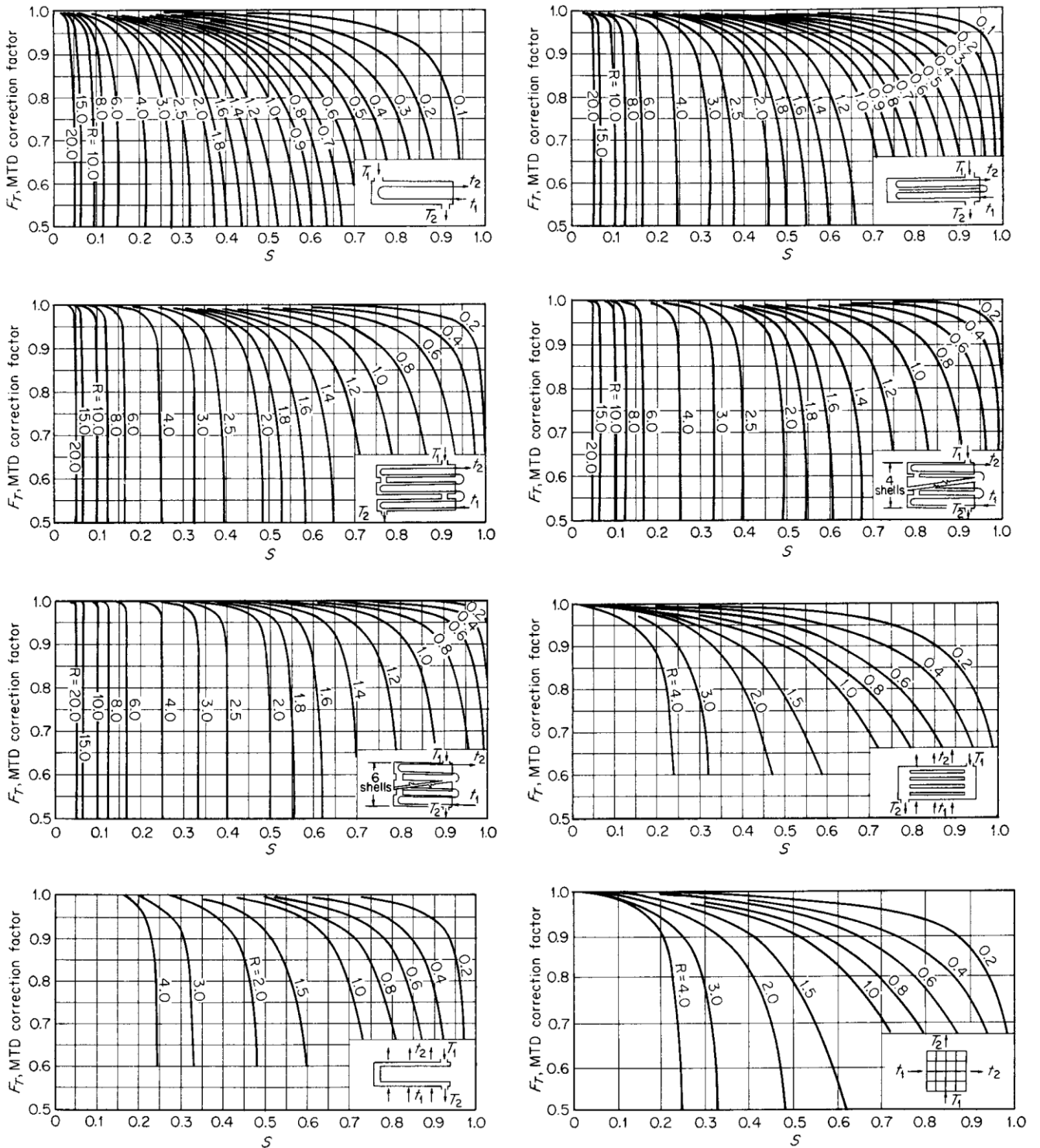
Figure 28: LMTD correction factors for heat exchangers (Source: Green & Perry, 2008)

When the temperature values for the interacting fluids is constant as seen in phase change conditions, or the thermal capacity ratio C* = 0:

$$F = 1 \qquad .187$$

2. Effectiveness and Number of Transfer Units (ε-NTU):

The **ε-NTU** design process is designed to enable the designer assess the capability of one or more heat exchangers to deliver a desired duty. This analysis is accomplished using 3 non-dimensional factors referred to as:

- o   Thermal Effectiveness, $\in$
- o   The Number of heat transfer units, NTU, and
- o   Thermal capacity ratio, C^*

Thermal Effectiveness $\in$:

$$\in = \frac{actual\ heat\ transfer}{maximum\ possible\ heat\ transfer} = \frac{q}{q_{max}} \qquad .188$$

The value $\in$ is the value of the ratio of actual heat transfer in the heat exchanger and the maximum heat transfer possible based on process conditions. This ratio can also be said to provide the designer with information related to the thermal performance of the heat exchanger unit when compared to the performance of a counter-current heat exchanger operating under equivalent conditions. In the counter-current flow arrangement described earlier, the maximum heat energy transferrable is only limited by the fluid with the lesser thermal capacity and the difference between the inlet temperatures of the interacting fluids, which is theoretically, the maximum temperature change possible in the unit. Therefore, Eqn. 56 can also be rearranged in the form:

$$q = \epsilon C_{min}(T_{h,i} - T_{c,i}) = \epsilon C_{min}\Delta T_{max} \qquad .189$$

Where

$$C_{min} = min\left[(\dot{m}C_p)_h, (\dot{m}C_p)_c\right], \ \Delta T_{max} = (T_{h,i} - T_{c,i})$$

$$q_{max} = C_{min}(T_{h,i} - T_{c,i}) \qquad .190$$

Considering the heat balance for a hot – cold fluid stream interaction, the energy equation can also be represented as:

$$Q = (\dot{m}C_p)_{smaller}|(T_{in} - T_{out})|_{larger} \qquad .191$$

$$Q = (\dot{m}C_p)_{larger}|(T_{in} - T_{out})|_{smaller} \qquad .192$$

Substituting either of Eqn. 59 or Eqn. 60 into Eqn. 57,

$$\epsilon = \frac{(T_{in} - T_{out})_{larger}}{\Delta T_{max}} \ x \ \frac{C_{min}}{C_{min}} = \frac{(T_{in} - T_{out})_{smaller}}{\Delta T_{max}} \ x \ \frac{C_{max}}{C_{min}} \qquad .193$$

$$\epsilon = \frac{(T_{in} - T_{out})_{larger}}{\Delta T_{max}} \qquad .194$$

The ineffectiveness in heat transfer of heat can also be evaluated as:

$$1 - E = \frac{|(T_{h,i} - T_{c,i})| - |(T_{in} - T_{out})|_{larger}}{|(T_{h,i} - T_{c,i})|} \qquad .195$$

$$1 - E = \frac{\Delta T_{smaller}}{|(T_{h,i} - T_{c,i})|} \qquad .196$$

The Number of Transfer Units (NTU):

This non-dimensional value refers to the ratio of the thermal conductance of the heat exchanger 'UA', to the smaller of the two thermal capacities of the interacting fluids. The NTU is also defined as the heat exchanging capacity between the fluids. It is expressed in the Eqn. 65.

$$NTU = \frac{UA}{C_{min}} = \frac{UA}{C_{min}} x \frac{C_{min} |(T_{in} - T_{out})|_{larger}}{UA\Delta T_m} = \frac{|(T_{in} - T_{out})|_{larger}}{\Delta T_m} \qquad .197$$

Average values of NTU for heat exchangers have been found to be between 0.5 and 4 Ref. [88]

Thermal capacity ratio, C*:

The thermal capacity of any of the interacting fluids is the product of the fluid mass flow rate and the fluid's specific heat capacity. For any multiple fluid heat transfer, one of the fluids will possess a lesser thermal capacity in comparison to the second fluid. Therefore, the thermal capacity ratio is the ratio of this lesser thermal capacity to the larger on. This is expressed as:

$$C^* = \frac{(mc)_{smaller}}{(mc)_{larger}} = \frac{|(T_i - T_o)|_{smaller}}{|(T_o - T_i)|_{larger}} \qquad .198$$

The thermal effectiveness is related to the thermal capacity ratio through the equation:

$$\epsilon = \frac{|(T_i - T_o)|_{smaller}}{C^* x \, \Delta T_{max}} \qquad .199$$

Considering the variations available in heat exchanger configurations, the values for the *NTUs, C** and Thermal Effectiveness ϵ will hardly be the same even for the same heat exchangers working under slightly different operational conditions. Ref. [88] has provided 3 methods through which the *NTUs, C** and ϵ can be evaluated. They include:

- Graphical: Provides graphs which plots the thermal effectiveness, ϵ against NTU for values of C* between 0 and 1.
- Analytical Relationships: are provided for the various configurations of heat exchangers possible using the form:

$$E = f \, (NTU, C^*)$$

- Empirical Relationships: provide numerical solutions for the various configurations of heat exchangers possible. The equations are related to pure counter current and parallel flow arrangements and take the form:

$$E = E_{co} + (E_{cu} - E_{co})\Gamma \qquad .200$$

$$E_{cu} = \frac{1 - exp[NTU\ (1 -\ C^*)]}{C^* - exp[NTU\ (1 -\ C^*)]} \qquad .201$$

$$E_{cu} = \frac{1 - exp[NTU\ (1 -\ C^*)]}{C^* - exp[NTU\ (1 -\ C^*)]} \qquad .202$$

$\Gamma -$ provides the empirical functio to solve other heat exchanager flow arrangments

$$\Gamma =\ \Gamma_{asymp} +\ \Gamma_{corr.} \qquad .203$$

$$\Gamma_{asymp} =\ a_0 +\ a_1 C^* +\ a_2 C^{*2} \qquad .204$$

$$\Gamma_{corr.} = BC^*[arctan(c_0 NTU)][exp(D\ NTU)] \qquad .205$$

$$B =\ b_0 +\ b_1 C^* +\ b_2 C^{*2} +\ b_3 C^{*3} + b_4 C^{*4} \qquad .206$$

$$D =\ d_0 +\ d_1 C^* +\ d_2 C^{*2} +\ d_3 C^{*3} + d_4 C^{*4} \qquad .207$$

Values for the coefficients vary for different heat exchangers and are available from ESDU 98003, Part 3.

Thermal Conductance, UA:

In ideal conditions, where there is steady state heat transfer (assumption 1 above), the process of heat transfer occurs by the hot fluid giving up its energy to the cold fluid firstly via convection to the wall then conduction through the tube wall and finally via convection from the tube wall to the cold fluid. The presence of a layer of material (scale or deposits) with poor thermal conductivity increases the resistance path over which the heat energy must travel before an exchange can take place. This layer resistance is referred to as the fouling resistance and usually represented by:

$$r_f =\ \frac{1}{h_f} \qquad .208$$

Factoring the possibility of fouling in the heat transfer process, the rate of heat transfer per unit area across a section dx of a tube wall section is represented by the equation below:

$$dq = \frac{T_h -\ T_{h,f}}{dR_h} =\ \frac{T_{h,f} -\ T_{w,h}}{dR_{h,f}} =\ \frac{T_{w,h} -\ T_{w,c}}{dR_w} =\ \frac{T_{w,c} -\ T_{c,f}}{dR_{c,f}} =\ \frac{T_{c,f} -\ T_c}{dR_c} \qquad .209$$
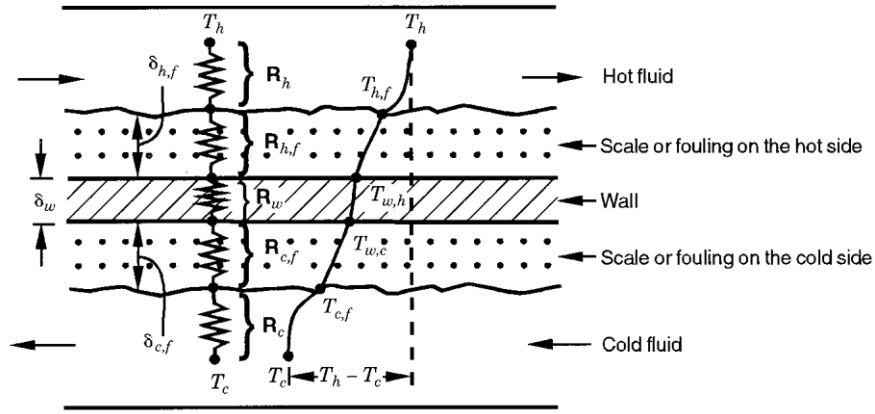
Figure 29: Thermal resistance to heat flow across a smooth surface (Source: Shah & Sekulić, 2003)

Eqn. 77 can also be summarised as:

$$dq = \frac{T_h - T_c}{dR_o} = U \, dA \, (T_h - T_c) \qquad .210$$

Where dR_o represents the summation of the resistances to heat transfer across the exchanger

$$\frac{1}{U \, dA} = dR_o = dR_h + dR_{h,f} + dR_w + dR_{c,f} + dR_c \qquad .211$$

$R_h -$ hot fluid convection resistance

$R_{h,f} -$ hot fluid fouling resistance

$R_w = \frac{ln\left(\frac{d_o}{d_i}\right)}{2\pi k_w L N_t} -$ cylindrical wall thermal resistance

$R_{c,f} -$ cold fluid fouling resistance

$R_c -$ coldfluid convection resistance

Eqn. 79 can also be written as:

$$\frac{1}{U \, dA} = \frac{1}{(\eta_o h \, dA)_h} + \frac{1}{(\eta_o h_f \, dA)_h} + dR_w + \frac{1}{(\eta_o h_f \, dA)_c} + \frac{1}{(\eta_o h_f \, dA)_c} \qquad .212$$

For heat exchangers without extended surfaces or fin$s$, $\eta_o = 1$ .In most cases, these extended surfaces are loosely bonded to the heat transfer tubes and thus present a resistance to heat transfer of their very own. The resistance must be considered in the calculation of the overall thermal resistance and denoted as the contact or bond resistance.

Appling the assumption that the heat transfer area is equal on both sides of the exchanger,

$$\frac{dA}{A} = \frac{dA_h}{A_h} = \frac{dA_c}{A_c} = \frac{dA_w}{A_w} \qquad .213$$

Replacing the differential areas in Eqn. 80 with the appropriate areas in Eqn. 81,

$$\frac{1}{U \, A} = R_o = \frac{1}{(\eta_o \, hA)_h} + \frac{1}{(\eta_o h_f)_h} + R_w + \frac{1}{(\eta_o h_f)_c} + \frac{1}{(\eta_o hA)_c} \qquad .214$$

The heat transfer equation thus becomes:

$$q = UA\Delta T_m = UA(T_h - T_c) = \frac{(T_h - T_c)}{R_o} \qquad .215$$

One set of the thermal resistances listed on the RHS of Eqns. 79 and 82 will be referred to as the controlling resistance if it represents over 80% of the overall resistance [65]. The aim of every heat exchanger design should therefore be to improve the efficiency of heat exchange by lowering the value of the controlling thermal resistance by as much as possible. This can be achieved by the addition of the extended surfaces especially on the gas side which usually has the controlling resistance. Therefore, where any side has a low heat transfer coefficient h, A is increased such that:

$$(\eta_o\, hA)_h \approx (\eta_o hA)_c$$

Alternatively, the overall heat transfer coefficient can be defined in terms of the areas of either fluid stream or the tube wall area.

$$UA = U_h A_h = U_c A_c = U_w A_w \qquad .216$$

The value UA is referred to as the overall thermal conductance of the heat exchanger. To evaluate the thermal conductance UA, the total Area, A must not be explicitly defined. On the other hand, the areas $A_h, A_c\ and\ A_w$ must be defined before U can be evaluated since $A_h \neq A_c$.

For heat transfer based on a unit surface area, the rate equation becomes:

$$\frac{q}{A} = U\Delta T_m \qquad .217$$

Eqn. 208 becomes, $R_o = 1/U$ and each resistance is evaluated on a unit area basis with A_h or A_c used as the basis for evaluating the overall thermal resistance.

$$\frac{1}{U_h} = \frac{1}{\left(\eta_o h\right)_h} + \frac{1}{\left(\eta_o h_f\right)_h} + R_w A_h + \frac{A_h/A_c}{\left(\eta_o h_f\right)_c} + \frac{A_h/A_c}{\left(\eta_o h\right)_c} \qquad .218$$

$$\frac{1}{U_c} = \frac{1}{\left(\eta_o h\right)_c} + \frac{1}{\left(\eta_o h_f\right)_c} + R_w A_c + \frac{A_c/A_h}{\left(\eta_o h_f\right)_h} + \frac{A_h/A_c}{\left(\eta_o h\right)_h} \qquad .219$$

For a plain tube $\eta_o = 1$ and:

$$R_w = \frac{\delta_w}{k_w} \qquad .220$$

Based on the inner and outer surfaces of the tube:

$$\frac{1}{U_o} = \frac{1}{h_o} + \frac{1}{h_{o,f}} + \frac{d_o\, ln(d_o/d_i)}{2k_w} + \frac{d_o}{h_{i,f}d_i} + \frac{d_o}{h_i d_i} \qquad .221$$

$$\frac{1}{U_i} = \frac{1}{h_i} + \frac{1}{h_{i,f}} + \frac{d_i\, ln(d_o/d_i)}{2k_w} + \frac{d_i}{h_{o,f}d_o} + \frac{d_i}{h_o d_o} \qquad .222$$

Appendix B

Introduction:

This chapter attempts to outline the requirements the heat exchanger design toolkit must fulfil to ensure it is suitable for the purposes of heat exchanger design. These requirements are not strict and should only act as guidelines to be considered by the toolkit developer. The final approval will be given by the end-users after much testing has been conducted.

Toolkit Requirements:

1. **User – manual:**

   The toolkit will be used by a design team familiar with input values required at each stage of heat exchanger design or at least as specified by a client. However, it should be anticipated that users with little or no technical knowledge of engineering terms would be able to operate the toolkit with ease based on a set of requirements sent in by a potential customer. Hence there exists a need for a user manual accompanied by a user manual to explain the meaning of terms and guide end – users on how to apply the toolkit for design purposes.

2. **Toolkit Description:**

   The general outline of the toolkit has been split into two parts, comprising the Front-End and the Back-End. The front-end comprises the visual part through which the designer interacts with the toolkit while the back-end is the section 'hidden' away from the designer and is the location where all calculations will be performed. These two parts are further described below:

   A. **Toolkit Front – End:** To ensure ease of operation, data input into the toolkit should be made possible through a graphic user interface (GUI) environment. Button controls present on the graphic user interface (GUI) should be able to trigger commands which in turn activate equations and produce desired results. Design results produced will be also need to be displayed on the GUI. The GUI will comprise:

      o Drop-down menus: that allow the designer choose design parameters such as fluid type, design approach desired (rating or sizing), etc. The drop-down menu functions should also allow for the selection of specific dimensions to which the potential designer already manufactures to, such as fin pitch, tube OD etc.

      o Blank input boxes: into which the designer would fill the initial conditions or information provided by the customer. The drop-down and the blank spaces would possibly be aligned side-by-side in most instances.

      o Button controls: that would be used to activate commands which in turn, activate the equations at the back-end of the toolkit, thus allowing the output of results.
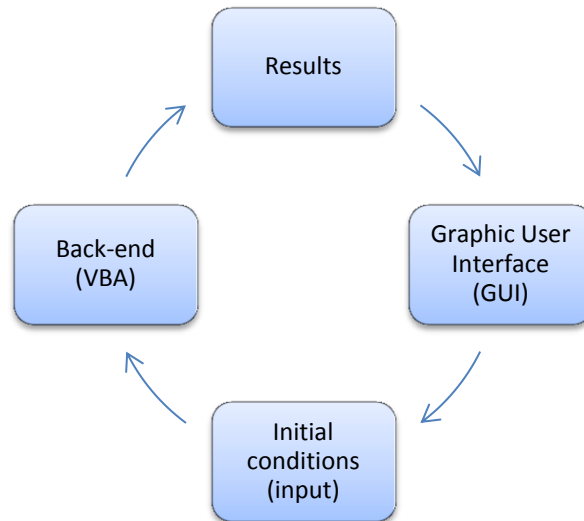
Figure 30: Toolkit calculation process.

As earlier mentioned, the types of heat exchangers studied for this project fall under 3 categories: Plain tube heat exchangers, circular-fin tube heat exchangers, and the tube-in-plate heat exchangers (where single or more tube rows share the same flat fin). Therefore, the front – end (also the graphic user interface, GUI) of the tool should firstly comprise of tab options indicating each of these heat exchanger types. Upon selection of the desired heat exchanger type, end-user would be presented with the option of selecting the condition of the tube-side fluid, which would either be a dual-phase or a single phase fluid. If the single phase button is selected, end-user will be further presented with the option of choosing whether the tube-side fluid will have heat added (heating) or extracted from it (cooling).

Figure 31: Sample Graphic User Interface (GUI) for selection based on type of heat exchanger

Once these initial conditions are set, the next stage of design would be largely dependent on the calculation process chosen by the end-user. The possible calculation processes are described below:

Calculation process:

Bearing in mind the relationship between geometrical characteristics, process conditions and eventual heat transfer, two ca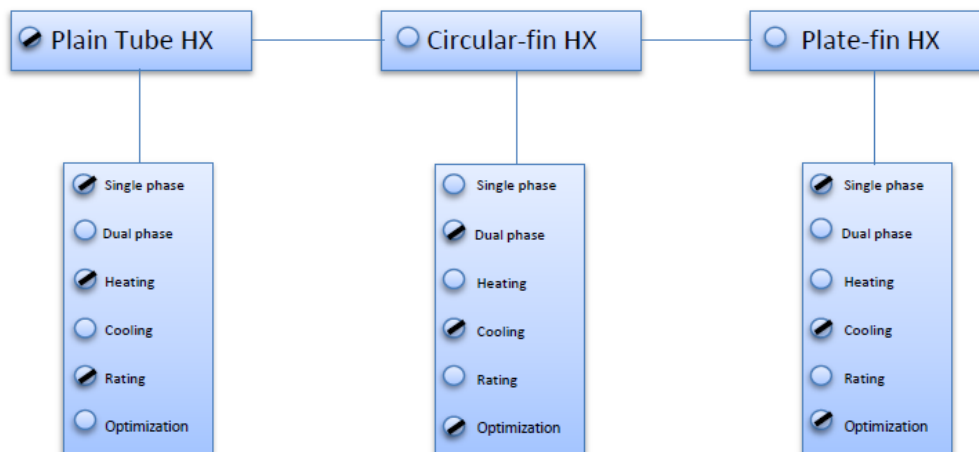lculation processes have been identified that will impact on the final structure of the front-end GUI. The first calculation process will be such that an initial set of values comprising process conditions and geometrical characteristics can be entered via the GUI, and results produced that will indicate the capability of the proposed dimensions to do the required duty whilst still staying within design boundaries. This calculation process will be termed the 'Rating' process. In the second calculation process, several results will be produced, giving the designer the freedom to choose which heat exchanger dimensions that not only best suits his needs but will also do the required duty. This calculation process will be referred to as the 'Sizing' process. The outline of the GUI depending on the designer selecting the 'Rating' or 'Sizing' calculation process, is described below.

Rating:

As described earlier, the rating calculation process refers to the calculations which are conducted to 'check' that pre-defined heat exchanger dimensions are able to deliver a set of design requirements. For example, due to space restrictions, the maximum allowable length for the heat exchanger could be so short as to cause an increase in the pressure drop across the unit. Therefore, the designer must 'rate' a heat exchanger unit made of that specific length against the desired pressure drop. The main advantage of the rating process is that it prevents the iterative process needed to arrive at an ideal heat exchanger size.

If the rating option is chosen, only one set of results will be produced which will give the designer a clear picture of the heat exchanger's efficiency under those operating conditions.

It is proposed, that the front-end, be split into 3 sections, consisting:

- Part A: Fluid flow conditions
- Part B: Bundle specifications
- Part C: Results.

If the rating process is chosen, then the end-user should be presented with the options listed below:

Part A: **Fluid flow conditions:**

- **Tube-side fluid type:** An accessible drop down menu would enable the end-user select a particular fluid from a pre-compiled list. Each fluid will be linked to the thermophysical properties database REFPROP, such that the fluid's thermophysical properties at the mean value of the inlet and outlet temperatures are computed. These values need not be visible to the end-user, and would include the following:

    i. Specific heat capacity, C_p: needed to calculate the heat duty from the fluid and also, its Prandtl number.

    ii. Specific Enthalpy, h_{fg}: needed to compute the heat duty if tube-side fluid is dual-phase (vapour & liquid combination).

- **Gas-side fluid type:** Another drop down menu should also be available to enable selection of an appropriate fluid on the gas-side. Fluid thermophysical properties will also be evaluated at the mean value of the inlet and outlet temperatures. Properties also include those listed above.

- **Inlet tube-side fluid temperature:** Blank spaces would be required for the end-user to input the inlet temperature of the fluid. A drop down menu right next to the blank spaces should then enable the end-user select whether the value is in SI or Imperial units format (^{0}C or ^{0}F)

- **Outlet tube-side fluid temperature:** If tube-side fluid is dual-phase, then the outlet temperature, should automatically indicate a value same as that at the inlet in this section. If however, the tube-side fluid is selected as being single-phase, then user should be allowed to fill the outlet temperature within the space provided. End-user would also be required to indicate whether this value is in ^{0}C or ^{0}F.

- **Inlet gas-side fluid temperature:** End-user should be able to input the inlet temperatures in either ^{0}C or ^{0}F. Preferably, a blank box would be present with a drop down menu next to it indicating its unit form, ^{0}C or ^{0}F.

- **Outlet gas-side fluid temperature:** Format should be same as the inlet temperature format.

- **Gas – side inlet pressure:** The default value will be set at atmospheric pressure, which will be available in a drop-down menu. The second option within the drop down menu will be the user-defined option, which will enable the end-user input desire values if they differ from atmospheric pressure. End-user should also be able to indicate whether this value is in SI or Imperial units.

- **Tube – side inlet pressure:** This section will only be a blank space where the end-user will need to input the inlet supply pressure. Drop down menu will also indicate the unit of the value

- **Gas-side volumetric/mass flow rate:** If the volumetric flow rate is available, blank space should be available to input the value. Then toolkit would need to automatically compute the mass flow rate by multiplying this value with the density of the fluid. If the volumetric flow rate path is chosen, then another drop down menu should be available, to enable end-user select units in either the SI or Imperial format (m^3/s, $m^3/hr.$, ft^3/s, or $ft^3/hr.$). The same goes for the mass flow rate (kg/s or kg/hr.). Therefore, drop down menu should show the SI & Imperial units (m^3/s, $m^3/hr.$, ft^3/s, $ft^3/hr.$, kg/s and kg/hr.) and the toolkit should be able to recognise these values for what they are and base heat duty calculations on these.

- **Tube-side mass flow rate:** Format should be similar to that described for the gas-side volumetric/mass flow rate.

- **Heat duty (tube-side):** Based on the fluid flow properties (Specific enthalpy, ΔH or Specific capacity, C_p, inlet & outlet temperatures and mass flow rate), the heat duty from the tube-side is calculated from the equation. $Q=m*h_{fg}$ (if fluid is condensing) or $Q=m*C_p*\Delta T$ (if fluid is a single phase fluid). This implies that if a dual-phase condition was selected at the start of the design, then the toolkit automatically picks the specific enthalpy of the fluid and delivers the output. While if a single phase condition was selected, the toolkit picks the heat capacity of the fluid, along with the temperature drop & flow rate and delivers a result. Preferably, a button would be required to activate this action.

- **Heat duty (gas-side):** Using the properties evaluated the mean values of the inlet and outlet temperatures, heat duty is calculated using same the equation for single phase flows, $Q=m*C_p*\Delta T$.

Also, available drop down menu should indicate whether result would be in SI or Imperial units (kW or BTU/h)

Toolkit would be programmed to ensure that the heat duties evaluated at both the fluid and gas sides are equal. Reasons for this lie in the fact that most times, flow conditions supplied by the customer under-predict the heat duty they desire. If this is the case, toolkit should prompt the end-user with an error message to adjust the flow conditions to match the heat duty.

Figure 32 below shows a sample of what this section of the toolkit should be.

KEY:

- Drop-down menu, user controlled.
- Blank Space, user controlled.
- Result box, not controlled by end-user.

	Tube-side		Gas-side	
Fluid	Steam		Air	
Inlet	133	°C	35	°C
Outlet	100	°C	75	°F
Flow rate	100	Kg/s	75	m³/s
Heat Duty	100	kW	75	Btu/h
Run				

Figure 32: Sample Graphic User Interface (GUI) for selection of process conditions

Part B: **Tube/fin dimensions and characteristics.**

- **Tube material:** a list of materials compiled in the form of a drop down menu, should be available to enable the end-user select an appropriate material type for the heat exchanger tubes. The most popular of these materials include: copper, stainless steel and mild steel. To ensure that problems are not encountered in the near future, as many metallic materials as possible would be included within this list. On selection, properties of the material specifically the thermal conductivity needs be extracted from the pre-installed thermophysical properties database.

- **Fin material:** would also be available in a drop down menu form, to enable the end user select a desired fin material. The common fin materials used for manufacture include: aluminium, stainless steel and mild steel. As mentioned earlier, as many metal materials as possible would be added to this list to ensure that the end user is presented with as many options as possible. The material properties as well, (material thermal conductivity) will also be required.

- **Tube outer diameter (OD) and thickness:** One option of presentation would be in a drop down menu format constituting of a list of the tube OD dimensions along with the thicknesses. For example, 25.4mm x 2.77mm, where 25.4mm represents the tube OD, while 2.77mm represents the tube wall thickness. Once selected, the Inner Diameter (ID) of the tube will be calculated from the equation: (OD − (2*tube-wall thickness)).

Alternatively, the tube thickness space could be offered to the end user as a drop down menu, with pre-filled values along with a user-defined option. Upon selection of the user defined section, a blank space will become available for the end-user to fill in the available thickness. To ensure consistency in values and units, end-user should be allowed to select whether this value is in mm or m.

- **Fin thickness:** also available in a drop down menu, this list will constitute all the fin thickness values used generally for manufacture. All the end-user need do, is select the desired one.

- **Tube length:** value would be fed manually, since this is a bundle rating exercise. Ideally, this value should remain in SI units of either m or mm, but end-user should be given the option of choosing Imperial units in the form of feet (ft.). Hence, a drop-down menu will also be available to indicate what unit the input values are in.

- **Number of fins/m:** Already limited in possible combinations, (98, 118, 157, 197, 236, 276, 315, 354, 394, 433 & 472 fins per m). A drop down menu will be made available with these values for the end-user to select from.

- **Number of rows:** End – user would be given the option to indicate the number of rows they want for that particular bundle. This will be in the form of a blank space, where the end user can simply fill in the desired number of rows.

- **Transverse Pitch:** End-user will be presented with a blank space, to input this value manually, drop down menu next to this blank space, should also indicate the unit of the value entered.

- **Longitudinal Pitch:** Outline will be same as the transverse pitch section.
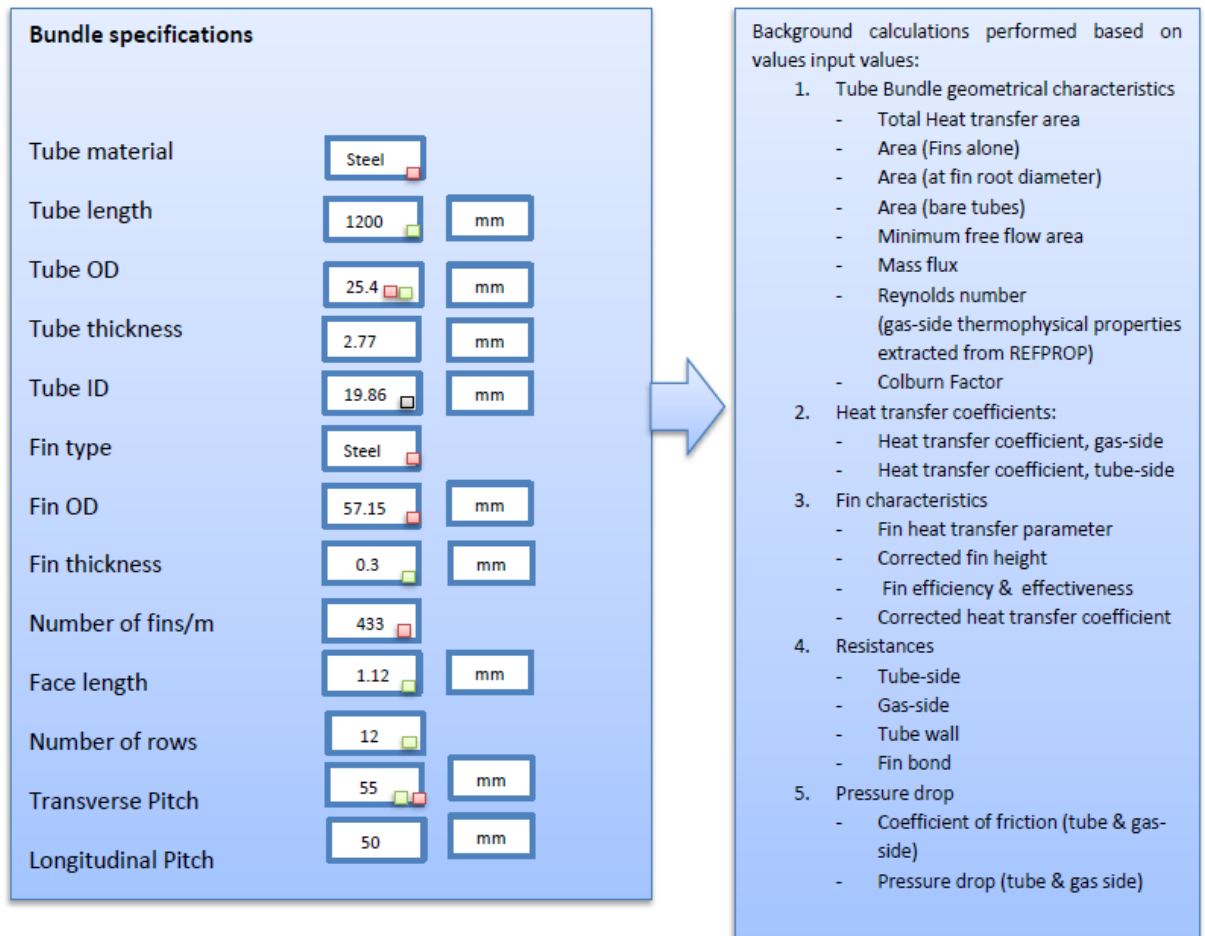
Bundle specifications			Background calculations performed based on values input values:

Bundle specifications

Tube material	Steel	
Tube length	1200	mm
Tube OD	25.4	mm
Tube thickness	2.77	mm
Tube ID	19.86	mm
Fin type	Steel	
Fin OD	57.15	mm
Fin thickness	0.3	mm
Number of fins/m	433	
Face length	1.12	mm
Number of rows	12	
Transverse Pitch	55	mm
Longitudinal Pitch	50	mm

Background calculations performed based on values input values:

1. Tube Bundle geometrical characteristics
   - Total Heat transfer area
   - Area (Fins alone)
   - Area (at fin root diameter)
   - Area (bare tubes)
   - Minimum free flow area
   - Mass flux
   - Reynolds number (gas-side thermophysical properties extracted from REFPROP)
   - Colburn Factor
2. Heat transfer coefficients:
   - Heat transfer coefficient, gas-side
   - Heat transfer coefficient, tube-side
3. Fin characteristics
   - Fin heat transfer parameter
   - Corrected fin height
   - Fin efficiency & effectiveness
   - Corrected heat transfer coefficient
4. Resistances
   - Tube-side
   - Gas-side
   - Tube wall
   - Fin bond
5. Pressure drop
   - Coefficient of friction (tube & gas-side)
   - Pressure drop (tube & gas side)

Figure 33: Sample Graphic User Interface (GUI) for selection of heat exchanger characteristics

Part C: **Results**

This section will be made up of results for calculations obtained from parameters set for both fluid sides and the bundle/fin dimensions. Most notably, it will include the pressure drops on the tube & gas sides. Two areas will be produced:

i.   Area, A_1 representing tube bundle area required to ensure specified heat duty is transferred.

ii. Area, A_2 representing area of tube bundle based on present configuration; A_2

The final aim, is to ensure that these two areas are equal, $A_1 = A_2$. If $A_2 \neq A_1$, end-user can return and amend the factors that affect A_2, e.g. the number of rows present in the bundle and if desired, tube length.

Based on this comparison, the end-user could go back and amend initially set dimensions in order to balance the two areas.
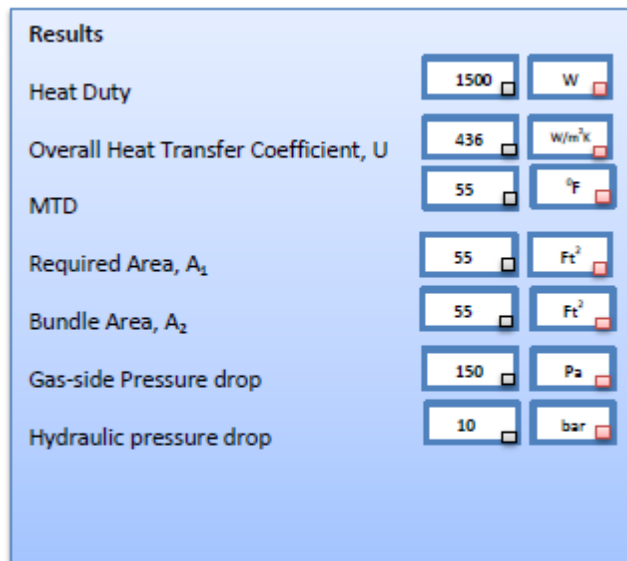
Results

Heat Duty	1500	W
Overall Heat Transfer Coefficient, U	436	W/m^2K
MTD	55	$^\circ F$
Required Area, A_1	55	Ft^2
Bundle Area, A_2	55	Ft^2
Gas-side Pressure drop	150	Pa
Hydraulic pressure drop	10	bar

Figure 34: Sample Graphic User Interface (GUI) for display of calculation results

Sizing:

Heat exchanger design tends to be a continuous iterative process in which several geometries are analysed to assess their suitability for a set of process conditions. This is because the customer could place certain constraints on the heat exchanger geometry based on process conditions beyond his control. These constraints might include: a maximum allowable pressure drop on the gas-side of the heat exchange, a minimum heat duty required etc. These constraints have to be accommodated in whatever final design is chosen. Due to the several iterations that need to be conducted, computer programs are chosen to run these calculations because they are fast and can run through several different configurations within minutes. These configuration(s) usually involve a trade-off of some sort. For example, tube length could be shortened in order to increase the number of tube rows or the number of fins/m on each tube can be increased to obtain more heat transfer but could invariably lead to an increased pressure drop across the bundle. Any heat exchanger configuration finally chosen from the group made available by the toolkit should provide the designer with the most effective option in terms of cost and functionality.
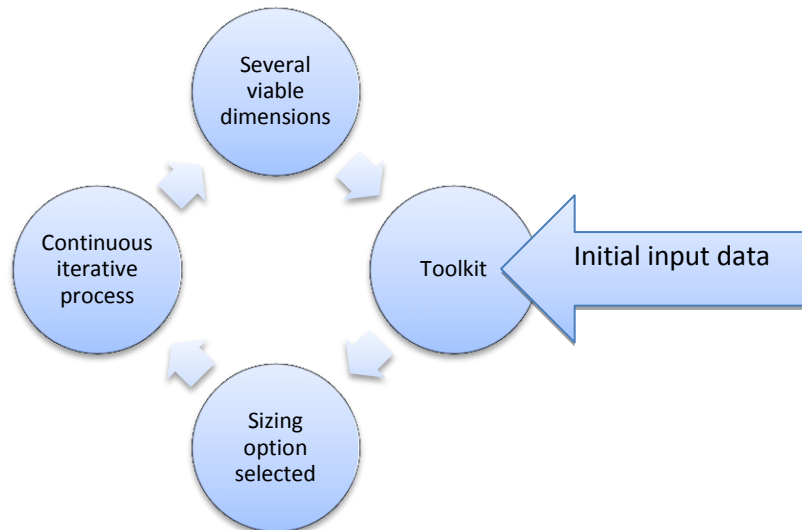
Figure 35: Sizing calculation process

When this calculation process option is selected, end-user will not be required to input as much information as the rating method described above. The procedure would normally include just the following, along with the enhancements described below:

- Part A parameters, including the desired pressure drop on both sides
- Part B parameters will be blanked out save for the tube length, number of rows and face length. End-user will still need to select these materials. Also to ensure that only feasible results are produced, certain sections would have a minimum and maximum column so that end-user can specify the limits of these values. Other sections will be greyed out with the toolkit ignoring the user-defined option and performing iterations solely on the values from the drop-down menus, while also, limiting the results to the maximum and minimum values entered by the end-user.

Using these values, toolkit performs several rapid calculations, by altering bundle dimensions as detailed in Part B, above. A list of possible tube bundle dimensions would then be made available to the end-user to select from.

Equations from Part B, remain the same as they are the building block of the main equations
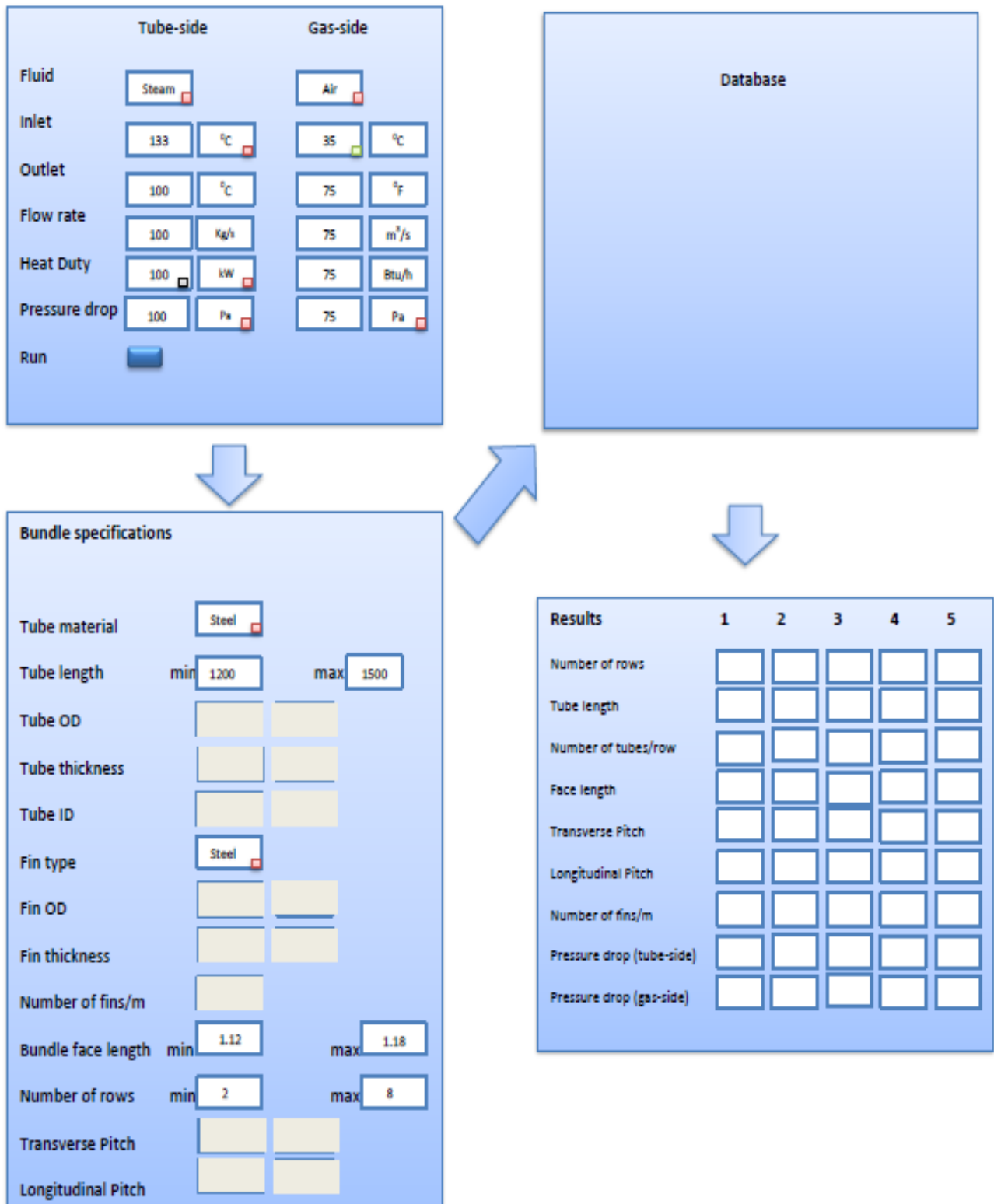
Figure 36: Sample GUI for the Sizing design option.

B. **Toolkit Back – End:** A text-user interface will represent the back-end of the toolkit; a convenient programming language would be used to link the toolkit to the fluid & material databases (REFPROP & ASTM), which are standalone programs, ensuring that the appropriate or desired properties are provided when needed. The figure on the RHS of Fig. 36 gives an example of this, and constitutes sections of the complex equations which would remain invisible to the end-user. The required equations will be 'coded' in the back-end and will be activated with the 'Run' button on the front-end GUI.
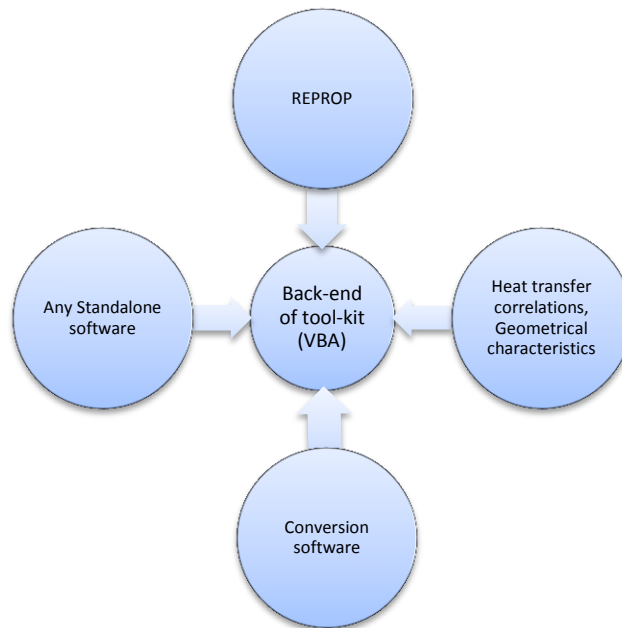

Figure 37: Depiction of toolkit back – end

Design data entered by the designer on the front-end GUI, will be then be processed using these equations. These calculations will be based entirely on the on the values entered for the tube/fin dimensions and the initial process conditions. Some of these equations include:

- **Tube bundle geometrical characteristics:** Geometrical characteristics correlations: Prior to the heat transfer coefficient being determined, the geometrical characteristics e.g. minimum flow area etc. of the heat exchanger has to be determined based on the dimensions such as tube length, tube OD, fin diameter, fin height, fins/m etc. These characteristics, are determined by equations dependent on the tube bundle type (plain, circular or plate fin). The preferred equations have been listed in the preceding chapters and include: Primary surface area (minus fins), Surface area at fin root diameter, Secondary surface area (fins alone), Minimum flow area, Mass flux, Reynolds number, Colburn factor, Fin surface parameter, Corrected fin height, Fin efficiency, Fin surface effectiveness

- **Heat transfer coefficient:** will constitute of 2 sub-equations, namely:

- Heat transfer coefficient, h_1 (tube-side): The equations required to calculate this value, will depend on state of fluid (single or dual-phase). If fluid is single phase, then the heat transfer coefficient will be computed using the Dittus-Boelter equation: $Nu=0.024Re^{0.8}.Pr^{0.4}$ (heating conditions) or $Nu=0.026Re^{0.8}.Pr^{0.3}$ (cooling conditions). If it is a dual phase fluid, then the appropriate equations should have been activated once the end user highlighted the single phase button at the beginning of the exercise.

- Heat transfer coefficient, h_2 (gas-side)**:** begins initially with the calculation of the geometric characteristics of the tube bundle. The dimension calculations will be based on the initial input values for the tube bundle, i.e. tube length, transverse & longitudinal pitch, number of fins/m, and heat exchanger type (circular, plate or plain tubes). From these calculations (geometric characteristics & Reynolds number), the Colburn factor is extracted and from this, the gas-side heat transfer coefficient. The transfer coefficient equation used, will also depend on the type of heat exchanger being designed (circular-fin, plain or tube-in-plate)

- **Thermal resistances:**
  - Tube-side: will be the inverse of the heat transfer coefficient obtained earlier using the Dittus-Boelter equation, multiplied by the tube OD/ID ratio.

  - Gas-side: will be the inverse of the heat transfer coefficient obtained from the gas side.

  - Tube wall: is the resistance to heat transfer as a result of both the tube wall thickness, and it material. Hence, the tube material's thermal conductivity will also be extracted from REFPROP.

  - Fin-bond resistance: computes the resistance produced as a result of incomplete adhesion of spiral bound fins on tubes. This equation, will only be required if the finned tubes are produced by as spiral wound fins. If they are sourced externally, it is highly likely they will be G-fins (fins are filled into grooves marked on the tube body)

    Summation of these values will be displayed in the overall heat transfer coefficient, U, block within the results section.

- **Pressure drop:**
  - Co-efficient of friction: will be required to compute pressure drop on both the gas and tube-side. Using a combination of both the frictional coefficient and relevant equations,

pressure drop across the bundle and the tube, will be computed and displayed in the results section of the user-interface

To ensure accurate results, potential tampering of the building blocks of the toolkit, must be prevented by ensuring that the back-end is never accessible to front-end users. On the other hand, the back end must be 'coded' with low-level programming language such that any modifications required in the future can be carried out by people with little or no experience in computer programming. An example is the software referred to as REFPROP, which will enable the designer evaluate fluid thermophysical properties required for heat transfer calculations without resorting to manual data sheets.

3. **Further Development:**

It should be anticipated that the toolkit will be continuously upgraded to include features that will improve its productivity. Examples of some these features are outlined below and by no means represent an end to the list. As the project unfolds, ideas would come up and this would be built into the toolkit.

- Data storage: Toolkit should allow the designer store bundle dimension output, against a particular customer's name. This would ensure that in the absence of the designer, tube bundle specifications for a particular customer can still be recalled if needed.

- Costing: Prices based on the chosen tube bundle should be one of the added functions of the toolkit.

- CAD drawing: toolkit should include a functionality which allows it produce a dimensioned CAD drawing of the tube bundle.

- Structural analysis: as part of the project, toolkit should be able to carry out structural analysis on the tube bundle based on codes governing pressure vessels and certify them safe to be installed within a human occupied environment. Hence, an addition to the rating process earlier described, would be that the end-user should select a design code to base the bundle dimensions on. These codes will include ASME & EN 13445 and when they are selected, bundle sizing for rating or optimization will be based on the prescribed equations.

- Weld-type recommendations: Based on the results of the structural analysis, toolkit would recommend best type of weld to append to certain joints to ensure complete safety.

- Complete bundle design: Presently, toolkit is being designed to specify just the tube bundle dimensions. Further parameters, like the flanges and headers sizes are

excluded. Future development should include these features so that the end product can go straight to manufacturing without further design.

Appendix C

GRG Non – Linear Solver

Generalized Reduced Gradient methods include most algorithms used to solve non-linear programs of general structure.

The nonlinear equation is usually expressed in the form;

$$minimize\ f(X)$$

$$subject\ to\ g_i(X) = 0\ ,i = 1, ..., m$$

$$l_i\ \leq\ X_i\ \leq\ u_i, i = 1, ..., n$$

Where X, is an $n -$ vector and u_i, l_i, are assigned upper and lower boundaries where $u_i > l_i$. It is assumed that $m < n$, because $m \geq n$, indicates an equation that requires a unique solution. Equations 1-3 above is generalized as the inequality constraints expressed in eqn. 3, can be transformed to equality constraints by the addition of variables designed to eliminate less-than constraints (slack variables). Vector $'X'$ usually comprises of the natural variables of the problem and the slack variables.

The main idea behind the generalised reduced gradient method (GRG), is to express the variables $'m'$ which are not equal to zero (basic variables) in terms of the variables $'n - m'$ which are equal to zero (non-basic variables) using the equalities in Equation 2. Assume that $\overline{X}$, is a feasible point and $'y'$ is a vector of the basic variables and $'x'$ the non-basic variables at $\overline{X}$, then $'X'$ can be split into:

$$X = (y, x), \overline{X}\ = (\bar{y}, \bar{x})$$

Equation 3 can then be expressed as:

$$g(y, x) = 0$$

$$where\ g = (g_i, ..., g_m)$$

If it is assumed that objective function $'f'$ and the constraints $'g_i'$ are differentiable, the implicit function theorem will allow for equation 5 to have a solution for all $'x'$ in the region of $\bar{x}$, provided that the $m\ x\ m$ basis matrix $'\partial g/\partial y'$ evaluated at $'\overline{X}\ '$ is non-singular. If the assumptions are correct, then the objective can be expressed as a function of $'x'$ alone in the form:

$$F(x) = f(y(x), x)$$

The non-linear equation is then altered for variables of $'x'$ close to $'\bar{x}\ '$ to a reduced form, with only upper and lower bounds.

$$Minimize\ F(x),$$

$$dependent\ upon\ l_{NB} \leq x \leq\ u_{NB}$$

$$l_{NB}\ and\ u_{NB}\ are\ the\ vectors\ for\ the\ boundaries\ of\ 'x'$$

The generalised reduced gradient (GRG) method, finds an optimal solution to a non-linear equation of the form eqns. (1) – (3) by following the sequence of eqns. (8) – (9). , for eqns. (8)-(9) to produce any meaningful results $'x'$ must have the freedom to vary about point $\bar{x}$. Unfortunately the boundaries of restrict the movement of x, but it is still easy for x to move in directions which keep the boundaries satisfied. On the other hand, if components of $\bar{y}$ are at their boundaries, an adjustment in x from $\bar{x}$ will likely cause a violation of the boundaries. To ensure this does not happen and that the function $y(x)$ remains, the following assumptions are made.

    i.   Assumption of non-degeneracy: which states that at any point X which satisfies the objective function and constraints [eqns. (2) & (3)], there should exist a demarcation of X into $'m'$ basic variables $'y'$ and $'n-m'$ non-basic variables $'x'$ such that

$$l_B \; < y \; < \; u_B$$

$$where \; l_B \; and \; u_B \; are \; vectors \; of \; bounds \; y$$

$$and \; B = \; \partial g / \partial y \; is \; non-singular$$

With the above assumption, consider beginning from $'\bar{X}\,'$ with y and x which are basic and non-basic variables respectively, then attempt to solve eqns. (8)-(9). At eqn. (7), in order to evaluate $F(x)$, the values of the basic variables $y(x)$, must be known. Unfortunately, $y(x)$, cannot be determined in its closed form except for linear and nonlinear conditions. However $y(x)$ can be evaluated for any values of x via iteration which solves the equalities in eqn. 5; therefore, a procedure to solve the reduced problem beginning from $X_o \equiv \overline{X}$, is:

- Set $i = 0$

- Substitute x_i into eqn. 5 and evaluate the equivalent values for i, y_i by an iterative process for solving nonlinear equations.

- Determine a direction of motion d_i for the non-basic variables x.

- Select a step size α_i to give $x_{i+1} = \; x_i + \; \alpha_i d_i$. This is achieved by solving the one dimensional problem

$$minimize \; F(x_i + \propto d_i),$$

$$where \; \propto is \; restricted \; to \; ensure \; that \; x_i + \propto d_i \; satisfies \; the \; boundaries \; on \; x.$$

$$This \; search \; need \; a \; repeated \; applicaton \; of \; step \; (1) in \; order \; to \; evaluate \; F \; for \; the \; values \; of \; \propto$$

- Test the present point $X_i = (y_i, x_i)$ for optimality. If optimality is not reached, set $i = i + 1$ and return to Step (1).

From Step (1), one or more components of y_i may exceed their bounds, if this happens, then the iterative process must be interrupted. To illustrate this, assume only one basic variable violates a bound. This variable must then be made non-basic and a component of x which is not bounded will be made basic. When this change of basis occurs, new functions $y(x), F(x)$ and a new reduced problem are formed.

ii. The Reduced Gradient: To minimize F using derivatives, a formula must exist for ∇F. The value F will be differentiable if f and g are differentiable and also if $\delta g/\delta y$ is non-singular. This ensures that the implicit function $y(x)$ is differentiable. From eqn. 7:

$$\delta F/\delta x_i = \delta f/\delta x_i + (\delta f/\delta y)^T \, \delta y/\delta x_i$$

To evaluate $\delta y/\delta x_i$, assume that

$$g_j \, (y(x), x) = 0, \qquad j = 1, \dots, m$$

For all x in the vicinity of $\bar{x}$ then

$$dg_j/dx_i = 0 = (\delta f/\delta y)^T \, \delta y/\delta x_i + dg_j/dx_i, \qquad j = 1, \dots, m$$

This can also be expressed in matrix form as,

$$(\delta g/\delta y) \, \delta y/\delta x_i + \delta g/\delta x_i = 0$$

Considering that $(\delta y/\delta y)$ is non-singular at the point $\bar{X}$ then,

$$\delta y/\delta x_i = -(\delta g/\delta y)^{-1} \, \delta g/\delta x_i \equiv B^{-1} \, \delta g/\delta x_i$$

Substituting eqn. 13 into eqn. 12, then

$$\delta F/\delta x_i = \delta f/\delta x_i - (\delta f/\delta y)^T \, B^{-1} \equiv \partial g_k \delta x_i$$

$$Let \; \pi = (\delta f/\delta y)^T \, B^{-1}$$

The $m - vector, \pi$ referred to as the Kuhn-Tucker multiplier vector for the constraint g. Rearranging eqn. 15, components of ∇F becomes:

$$\delta F/\delta x_i = \delta f/\delta x_i - \pi^T \, \delta g/\delta x_i$$

Equation 16 then reduces to the equation for the relative cost factors in **[Ref. 1]** if f and all g_i are all $linear$.

Then, $\delta y/\delta x_i = c_i, \delta f/\delta y = c_B$ $(objective \; coefficients \; of \; the \; basic \; variables)$ and

$$\delta y/\delta x_i = P_i, \; the \; column \; of \; constraint \; coefficients \; for \; x_i.$$

$$The \; vector \; \pi \; is \; the \; simplex \; multiplier \; vector.$$

Relationship of the Reduced Gradient Formula and Kuhn-Tucker Conditions

Assume that $\bar{X}$ is optimal for eqns. (1) – (3), also assume that the gradients of the binding constraints of $\bar{X}$ are independent, the Kuhn-Tucker conditions will be valid at $\bar{X}$. Let π be a Lagrange multiplier vector for the equalities of Eqn. 2, and α and β multipliers for the upper and lower boundary constraints respectively. Thus the Lagrangian for eqns. (1) – (3) becomes

$$L = f + \pi g + \alpha(l - X) + \beta(X - \pi)$$

The Kuhn-Tucker conditions when written in terms of y and x, become:

$$\delta L/\delta y = \delta f/\delta y + \pi B - \alpha_y + \beta_y = 0$$

$$\delta L/\delta x = \delta f/\delta x + \pi \delta g/\delta x - \alpha_x + \beta_x = 0$$

$$\propto \geq 0, \beta \geq 0$$

$$\alpha(l - x) = \beta(x - \pi) = 0$$

Where α_y, β_y are sub-vectors of α and β which correspond to the basic variables y , and also for α_x, β_x; If $\bar{X}$ is optimal, then vectors $\bar{\pi}, \bar{\alpha}$ and $\bar{\beta}$ together with $\bar{X}$ will satisfy eqns. (17) – (20).This ensures that $\bar{y}$ is well within the bounds and thus eqn. (20) suggests that

$$\alpha_y = \beta_y = 0$$

  Equation 17 then becomes:

$$\pi = \delta f/\delta y \, B^{-1} = 0$$

Therefore, the vector π from eqn. 15 is the multiplier vector for the equalities in eqn. 2. Eqn. 18 can then be written as:

$$\delta f/\delta x + \pi \, \delta g/\delta x = \alpha_x - \beta_x$$

The LHS of Equation 21 is the reduced gradient, $\nabla F(x)$. to find the relationship of eqns. (8) – (9) to eqn. 21, if x_i remains strictly between its boundaries, then $\alpha_{xi} = \beta_{xi} = 0, from \, eqn. 20$. Therefore,

$$\delta F/\delta x_i = 0$$

If x_i exists at the lower boundary, then $\beta_{xi} = 0$ such that

$$\delta F/\delta x_i = \propto_{xi} \geq 0$$

If x_i exists at the upper boundary, then $\propto_{xi} = 0$ such that

$$\delta F/\delta x_i = -\beta_{xi} \leq 0$$

However, eqns. (22) – (24) are the optimality conditions for the reduced equations of eqns. (8) – (9). Therefore, the Kuhn-Tucker conditions for eqns. (1) – (3) can be viewed as the optimality conditions for the reduced eqns. (8) – (9).The value π in the equation for the reduced gradient is the Kuhn-Tucker multiplier vector. The vector π is valuable for sensitivity analysis and the GRG nonlinear solver provides it as a by-product of its calculations.

Appendix D

Toolkit Design and Development

Introduction:

This chapter describes the actual development of the design toolkit with the incorporation of some the guidelines from the preceding chapters. It has been written such that it doubles as the user manual for the toolkit. It is split into five sections; General Information, System Summary, Getting Started, Using the System, Reporting and Troubleshooting. Each section is further described below and where appropriate, the end – user has been given a sample exercise to work through, to ensure that the toolkit is installed correctly and is producing accurate results.

General information:

General Information section explains in general terms, the toolkit and the purpose for which it is intended.

Toolkit Description

This tool is a design toolkit comprised of 3 Excel Workbooks, from which 3 macros have been developed using Visual Basic for Applications (VBA). These spreadsheets are titled:

i. **Circular-Fin Heat Exchangers:** used primarily for the thermal design of circular-fin heat exchanger bundles.

ii. **Plate-Fin Heat Exchangers:** used primarily for the thermal design of plate-fin heat exchanger bundles.

iii. **Plain Tube Heat Exchangers:** used primarily for the thermal design of plain tube heat exchanger bundles.

An activation button is located within each spreadsheet, with which the macros can be "called". Each macro consists of 4 tabs named:

i. Heat Exchanger Design: developed to enable the designer correctly size a heat exchanger bundle. Its final results, will tell the designer how sufficient his actual dimensions are, when compared to the required size that should do the desired heat duty. It is further sub-divided into:

- Air-cooled
- Heat Recovery
- Steam coil

Equations used in these calculations, were collated from the fundamental heat transfer equations and fluid flow equations outlined in the preceding chapters. Please refer to the reference for sources of these equations.

ii.   Structural Calculations: were developed, using fundamental equations to determine the stresses in the heat exchangers as a result of pressure loading only. The design strengths for the tubes and plates were obtained from the PD5500, with the appropriate factors of safety already worked in.

iii.   Weld Calculations: should enable the designer determine the volume of each weld and the load it can carry with respect to the current pressure loading.

iv.   Conversion tool: was designed for quick conversions between the SI and Imperial unit systems.

System Summary

This section provides information on the additional software that must be installed on the user's computer for full functionality of the toolkit. It also provides information on the disk size required for installation.

System Configuration

The toolkit is designed to operate on computers running on a Microsoft Operating System. It has not been tested on any other OS. It is compatible with Microsoft Office 2007 and higher versions. The toolkit requires Microsoft Excel in order to run because it is written in the Excel Visual Basic for Applications (VBA) code, Microsoft Word for saving results and most importantly, connection to the thermal fluids database Reference Fluid Thermodynamic and Transport Properties (REFPROP), which it requires for extracting the thermal properties of fluids used in the heat exchanger sizing calculations. REFPROP is a standalone program, which must be installed on any computer system prior to installing the design toolkit.

Internet connection is not required for functionality of this design toolkit.

User should have a disk space of roughly, 1.00 MB (1,056,768 bytes) on their computer for installation.

User Access Levels

Anyone can use this toolkit, so long as they have the Microsoft Office Application and the REFPROP program installed on their computer system.

Getting Started

This section describes where the toolkit can be obtained, and how to install it on the users' computer system. This section also presents briefly, the individual menus of the tabs in the toolkit.

Installation

The toolkit can be obtained by copying the main Excel spreadsheet files from any computer system it has been installed. This can be transferred via any storage device to the new computer bearing in the mind the minimum system requirements mentioned earlier. To transfer, highlight and copy all the Excel

workbooks. Create and name a folder in your personal computer system, preferably in the Documents Folder. Paste the copied Excel workbooks within this folder.

Double click on any of the workbooks to activate. The toolkit GUI should immediately appear. The Excel spreadsheet might issue a warning to enable or disable the Macros, user must enable this function.

For cases where the calculations have already been executed, and the graphic user interface closed, the toolkit can be "called" by clicking the buttons situated on the spreadsheets labelled 'Sizing'. The figure below shows what this button looks like.
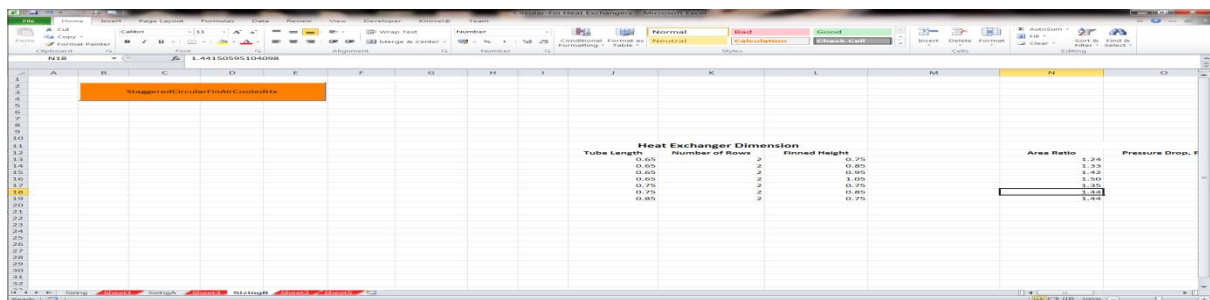

Figure 38: Toolkit activation button

System Menu

This design tool is a tab styled application, which consists of 4 tabs. The first tab called **Heat Exchanger Design**, handles the thermal design of the heat exchangers. The second tab called **Structural Calculations** handles basic structural analysis of the heat exchanger parts. The third tab called **Weld Calculations** is used to calculate the volume or area of weld configurations and checks to ensure that they can bear the pressure load of the fluid. The final tab called **Conversion Tool** is used to convert values from one unit system to the other. The unit systems in this section include the SI and Imperial system of units. The outline of each individual tab is further described. Figure 34 below shows an outline of these tabs.

Figure 39: Design tabs available within toolkit

Heat Exchanger Design Tab:
The Heat Exchanger Design tab consists of 83 possible input fields, with 14 output fields. Please note that not all these output fields, will have results as they are dependent on the design option selected. The number of input fields made available to the designer, is also dependent on the selected design option. Design option selection and its effects, are further explained in the next section. Below the input

fields, an execute button has been attached. Figure 40 below shows this tab. But please note that this GUI is different for each of the 3 different heat exchanger types.
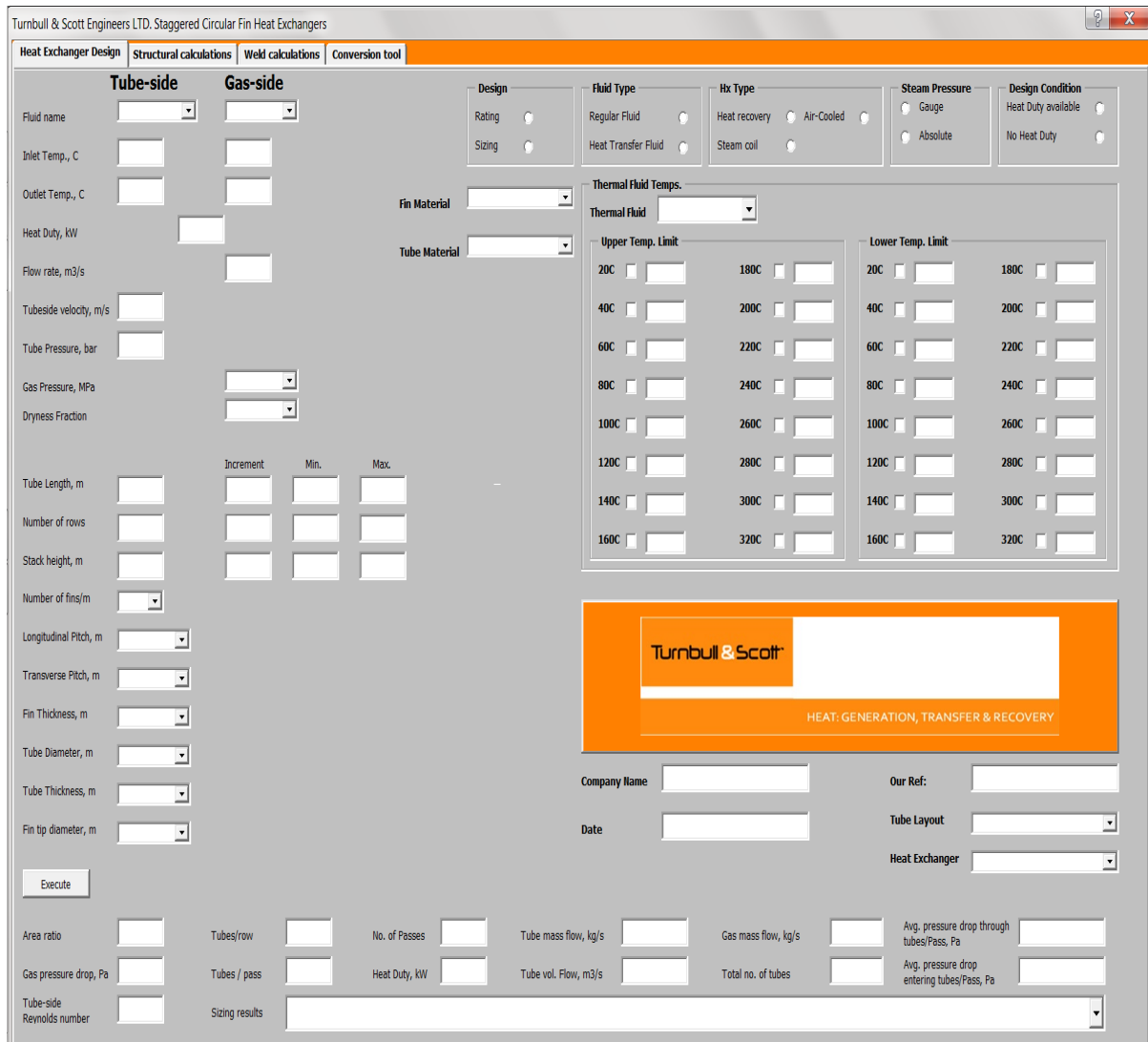

Figure 40: Heat exchanger design Graphic User Interface (GUI)

Structural Calculations Tab

The Structural Calculations tab consists of 36 possible input fields, with 19 output fields. The number of input fields made available to the designer, is also dependent on the selected design option. Design option selection and effects are further explained in the next chapter. Unlike the Heat Exchangers Design tab, all 19 output fields are expected to produce results for every calculation run. An execute button lies below the last input field. A screenshot of this tab is displayed below (Fig. 36) and is common to all the heat exchanger types.

Figure 41: Heat exchanger structural calculations Graphic User Interface (GUI)

Weld Calculations Tab

The Weld Calculations tab, consists of 3 sub-tabs named; Fillet Weld, Butt Weld and Bevelled Butt Weld. Each sub-tab has a combination of option buttons, and input fields, with an output field section. Each sub-tab, has an execute button to execute calculations for that particular sub-tab. A screenshot is shown below (Fig. 41).
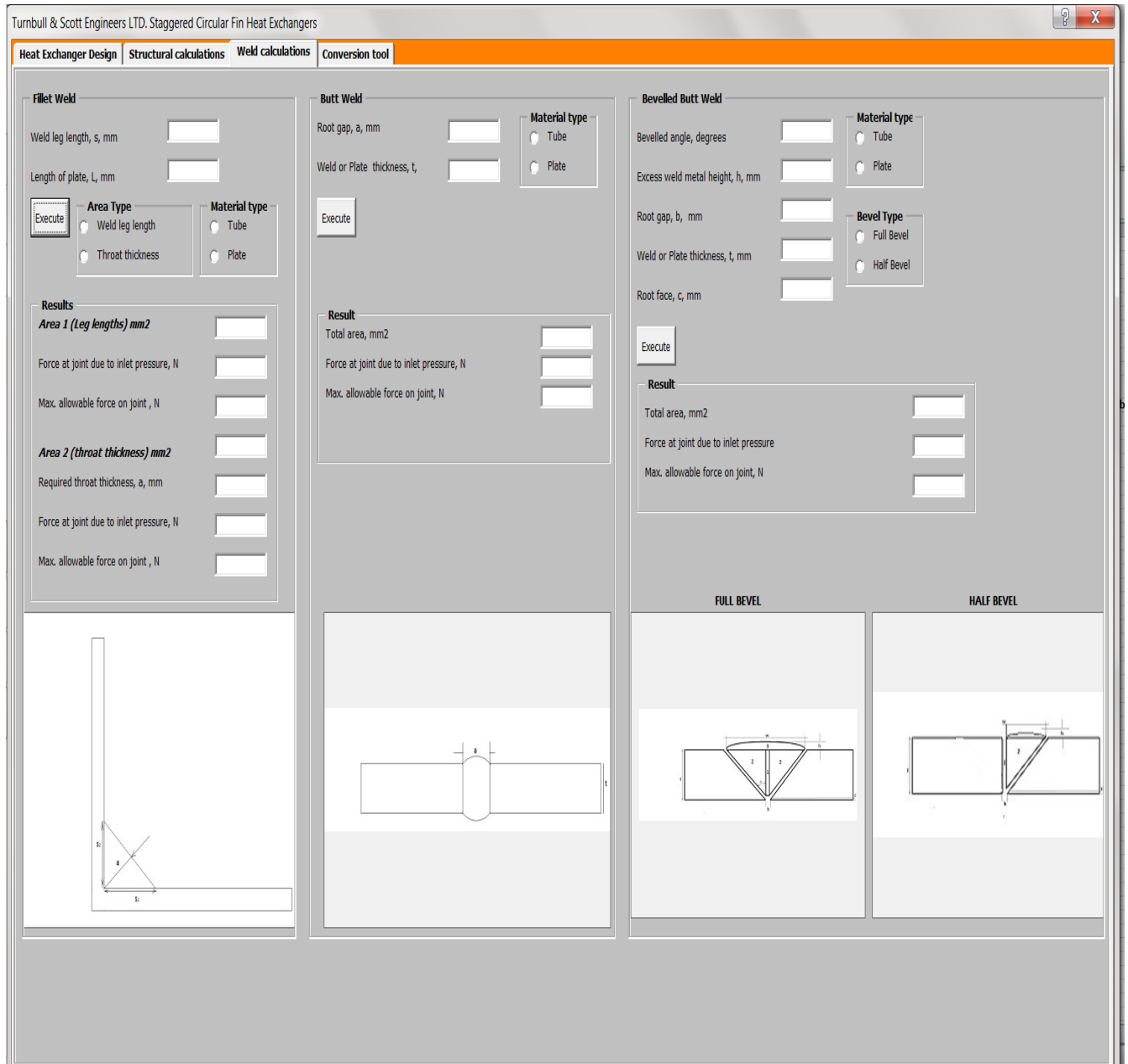
Figure 42: Heat exchanger weld calculations Graphic User Interface (GUI)

Conversion Tool Tab

The Conversion Tool tab consists of 5 sub-tabs, namely; Length, Pressure, Temperature, Volume Flow Rate and Power or Heat Flow Rate. Each sub-tab contains 1 input field, 1 output field, and a number of option selection buttons arranged on the right-hand-side and left-hand-side of each of the boxes. Figure 42 below shows what the tab looks like, and it is common to all the heat exchanger types.
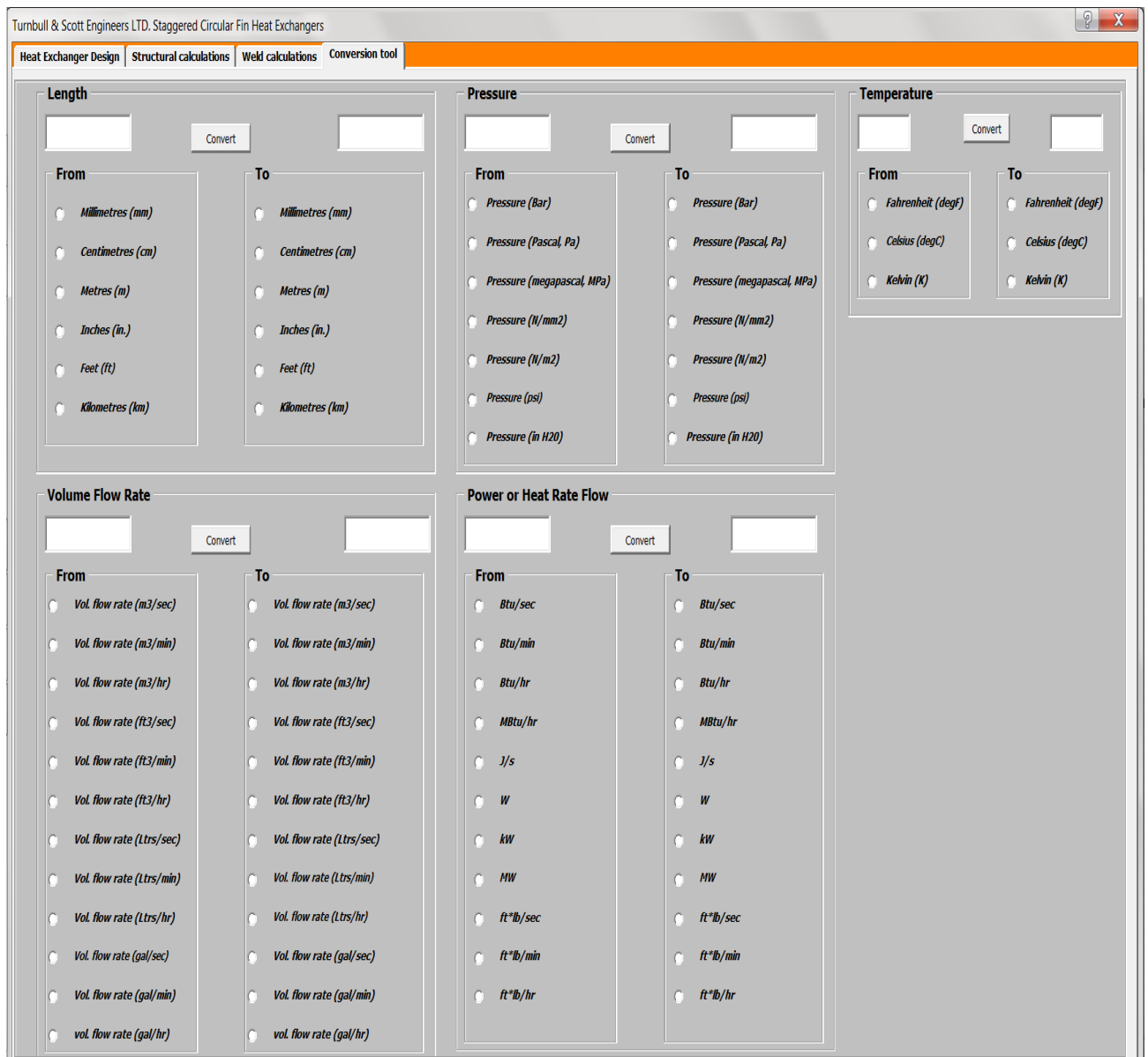
Figure 43: Heat exchanger conversion tool Graphic User Interface (GUI)

Using the System

This section provides a detailed description of the toolkit and its functions. It concludes with an exercise which potential designers should try in order to familiarise themselves with the toolkit and its functions.

Thermal Design:

Thermal design begins with the designer deciding on the configuration of the heat exchanger. The configurations available include:

i.   Circular – Fin Heat Exchangers: These heat exchangers are made with circular fins attached to each tube. These fins are made of metal strips, which are tension wound around the tubes to form the fins. In some cases, the heat exchanger tubes are bought with the fins already attached by the manufacturer.

ii.   Plate – Fin Heat Exchangers: Also called tube-in-plate heat exchangers, these heat exchangers are also extended surface type heat exchangers. However, rather than having circular fins, their fins are rectangular thin plates mostly made of aluminium. These plates have holes drilled in them, and the tubes passed through the drilled holes and then expanded. Hence, the tubes share common fins rather than have individual fins.

iii.   Plain Tube Heat Exchangers: These heat exchangers have no extended surface and are manufactured plain with no extended surface.

These configurations exist as separate workbooks, and the correct configuration must be selected from one of the workbooks in the design folder earlier created.

Heat Exchanger Design Tab

Note: It is advisable to have this spreadsheet already pulled up on the user's screen. This will make it easier to work through this section.

Upon selection of the heat exchanger type, designer is presented with a graphic user interface similar to Fig. 40. The appropriate sub-tab options at the upper-right-hand corner must first be selected before the options at the left-hand side are chosen. These sub-tabs are listed below, with their functionalities explained:

i.   Design: Consists of 2 option buttons labelled:

-    Rating: The Rating option button should be selected when the designer has the exact values for tube length, number of rows and the stack height (finned height) for the desired heat exchanger. The designer will be checking to see that the proposed configuration can deliver the desired duty. In another instance, the designer might be restricted already by the duct dimensions into which the heat exchanger will be installed. Either way, selection of this option, renders the boxes labelled; Increment,

Min. & Max; invalid for numerical input. These are the only fields affected by this selection.

When this option is selected, the designer is required to input numerical values for Tube length, Number of tube rows and the Stack height of the heat exchanger.

These values must be in the SI unit system. The stack height will in this case, refer to the distance measured across the face of the heat exchanger.

- **Sizing:** The Sizing option button should only be selected for cases where the designer is most importantly not restricted by space. It could also be selected when the designer is undecided about the heat exchanger geometry which includes: Tube Length, Number of rows and Stack or Finned Height. When this option is selected, the fields next to tube length, number of rows and stack height, are rendered invalid for numerical value input. The fields under Increment, Min. and Max, then become available for input.

When this option is selected, the designer must define the incremental values desired, the minimum value desired, and finally the maximum value. For example, the designer could decide to increase the tube length by 0.1m, starting from a minimum of 0.82m to a maximum of 1.02m. This means that calculations will be carried out for cases where the tube length is 0.82m, 0.92m, and 1.02m. Although restrictions on increment do not exist, it is advisable to choose workable increments, minimum and maximum values.

ii. **Fluid Type:** Within this sub-tab, are option selection buttons for:

- **Regular fluid:** This button refers to all types of fluids that are not Heat transfer Fluids, which are usually in the form of oils. It also refers to any fluid found in the drop down menu titled "Fluid Name" at the left-hand-side of the interface. When this option is selected, the drop-down menu labelled Fluid name, becomes valid for fluid selection, while the tab titled Thermal Fluid Temps, will become completely invalid for fluid selection.

- **Heat Transfer Fluid (HTF):** This option should be selected when the tube-side fluid is heat transfer oil and not found within the drop down menu titled "Fluid Name". When selected, the Thermal Fluid Temps. Tab becomes available for selection, while the drop down menu labelled Fluid name at the top-right-hand-corner becomes invalid for selection.

iii. **Hx Type:** This tab enables the designer select the main function of the heat exchanger. The available option buttons included, include:

- **Heat recovery:** occurs when the outside fluid is at a higher temperature than the tube-side fluid. These heat exchangers are used to recover heat from the outside fluid and

this heat is transferred to the tube-side fluid. This is quite common in flue stacks. It must be highlighted that results produced in heat recovery conditions using this toolkit, are not entirely accurate as the thermal properties of flue are unavailable and are quite different from the properties of ordinary air. When this option button is selected, the Steam Pressure tab becomes inactive.

- **Air-Cooled:** occurs when the tube-side fluid is at a higher temperature than the outside (gas-side) fluid. Most times, the designer seeks to lower/cool the temperature of the tube-side fluid. It should be noted that in this notation, it is assumed that the **Air-cooled** and **Heat recovery heat exchangers,** use single phase fluids e.g. water at the tube side. When this option button is selected, the Steam Pressure tab becomes inactive.

- **Steam coil:** Here, the tube-side fluid is predominantly steam and the outside fluid, possibly air. When this option button is selected, the Steam Pressure tab becomes active. Also when selected, the input fields for Tube-side **Inlet and Outlet Temps** become inactive. The designer only has to input the supply pressure at the Tube Pressure field.

iv. **Steam Pressure:** When the designer selects the Steam coil option and this tab becomes active, he must decide whether the steam values were supplied in Gauge or Absolute conditions.

- When Gauge conditions are selected, an approximate value of 1 is added to the steam supply pressure, and thermal properties are read at this value. The value of 1 is an approximation of atmospheric pressure, which is roughly 1.01325bar. E.g. steam at 3bar gauge, will have a temperature of 143^0C.

- Absolute conditions are selected only when the designer is completely sure that the steam values are supplied in absolute condition. This is because as mentioned above, the thermal properties are bound to be different. Still using the example from above, temperature at 3bar absolute will be 133.5^0C.

v. **Design Condition:** Has 2 options buttons labelled;

- **Heat Duty Available:** which simply refers to the instance where for the gas-side fluid, the manufacturer has only supplied a desired heat duty and the outside (gas-side) fluid inlet temperature. When this option is selected, the **Gas-side Outlet Temp** field becomes inactive, and the **Heat Duty** field becomes active. Designer must then supply the inlet temp of the gas-side fluid, and the desired heat duty.

- **No Heat Duty:** in this condition, the designer has both inlet and outlet temp values for the gas-side fluid. When this option is selected, a reverse of the condition above occurs.

The **Outlet** field of the Gas-side fluid temp becomes active, while the **Heat Duty** field becomes inactive. Designer must then supply these 2 values.

vi. **Thermal Fluid Temps:** In the 2nd tab described above, the designer is presented with the Regular Fluid & Heat Transfer Fluid options. When the Heat Transfer Fluid option is selected, this tab becomes available for selection. Thermal fluids are mostly oils used as the tube-side heat transfer medium. Within this tab, 3 options are available, which must be filled by the designer.

- **Thermal Fluid:** This exists as a drop-down menu, from which the designer must select the desired thermal fluid.

- **Upper Temp. Limit:** is a combination of numerical values, check boxes and output fields. In this section, the designer simply has to check the box corresponding to the temperature just greater than the thermal fluid upper temperature. In the output field, the density of the thermal fluid at that temperature will be displayed. This acts as a check, to ensure that thermal property values exist at that temperature for that fluid. For example, if the thermal fluid is supplied at 83^{0}C, then the designer must select 100^{0}C as the upper temp limit value. In cases where there are no values for the selected temperature, an error message in the form of **"Fluid properties are not available for … Please try the next lower or higher value"**. When this happens, designer only has to check the box for the next higher value. However, if the Fluid is supplied at 80^{0}C, then designer must first select 80^{0}C at the table. This is because, the large the distance between the interpolated, the larger will be the deviation for the final answer.

  Note that when the thermal fluid is changed, the appropriate check box must be unchecked and checked again, to ensure that the properties actually exist at that temperature. This should only be done when the thermal fluid has been changed.

- **Lower Temp. Limit:** Designer must select the temperature values lower than that for the outlet temperature of the thermal fluid. For example, if the fluid exits at 65^{0}C, then the designer must select the Lower Temp. Limit at 60^{0}C. All other factors as seen in the Upper Temp. Limit case, are also applicable. Most importantly, if the thermal fluid is changed, the appropriate check box must be unchecked and then checked again to ensure that the properties exist at that temperature.

  PLEASE NOTE THAT THIS FIELD IS ONLY AVAILABLE FOR THE THERMAL DESIGN OF CIRCULAR-FIN HEAT EXCHANGERS. IT IS NOT AVAILABLE FOR THE PLATE-FIN AND PLAIN TUBE HEAT EXCHANGERS DESIGN TOOLKIT.

vii.   **Fin Material:** is the drop-down menu from where the designer must select the material from which the fins of the heat exchanger are to be made. Please note that this option does not exist for the **Plain Tube heat exchanger design tool**. Designer must select a material from this list before the execute button is activated.

viii.   **Tube Material:** is the drop-down menu of materials from which the heat exchanger tubes will be made from. Designer must select a material from this list before the execute button is activated.

ix.   **Tube-side conditions:** Refers to parameters pertaining to the tube-side fluid.

- **Fluid name:** is the drop-down menu, from which the fluid at the tube-side will be selected. This option becomes invalid for selection, when the **Heat Transfer Fluid** option under **Fluid Type** is selected. However, when the **Regular Fluid** option is selected, this option once again becomes valid for selection.

- **Inlet Temp:** is the field where the inlet temperature of the tube-side fluid must be indicated. **Please note the units for each term and ensure that whatever value you are calculating for, corresponds to this unit.** For temperature, the units are all in Degrees C (^{0}C).

    Also note that when the **Steam Coil** option in the **Hx Type** tab is selected, this field becomes invalid for selection.

- **Outlet Temp:** is the field where designer should indicate the outlet temperature of the tube-side fluid. However, also note that when the **Steam Coil** option in the **Hx Type** tab is selected, this option will become invalid for selection, and only becomes valid when either the **Air-Cooled** or **Heat Recovery** options are selected.

- **Tube-side velocity:** in this field, the designer must decide at what velocity he wants the tube-side fluid to flow per tube. This value should ideally be anything from **0.5m/s – 1.0m/s** for water. This will ensure that the flow is sufficiently turbulent to get the best heat transfer. For thermal fluids, this value will be considerably higher as a result of the viscosity of thermal oils. Note that when the **Steam Coil** option is selected, this field becomes invalid for selection.

- **Tube Pressure:** refers to the supply pressure of the tube-side fluid and must be supplied for both **Fluid Type** and **Hx Type** conditions. When the **Steam Coil** option is selected, designer must be careful to indicate whether the supply pressure is in **Gauge** or **Absolute** conditions.

x.   **Gas-side conditions:** Refers to parameters pertaining to the gas-side fluids. That is, fluids flowing on the outside of the tubes.

- **Fluid name:** is the drop down menu from where the name of the gas-side fluid is selected. This field is not rendered invalid under any condition, and must always be selected.

- **Inlet Temp:** indicates the inlet temperature of the gas-side fluid. As mentioned earlier, this must be in Degrees C (^{0}C). This field is not rendered invalid under any circumstance, and must be filled before the execute button is pressed.

- **Outlet Temp:** this field is made available for the designer to input the desired outlet temp of the gas-side fluid. However, when the **Heat Duty available** option is selected, this field becomes invalid for selection and only becomes valid for selection when the **No Heat Duty** option is selected.

- **Heat Duty:** When the **Heat Duty available** option is selected, the designer will be required to state the appropriate heat duty in kilowatts (kW). This option becomes invalid when the **No Heat Duty** option is selected. Please note that the unit system used here is SI.

- **Flow rate:** Refers to the volumetric flow rate of the gas-side fluid. This value must be obtained from the manufacturer, and supplied before calculations are executed.

- **Gas Pressure:** refers to atmospheric pressure. This value is required for obtaining the thermal properties at the gas-side. This field exists as a drop down menu and is already set at 0.101325MPa. However, if atmospheric conditions do not correspond to this value, designer is free to manually input the correct values. However, he must be careful to ensure that they are in Megapascals (MPa).

- **Dryness Fraction:** refers to the extent of dryness of the steam. This option only becomes available for selection when the Steam Coil option is selected. It is currently set at 0.99, which assumes that the steam is almost 100% dry. But in reality, the steam might be less. If the dryness fraction value is supplied by the manufacturer, the designer is at liberty to change it, simply by typing in the value in this field.

xi. **Hx Geometry:** This tab enables the designer select all parameters related to the heat exchanger geometry. These include

- **Tube Length:** refers to the desired length of each tube. When the **Rating** option is selected, only the first field becomes available for selection, and the designer is only required to input a single value for the tube length. The other fields under **Increment, Min** and **Max**, become invalid for selection. However, when the **Sizing** option is selected, the reverse occurs. The first field becomes invalid for selection, and the fields under **Increment, Min** and **Max**, become available for selection. Designer must then

indicate what he desires his incremental values to be, at what minimum value the calculation should start and at what maximum value they should end. Please note that the tube length units are in meters (m).

- **Number of rows:** refers to the number of rows desired in the heat exchanger. When this value is certain, the designer sets it simply by selecting the **Rating** option as explained earlier. However, if this value is not known for certain, then the **Sizing** option is to be selected and the same procedure as described above must be followed.

- **Stack height:** also referred to as the finned height, refers to the length measured across the face of the heat exchanger, perpendicular to the direction of the incoming gas-side fluid. Just as before, when this value is known beforehand, such as when the heat exchanger is to be fitted in a duct, the designer simply supplies this value within this field. However, when this is not for certain, the **Sizing** option should be selected and the same procedure followed for the **Tube Length** and **Number of rows** method stated above. Calculations are executed in meters (m) for this value.

  Note: The sizing option is only applicable to the three (3) parameters; Tube Length, Number of rows and Stack height mentioned above.

- **Number of fins:** refers to the number of fins per tube required in the heat exchanger. Designer must note that rather than the traditional fins per inch (F.P.I), these values have been changed to fins per meter (F.P.M). Also, this field is not affected or rendered invalid by selecting any of the tabs described above. This field is currently in the form of a drop-down menu from which designer simply selects an appropriate value. When the values indicated are outside the values desired by the designer, he is at liberty to input the appropriate figures. This option is unavailable for the design of plain tube type heat exchangers.

- **Transverse Pitch:** refers the distance measured from one centreline to the other of two tubes, along the distance perpendicular to the direction of flow of the gas-side fluid. This field exists as a drop down menu, with values already made available in meters (m). However, if the designer wishes to change them, he is free to do so simply by typing in the values manually. Transverse Pitch values, apply to all heat exchangers; Circular-fin, Plate-fin and Plain tube.

- **Longitudinal Pitch:** refers to the distance measured from one centreline to the next of two tubes, along the distance in the direction of flow of the gas-side fluid. This field exists as a drop down menu, with values already made available in meters (m). However, if the designer wishes to change these, he is free to do so simply by typing in

the values manually. The Longitudinal Pitch values apply to all heat exchangers; Circular-fin, Plate-fin and Plain tube heat exchangers.

- **Fin thickness:** refers to the thickness of the fins. This applies to just the Circular and Plate fin type heat exchangers. This field is unavailable for the plain tube heat exchanger. Designer is required to select the fin thickness value from an available drop-down menu. If the desired values are not in this list, he can provide them manually.

- **Tube Diameter:** refers to the outside diameter (OD) and not the nominal bore (NB) of the tube. An already populated drop-down menu is available for the designer to select an appropriate value. However, he is also at liberty to input a desired figure, if it is not found within this list.

- **Tube thickness:** refers to the thickness of the selected tube. Again, this already exists as a prepopulated drop down menu, which designer can choose to ignore and manually input his desired figures. However, note that these values are in meters (m).

- **Fin tip diameter:** refers to the overall diameter of the fins attached to the tubes. This field is absent for plain tube heat exchanger types. It is also available as a prepopulated drop down menu which can be overridden by the designer with desired values.

xii. **Execute:** is the button which must be depressed in order to activate the calculation process. **DESIGNER MUST ENSURE THAT ALL THE REQUIRED FIELDS HAVE BEEN CORRECTLY FILLED BEFORE THIS ACTION IS PERFORMED.**

xiii. **Results:** Relates to all fields below the **EXECUTE** button. All the fields except the **Sizing results** field are almost all populated when the **Rating** option is selected. However, when the **Sizing** option is selected, these fields become void except the **Sizing results** field. The fields and meanings are described below:

- **Area ratio:** This field offers the designer a comparison between the actual areas of the current configuration of the heat exchanger to the area required to meet the specified heat duty. Designer should aim to get this ratio to at least 1.10, which would be interpreted as being that "the actual area based on the current heat exchanger configuration from calculations, is 10% greater than the area required to meet the specified heat duty". This value should always be slightly greater than 1, in order to accommodate calculation errors.

- **Tubes/row:** This field tells the designer the number of tubes required for each row of the heat exchanger. As a result of approximations encountered in design, designer might need to approximate sometimes for this value.

- **No. of Passes:** Tells the designer, the number of passes required in the heat exchanger. When the Steam Coil option is selected, this field is void as all steam coils are designed with a single-pass configuration. As mentioned earlier, due to approximation issues encountered during calculations with Microsoft Excel, the number of passes might not tally entirely with the **total number of tubes**, **Tubes / Pass** and **Tubes / Row.** Please note, that this does not render the calculations invalid at all. Designer will only have to use his discretion to either approximate by adding an extra tube, to ensure that each pass contains the same number of tubes, or remove the extra tube in order to achieve the same purpose.

- **Tube mass flow rate:** refers to the mass flow rate of the tube-side fluid. This value is calculated from the inlet and outlet temperatures of the tube-side fluid, earlier specified before the calculation was executed. This must not be confused with the volume flow rate of the tube.

- **Gas mass flow rate:** refers to the mass flow rate of the gas-side fluid. Designer must also not confuse this with the value for the volume flow rate of the fluid.

- **Avg. pressure drop through tubes/Pass:** is the pressure drop experienced per pass by the fluid, as it flows through the tubes. Designer should take note that this is expressed in Pascal, Pa. Please note that for the **Steam Coil** heat exchanger design, this value, is not calculated. It exists only for single phase fluid condition.

- **Gas pressure drop:** is the pressure drop experienced by the gas-side fluid, as it flows across the heat exchanger. This value is produced for all the heat exchanger types; Circular-fin, Plate-fin and Plain tube.

- **Tubes / pass:** Value produced in this field, tells the designer how many tubes will be segregated for each pass. As mentioned in the No. of Passes section, this value might not entirely correlate with the **total number of tubes**, **Number of passes** and **Tubes / Row.** Designer must ensure that the results are as accurate as possible. For **Steam Coil** conditions, this value is also void.

- **Heat Duty:** Field indicates the heat duty required from the heat exchanger. For cases where the **Heat Duty Available** option has been selected, a result is still produced in this field. This acts as further confirmation that the proper heat duty is being calculated.

- **Tube vol. Flow:** is the volume flow rate value for the tube-side fluid. This value is different from the tube-side mass flow rate, and must never be confused with it.

- **Total no. of tubes:** is the total number of tubes in the heat exchanger bundle.

- **Avg. pressure drop entering tubes/Pass:** is the pressure drop experienced by the fluid as it enters each tube for each pass.

  NOTE: DESIGNER MUST EVALUATE THE TOTAL PRESSURE DROP PER PASS AND THROUGH THE TUBES, FOR THE TOTAL NUMBER OF PASSES, AND ENSURE THAT THIS VALUE IS BELOW THE SUPPLY PRESSURE AT THE TUBE-SIDE. IF THIS VALUE IS HIGHER THAN THE SUPPLY PRESSURE, PROBLEMS WILL BE EXPERIENCED WITH THE HEAT EXCHANGER AS THE EXCESSIVE PRESSURE DROP WILL HINDER FLUID FLOW.

- **Tube-side Reynolds number:** indicates the Reynolds number for the fluid at the tube-side. When this value exceeds 50'000, a warning message flashes to indicate that the fluid is too turbulent. When it is below 10'000, a warning message also flashes indicating that flow is too laminar to ensure proper heat transfer. In the first condition, designer should lower the value of the velocity of fluid flow and in the second condition; designer should increase the tube-side fluid flow velocity.

- **Sizing results:** When the Sizing option is selected in the **Design** tab, appropriate fields populated and the execute button clicked. The **Tube Length** will be increased from the minimum to the maximum value as specified in the **Increment** section. The same process is carried out for the **Number of rows** and **Stack height** sections. These values are then inserted into the spreadsheet, incrementally and results produced. E.g. when the tube length is increased from 0.85 (min.) to 0.92m (max.) at intervals of 0.1m , the values produced are 0.85m, 0.86m, 0.87m, 0.88m, 0.89m, 0.90m, 0.91m and 0.92m. Each of these values is then placed in the heat transfer equations and results for when the tube length is 0.85m – 0.92m, are produced. The calculations have been written, to delete all **Area Ratios** below 1.0 and above 1.5. This will enable the designer make a quick decision as to what configuration best suits his manufacturing process. Selected configuration must also conform to the manufacturer's requirements, e.g. allowable pressure drop in heat exchanger.

  When a configuration is selected, the designer heads back to the **Design** tab and changes it to from **Sizing** to **Rating.** The **Increment, Min and Max** fields become invalid for selection, while the fields right of **Tube Length, Number of Rows and Stack height** become valid for selection. Designer must then insert the chosen configuration in these fields and click the **Execute** button. Figure 44 shows a typical sizing calculation and the results produced.
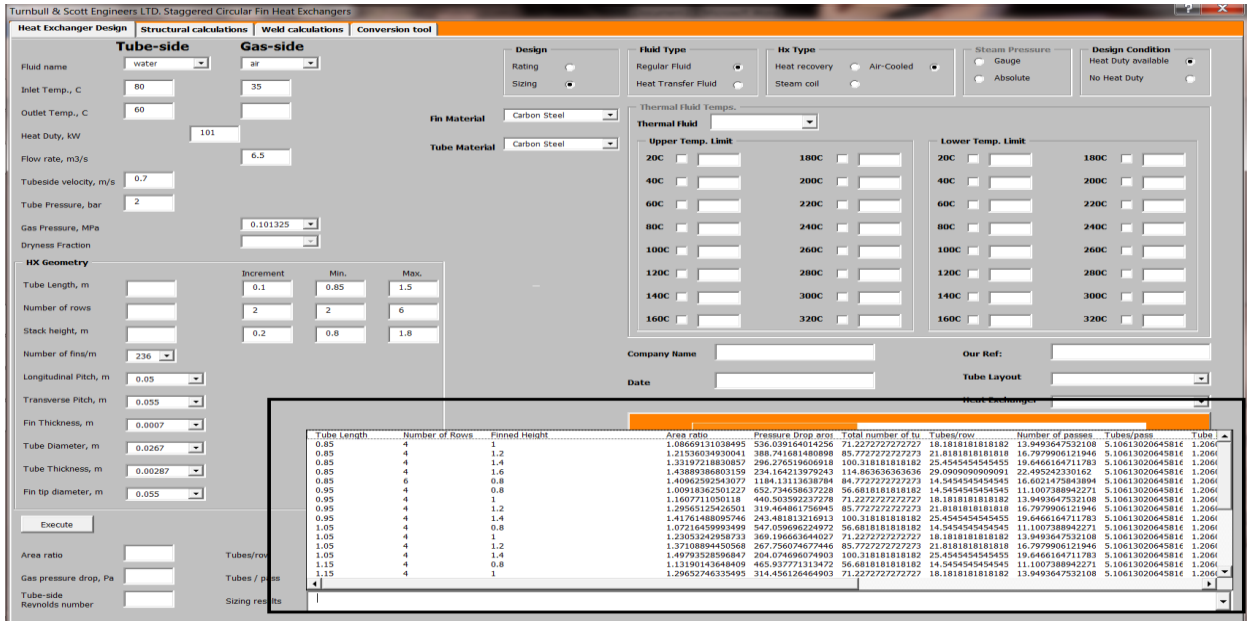
Figure 44: Display of results from a Sizing calculation process

xiv. **Miscellaneous Information:** This would refer to information found just below the **Thermal Fluid Temps**. Table. It contains the following details related to the heat exchanger, and is only useful for documentation purposes. Calculations can be executed without completing these fields;

- **Company name:** Designer is required to fill the client's company name in this field.

- **Date:** Current date of the design is filled in this field.

- **Our Ref:** A reference number for traceability purposes is penned here

- **Tube Layout:** This is a prepopulated field with only one option; the staggered tube layout option or in the case of plain tubes, an inline layout option.

- **Heat Exchanger:** The designer will select the option of defining the heat exchanger as; a steam coil, heat recovery, or air-cooled heat transfer equipment

Thermal Design Demonstration:

Scenario 1

A client Starship Enterprise has tasked the designer with sizing/designing a heat exchanger bundle based on the parameters listed below.

Data:

Air volume flow-rate	$= 5.5 m^3/s$
Duct size	$= 0.85 \times 1.11$ m (L x B)
Heat duty required	$= 100kW$
Inlet air temperature	$= 30^0C$ (possibly ambient)
Heat exchanger type	$=$ Circular-fin
Tube-side fluid	$=$ Water

Gas-side fluid   = air

Solution:

Based on preferred in-house manufacturing dimensions, designer has selected the following parameters for the design.

Transverse pitch   = 0.055m
Longitudinal pitch   = 0.050m
Tube OD   = 0.0267m
Tube thickness   = 0.00287m
Fin material   = Carbon steel
Tube material   = Carbon steel

Step 1: Since the duct dimensions have already been given, heat exchanger dimensions (length & breath) will have to conform to it. Therefore this will be a rating exercise and the designer selects the **Rating** option under **Design.**

Step 2: The **Regular fluid** option button is selected under the **Fluid Type** heading, since the fluid type is water. This renders the **Thermal Fluid Temps,** option box invalid.

Step 3: Select the **Air-Cooled** option under **Hx Type.** This action renders the next field invalid.

Step 4: Select the **Heat Duty available** option under the **Design Condition** box. This is because we have been given the desired heat duty, an inlet air temperature, but no outlet air temperature.

Step 5: Under the **Tube-side** heading, input the following values under the appropriate headings:
    Fluid name   = Water
    Inlet Temp   = 80
    Outlet Temp   = 60
    Heat Duty   = 100
    Tube-side velocity = 0.45
    Tube Pressure   = 2

Step 6: Under the **Gas-side** heading, input the following values under the appropriate headings:
    Fluid name   = Air
    Inlet Temp   = 30
    Outlet Temp   = should have been rendered invalid because **Heat Duty** available was selected earlier, so ignore it.
    Flow rate   = 5.5
    Gas pressure   = 0.101325MPa
    Dryness Fraction   = has been rendered invalid because **Air-Cooled** option was   selected earlier.

Step 7: Under the **HX Geometry** heading, select the following values under appropriate headings:
    Tube Length   = 0.85
    Number of rows   = 4
    Stack height   = 1.11
    Number of fins   = 236

Longitudinal Pitch	= 0.05
Transverse Pitch	= 0.055
Fin Thickness	= 0.0004
Tube Diameter	= 0.0267
Tube Thickness	= 0.00287
Fin tip diameter	= 0.055

Step 8: Under the following headings, select the appropriate heat exchanger material

| Fin Material | = Carbon steel |
| Tube Material | = Carbon steel |

Step 9: Fill in the fields

Company Name	= Starship Enterprise
Date	= 25/04/2012
Our Ref	= T/S 001
Tube Layout	= Staggered
Heat Exchanger	= Air-cooled

Step 10: Ensure that all fields are filled with the correct values, click **Execute.**

Step 11: Results

Area ratio	= 1.08
Tubes/row	= 20
No. of Passes	= 10
Tubes mass flow	= 1.1942
Gas mass flow	= 6.4044
Avg. pressure drop through tubes/pass	= 101
Gas pressure drop	= 292
Tubes/pass	= 8
Heat Duty	= 100
Tube vol. Flow	= 0.001221
Total no. of tubes	= 79
Avg. pressure drop entering tubes/pass	= 141
Tube-side Reynolds number	= 22853
Sizing results	= Blank because the **Rating** option was selected earlier

Observations and Inference:

Step 12: At this point, the designer decides if the dimensions are favourable, and this is chiefly dependent on the **Area Ratio** value. This must always be above 1.0, but preferably below 1.5.

Step 13: The **Total no. of tubes** must agree with **Tubes/pass x No. of Passes**. In this case, total number of tubes is 79, and tubes/pass x no. of passes is 80. This value is almost acceptable, considering approximations expected in Excel.

Step 14: If the results in Step 2 are totally unacceptable, designer can alter the fluid-side flow velocity, to anything between 0.5 and 1. **Note,** fluid velocity is bound to be different for **Thermal fluids** as a result of viscosities. In either case, designer must ensure that flow is turbulent, i.e. the **Tube-side Reynolds number** must be above 10,000. This is to ensure good heat transfer and also correct use of the fluid equations on which the toolkit has been designed.

Step 15: If all conditions above are acceptable, designer can go ahead and save the Results that will be pulled up if the **Yes** option is selected. If not entirely satisfied, the **No** option is selected and the designer can go back and modify initial input values.

Scenario 2

The same company Starship Enterprise has supplied the same data except the duct dimensions. The designer is at liberty to decide those values.

Step A: Rather than select the **Rating** option under the **Design** heading, the designer selects **Sizing**.

Follow through all processes till Step 7 (from above)

Step 7:

	Increment	Min.	Max.
Tube Length	0.1	0.85	1.15
Number of rows	1	2	6
Stack height	0.1	0.9	1.2

Please note that all other values remain as before

Follow through all other steps to **Step 11**

Step 11: Results

All fields become empty, and the **Sizing** field becomes the area of focus for the designer. It should resemble Fig. 44 below:
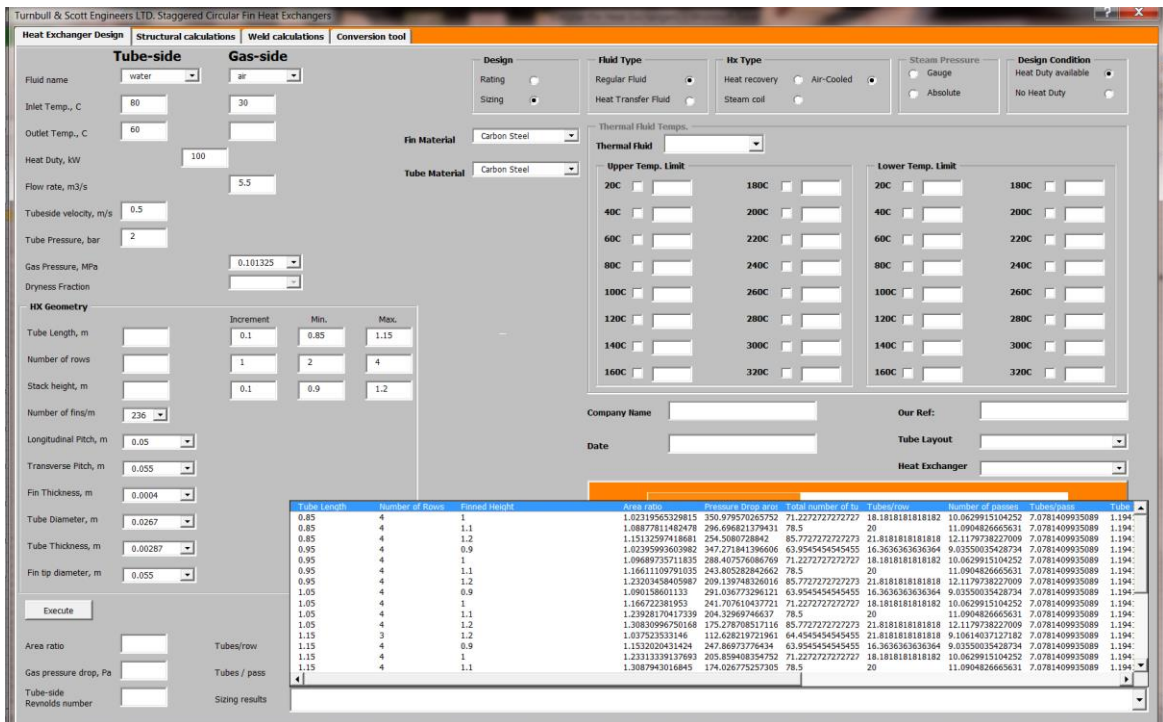
Figure 45: Sizing Results

Observations and Inference:

Follow through from **Step 12** – **Step 15**.

Step B: When the most preferred configuration has been selected, designer heads back to the **Design box,** to select the **Rating** option. Designer then fills the appropriate values in these sections, and executes, following through as before.

Structural Calculations Tab

For cases where the designer needs to ensure that the thicknesses of the materials used in the manufacture of the heat exchanger are suitable to hold the pressure loading from the fluid, he employs the use of the structural calculations tab. This is the second tab in the toolkit, and it functions independent of the other tabs:

- Provides the designer with minimum thickness requirements for the tubes and plates used in the heat exchanger manufacture.

- Provides the designer with the design strength for the materials used in the heat exchanger manufacture.

- Calculates the stresses experienced by the components as a result of pressure loading **from the fluids** only.

- Classifies the heat exchanger according to PED requirements.

When the structural calculations tab is selected, the designer is required to fill the following fields before calculations can be executed;

i. **Tube Dimensions:** This section covers all cylindrical shaped materials in the heat exchanger manufacture.

- **Tube grade:** This is exists as a prepopulated dropdown menu, from which the designer is required to select the grade of tube used in the manufacture. The designer **IS NOT** at liberty to fill in a desired tube grade because these materials were selected from the materials made available and recognized by the Pressure Vessel Code, PD5500. In addition to this, the PD5500 has made available design strengths for these materials with the appropriate factors of safety built in according to working temperature of the heat exchanger. Therefore if the tube materials used by the designer are not in the group provided, he must notify the senior design engineer.

- **Nozzle OD:** Designer is then required to select the inlet nozzle outer diameter (OD). Although this drop-down menu is already prepopulated with values, designer is at liberty to insert a value missing from the list. However, a corresponding DN value will not be available. Please note these values are in millimetres (mm) and refer to the Outer Diameter (OD) and not the Nominal Diameter (DN) of the inlet nozzle.

- **HX tube OD:** This refers to the outer diameter of the heat exchanger tubes, and this menu is exactly the same as the menu for the Nozzle OD. Same restrictions are also applicable.

- **Header OD:** Conditions applicable in the Nozzle and HX tube, are also applicable here, and should be treated as such by the designer.

- **Nozzle thickness:** Designer simply selects the thickness of the inlet nozzle. Designer can also populate this field with preferred data. Please also note that this field takes only values in SI units, millimetres (mm) to be exact.

- **HX tube thickness:** The same conditions seen in the nozzle thickness field are also seen here. Designer should also treat this field with the same restrictions as the nozzle thickness field.

- **Header thickness:** Same conditions are applicable as the field above.

ii. **Plate Dimensions:** refers to all plates used in the heat exchanger manufacture. These mostly include the tube-plate and the end-blanks. The fields found under this section include:

- **Plate grade:** Designer is required to select the grade of the plate material used for manufacture. As mentioned for the tube section, the designer **IS NOT** at liberty to fill in preferred materials, for the same reasons already explained in the tube section.

- **Plate thickness:** Designer only has to indicate the thickness of the plates used. Designer is at liberty to populate this field with his preferred values.

iii. **HX Dimensions:**

- **Longitudinal Pitch:** Designer selects the design longitudinal pitch from a prepopulated dropdown menu. Designer can also populate this field with preferred values.

- **Transverse Pitch:** Same conditions as in the longitudinal pitch field mentioned above, are also applicable in this field

- **Number of rows:** Number of rows in the heat exchanger is required in this field.

iv. **Fluid type:**

- **Design temp:** The designer will be required to specify the maximum tube-side fluid temperature that the vessel will experience while in service, within this field. This value must never be lower than the exit temperature of this fluid. Preferably, it should be slightly higher than the inlet temperature of the tube-side fluid.

- **Design pressure:** This field requires the designer to specify the supply pressure of the tube side fluid.

- **Steam:** When steam is the heat transfer medium at the tube-side, designer will be required to check this option button.

- **Water:** When water is the heat transfer medium within the tubes, then this option button should be checked.

v. **Temperature ranges:** Consists of 2 sub-tabs namely;

- **Tube temp range:** This tab is a combination of checkboxes and output fields. As earlier mentioned, the design temperature specified for structural calculations should be governed by the upper temperature of the tube-side fluid. Bearing this in mind, designer will be required to select two of the checkboxes, with the design temperature lying between these values. For example, if the upper design temperature is 170^0C, then the designer will be required to select the checkboxes for 150^0c and 200^0C.

  This is all the action required of the designer for this section.

- **Plate temp range:** Involves the same procedure as for the section described above. Please note that the temperature range selected for the plate temperature range must always be the same as selected for the tube temperature range. This is because, it is expected that the heat exchanger components will experience the same temperature increase. As mentioned earlier, the designer simply selects the appropriate check boxes for temperatures between which the design temperature lies.

vi. **Execute button:** This button is used to activate the calculations required for structural analysis. It should only be depressed when the designer has filled the input fields as described above.

vii. **Results:** This tab consists of 3 sub-tabs, which represent results obtained from the structural analysis calculation. They include:

  - **Design strength values:**

    ➤ **Tube design strength at design temp:** will give the designer, the strength of the tube material at the elevated working temperature of the heat exchanger. This value is interpolated from the design strength values for tube materials in Annex K of the PD5500 pressure vessel code.

    ➤ **Plate design strength at design temp:** producing the same values as above but only for plates, this section will give the strength values of the plate at its elevated working temperature. This information is also based on interpolated values from the PD5500.

    ➤ **Transverse stress in Nozzle:** gives the designer results for the transverse stress experienced by the nozzle, as a result of fluid pressure loading only. Calculations have been done, to ensure that if this value exceeds the design strength of the nozzle material at the design temperature, a warning message appears.

    ➤ **Transverse stress in HX tubes:** same as above, results are given for the primary stresses in the heat exchanger tubes as a result of fluid pressure loading only. If

this value exceeds the design strength of the material, a warning message is displayed. This follows guidelines according to the PD5500.

➢ **Transverse stress in Headers:** produces calculated results for stress as a result of pressure loading in the heat exchanger headers. The PD5500 guidelines have also been adhered to in calculating this value, and because it is a primary membrane stress, once it exceeds the strength of the material, a warning message is displayed to the designer.

➢ **Longitudinal stress in Headers:** This value shows the designer, the longitudinal stresses in the headers. Because this is not the controlling stress, often found to have less significant damaging effect when compared to the primary stress, it has been allowed to exceed the design strength by just 50%. When this value is exceeded, a warning message is displayed to the designer.

➢ **Transverse stress in tube-plate:** calculates the transverse stresses in the heat exchanger tube plate. It takes into account, the stress concentrations brought about by the tube holes drilled in the tube-plate.

- **Required material thickness:**

➢ **Nozzle minimum thickness:** Provides the designer with the minimum thickness required for the inlet nozzles, based on pressure loading only.

➢ **HX tube minimum thickness:** Provides the designer with the minimum thickness required for the heat exchanger tubes, based on pressure loading only.

➢ **Header minimum thickness:** Provides the designer with the minimum thickness required for the heat exchanger headers, based on fluid pressure loading only.

➢ **Plate minimum thickness:** Provides the designer with the minimum thickness required for tube-plate and the end blanks, based on fluid pressure loading only, in the plate's **unperforated condition**.

- **Other information:**

➢ **Plate length/diameter:**

➢ **Maximum allowable pressure:** Provides the maximum allowable pressure based on loading from the fluid only.

➢ **Vessel category:** According to the stipulations of the pressure equipment directive, each pressure vessel must be placed in a category defined by the nominal bore and pressure in the vessel. These categories include:

- **Sound engineering practice (SEP):** which simply states that the vessel must be manufactured according to sound engineering practice. These vessels must also not be CE marked and are not governed by strict design guidelines.

- **Category 1 (CAT I):** This category has more design and manufacturing fulfilments than the SEP category. When the vessel falls into this category, a warning message alerts the designer to the change in vessel category. The designer is then required to refer to the pressure equipment directive (PED) for the manufacturing requirements of this category.

- **Category 2 (CAT II):** it must be stated that the company's vessels hardly ever go as far as this category. However, when it does occur, the designer is given a warning message and the designer will have to refer to the pressure vessel code for the design and manufacturing requirements required from vessels in this category.

➢ **Tube material group:** provides the designer with the material group of the tube according to the tables in the PD5500. This group is also influenced by the material table in the BS 15609.

➢ **Plate material group:** Also gives the designer, the material group of the plates used in the HX manufacture.

➢ **Nozzle nominal diameter:** provides the nominal diameter of the inlet nozzle, which should be noted as being different from the inlet nozzle OD.

➢ **Header nominal diameter:** provides the nominal diameter of the heat exchanger headers, which is different from the inlet nozzle OD.

➢ **Hx nominal diameter:** provides the nominal diameter of the heat exchanger tubes.

Structural Calculation Demonstration:

Based on the results obtained earlier, designer may wish to determine the stresses set up in the system as a result of pressure loading. At this stage, designer must have decided on more dimensions for the heat exchanger parts such as the headers and the tube sheet/plate thickness. He must have also decided the material grades from which the tubes and the plates will be formed.

The material grades have been selected for demonstration purposes only.

Step 1: Select the **Structural Calculations tab.**

Step 2: Under the **Fluid Type** heading, designer will select the **Water** option button

Design temp   = 80
Design Pressure   = 2
Steam Pressure   = becomes void, because water option was selected.

Step 3: Under the **Material** option, select **Steel.**

Step 4: Under the **Tube Dimensions** option,

Tube grade	= BS 3601 - 430
Nozzle OD	= 26.7
HX tube OD	= 26.7
Header OD	= 168.3
Nozzle thickness	= 2.77
HX tube thickness	= 2.87
Header thickness	= 3.2

Step 5: Under **Plate Dimensions**

Plate grade	= BS 1501 – 1 – 151, 161, 430
Plate thickness	= 8

Step 6: Under **HX Dimensions**

Longitudinal Pitch	= 50
Transverse Pitch	= 55
Number of rows	= 4

Step 7: Under the **Temperature ranges** tab,
Check the boxes for **Design strength @ 50^{0}C** and **Design strength @ 100^{0}C**   **(Tube temp. range)**
Check the boxes for **Design strength @ 50^{0}C** and **Design strength @ 100^{0}C**   **(Plate temp. range)**

Step 8: Ensure all fields are have been filled appropriately, and then click the **Execute** button**.**

Step 9: Results

Tube design strength @ design temp	= 172.8 N/mm^2
Plate design strength @ design temp	= 161 N/mm^2
Transverse stress in Nozzle	= 0.8 N/mm^2
Transverse stress in HX tubes	= 0.7 N/mm^2
Transverse stress in Headers	= 5.1 N/mm^2
Longitudinal stress in Headers	= 93.9 N/mm^2
Transverse stress in Tube-Plate	= 79.5 N/mm^2
Nozzle minimum thickness	= 0.02 mm
HX tube minimum thickness	= 0.02 mm
Header minimum thickness	= 0.1 mm

Plate minimum thickness	= 2.35 mm
Plate length/diameter	= 200 mm
Max. Allowable pressure	= 66.98 bar
Vessel category	= SEP
Tube material group	= 1.1
Nozzle nominal diameter	= 20
HX nominal diameter	= 20
Header nominal diameter	= 150
Plate material group	= 1.1

Based on these results, toolkit should declare that the design is safe and that stresses generated are within the strength limits of the materials being used. Designer can go ahead and save generated data in MS word format.

However, if the stress values have exceeded the strength values of the construction materials or a case where the vessel category is outside of the Safe Engineering Practice (SEP) region, then a warning sign is displayed. Designer then has to amend the dimensions of the heat exchanger parts.

Weld Calculations Tab

This tab was developed to enable the designer calculate the volume/area of welds. It is tied to values obtained from calculations in the structural design tab. This means that before this tab is used, prior calculations must have been carried out for the structural analysis of the heat exchanger.

This tab consists of 3 sub-tabs titled: Fillet Weld, Butt Weld and Bevelled Butt Weld. Values can be obtained individually for each tab, but as earlier mentioned designer **MUST** have performed calculations with the structural tab beforehand. This is because; the design strength of the weld metal must be the same as the parent metal. Each sub-tab and its functionality are described below. Also note that this tab does not offer the designer the opportunity to save calculated data.

A diagrammatic description of each joint type is shown for each tab in Fig. 25. Each sub-tab also has its individual **Execute** button.

Sub – tabs:

    A. Fillet Weld:

        i.   **Weld leg length:** Designer will be required to input the desired leg length of the fillet weld. He must also be aware that this value is measured in millimetres and usually ranges from 1mm – 5mm.

        ii.   **Length of plate:** When the

        iii.   **Area type:** comprises of the 2 options described below.

- **Weld leg length:** When this option is selected, the area of the weld is calculated using the length of the plate earlier indicated.

- **Throat thickness:** This calculation is independent of the length of the plate, and only depends on the leg length of the fillet weld. The area of the weld is calculated through the throat of the weld.

iv. **Material type:** The designer has to indicate whether the material is a **Tube** or **Plate**. This is necessary because the design strengths for tubes, will differ from that of plates, and this would have been seen from the **Structural calculations** tab

v.   **Results:** The results section has two sub-tabs named:

- **Area 1 (Leg lengths):** is the area calculated when the **Weld leg length** option has been selected. Its value is in mm^2, and the following results are also produced;

  - Force at joint due to inlet pressure: Indicates the pressure experienced by the joint as a result of inlet pressure only. Please note that this value is in Newton (N)

  - Maximum allowable force on joint: Tells the designer, the bearable load on this joint, based on the area earlier calculated. This is also in Newton (N).

- **Area 2 (throat thickness):** is the area measured when the **Throat thickness** area calculation option has been selected. Its value is in mm^2, and the following results are also produced;

  - Required throat thickness: Indicates to the designer, the minimum throat thickness required to bear the pressure load.

  - Force at joint due to inlet pressure: also as described above, this result tells the designer the force experience by this joint as a result of pressure loading, especially when calculated through the throat of the weld. This is especially useful when calculating stresses at the fillet weld around a tube diameter.

  - Maximum allowable force on joint: shows the maximum allowable force, this joint can bear. This value is also in Newton (N)

B. **Butt weld:**

i.   **Root gap:** Here, the designer indicates the space to be allowed between the plates in millimetres (mm).

ii. **Weld or Plate thickness:** is an indication of the thickness of the plate, which must also correspond to the thickness of the weld metal. This value is also in millimetres (mm)

iii.   **Material type:** User selects whether the material is a tube or plate.   The reason why this selection is necessary has already been mentioned.

iv.   **Results:** Presents the results of calculations based on the initial input data. It also consists of the following output fields, similar to the **Fillet Weld** field.

-    **Total area:** measures the area of the weld metal in mm^2.

-    **Force at joint due to inlet pressure:** measures the force experienced by the joint, as result of the inlet pressure of the fluid. This is also in Newton (N).

-    **Maximum allowable force on joint:** gives the designer, the maximum allowable load for that joint.

C.   **Bevelled Butt Weld:** This type of joint preparation, applies to parts where the edges have been machined. Examples are shown in the diagrams under this tab.

i.   **Bevelled angle:** refers to the angle made by the machined edges. This is usually in degrees.

ii.   **Excess weld metal height, h:** refers to the desired height of the weld metal on the joint. This is indicated in the diagram as '**h'.**

iii.   **Root gap:** refers to the smallest distance between the edges to be joined. This is indicated as 'b' in the diagram.

iv.   **Weld or Plate thickness:** refers to the thickness of the edges to be joined.

v.   **Root face:** refers to the face height at the end of the bevels. This height is usually no greater than 2-5mm.

vi.   **Material Type:** Has been described above.

vii.   **Bevel type:** Designer will be required to select the edge condition of the edges.

-    **Full Bevel:** means the two edges have been machined at an angle.

-    **Half Bevel:** means just one of the edges has been machined, while the other is left intact.

viii.   **Result:**

-    **Total area:** Tells the designer, the total area of the joint. This value will be dependent on the **Bevel Type** option earlier selected. This value is in mm^2.

-    **Force at joint due to inlet pressure:** as described earlier, this is the force experienced by the joint as a result of pressure loading from the tube-side fluid. This value is also bound to be different for the **Full** & **Half Bevel** conditions.

-    **Maximum allowable force:** measured in Newton (N), this refers to the maximum allowable force on the joint. This value is also bound to be different for the **Full** & **Half Bevel** conditions.

Conversion Tool Tab

This is the fourth tab in the toolkit design group. The conversion tool, offers the designer a quick and easier means to make conversions between selected values in the Imperial and SI unit format. It consists of 5 sub-tabs. These sub-tabs are composed of a heading stating the dimension (e.g. length, pressure, etc.), 1 input field (Left-Hand-Side), 1 output field (Right-Hand-Side) and 2 side-by-side aligned option buttons labelled "From" & "To".

Process of calculation is common across all the sub-tabs. User is required to follow the steps outlined below:

i.   User decides which dimensions to convert. The dimension available include: Length, Pressure, Temperature, Volume flow rate, and Power or Heat Rate Flow.

ii.   User types the value he needs converted in the LHS textbox.

iii.   User selects the current dimension of this unit in the "From" box.

iv.   User selects the new desired dimension of this unit in the "To" box.

v.   User finally clicks the convert button located between the two textboxes.

vi.   The converted value is produced in the RHS textbox field.

Available Sub-tabs:

i.   **Length:** User can choose from 5 options that include; Millimetres, Centimetres, Metres, Inches, Feet, and Kilometres.

ii.   **Pressure:** available dimensions include; Bar Pascal, Megapascals, Newton/millimetres^2, Newton/metres^2, Pounds per Square Inch, and Inches water column.

iii.   **Temperature:** dimensions include; Fahrenheit, Celsius, and Kelvin.

iv.   **Volume Flow Rate:** includes; metres^3/sec, metres^3/min, metres^3/hr., feet^3/sec, feet^3/min, feet^3/hr., Litres/second, Litres/min, Litres/hr., gallons/second, gallons/min, and gallons/hr.

v.   **Power or Heat Rate Flow:** British Thermal Units/sec, British Thermal Units/min, British Thermal Units/hr., Mega British Thermal Units/hr., Joules/sec, Watts, Kilowatt, Megawatt, Foot-pounds/sec, Foot-pounds/min, Foot-pounds/hr.

Reporting

This section describes actions the designer is bound to encounter after the thermal design and structural calculations only.

Saving the document

When the execute button is triggered and calculations performed, designer is presented with an option to either save or discard the produced result. The steps involved are shown below:

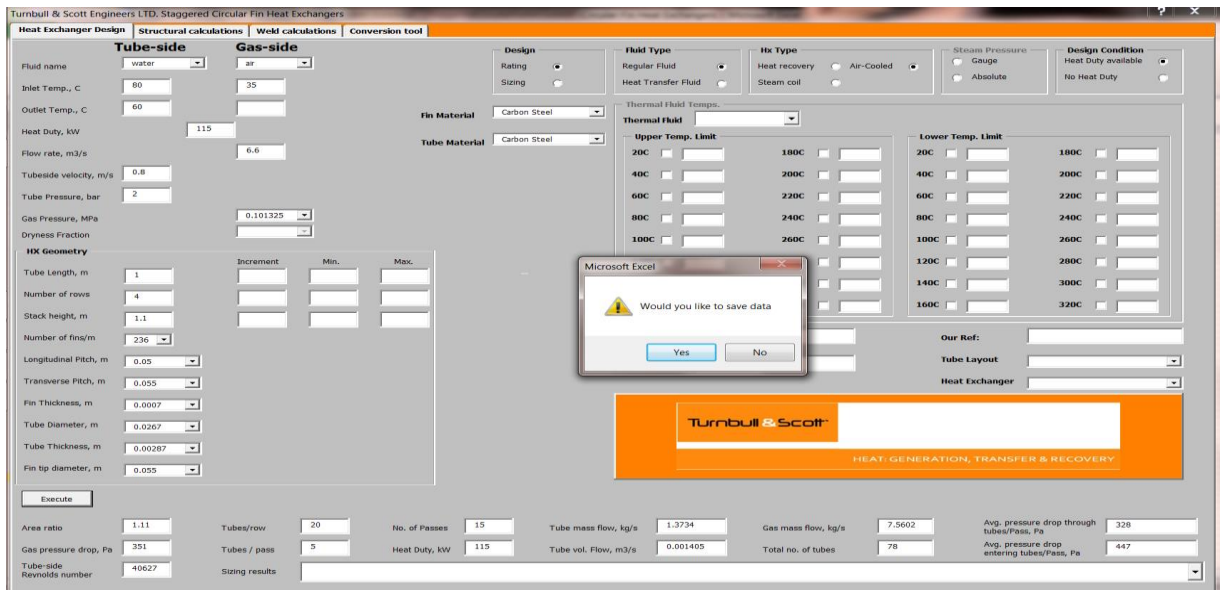A. Designer is offered the option to save calculated data, (Fig. 29 below)

Figure 46: Saving option

B. If "Yes" is the above answer, the screen below which represents the result sheet is produced and designer can view it.
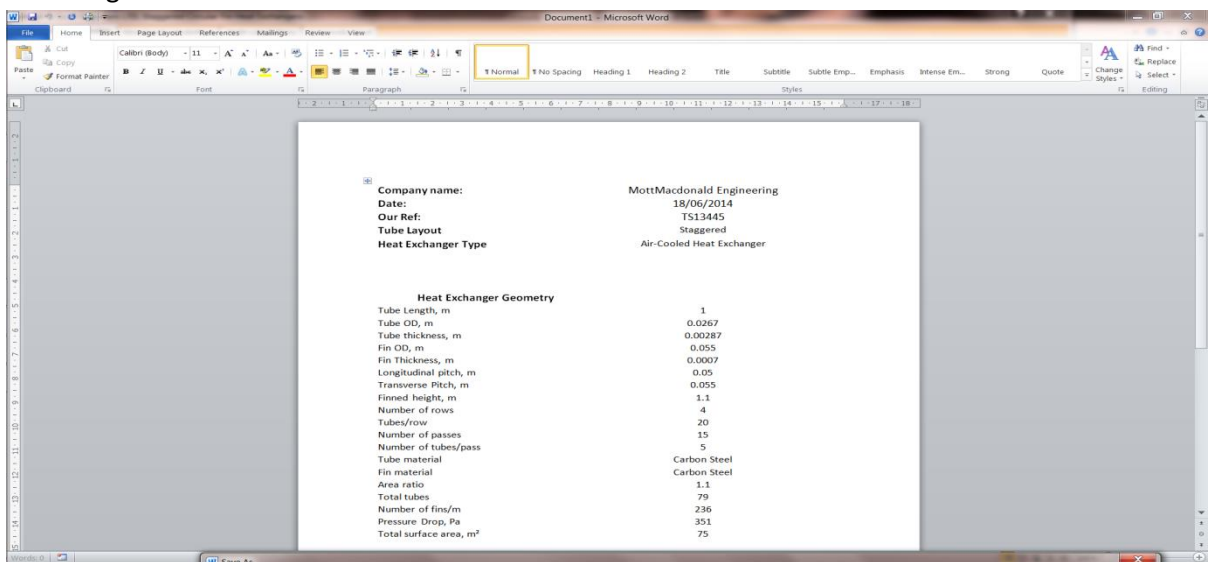

Figure 47: Calculations result sheet

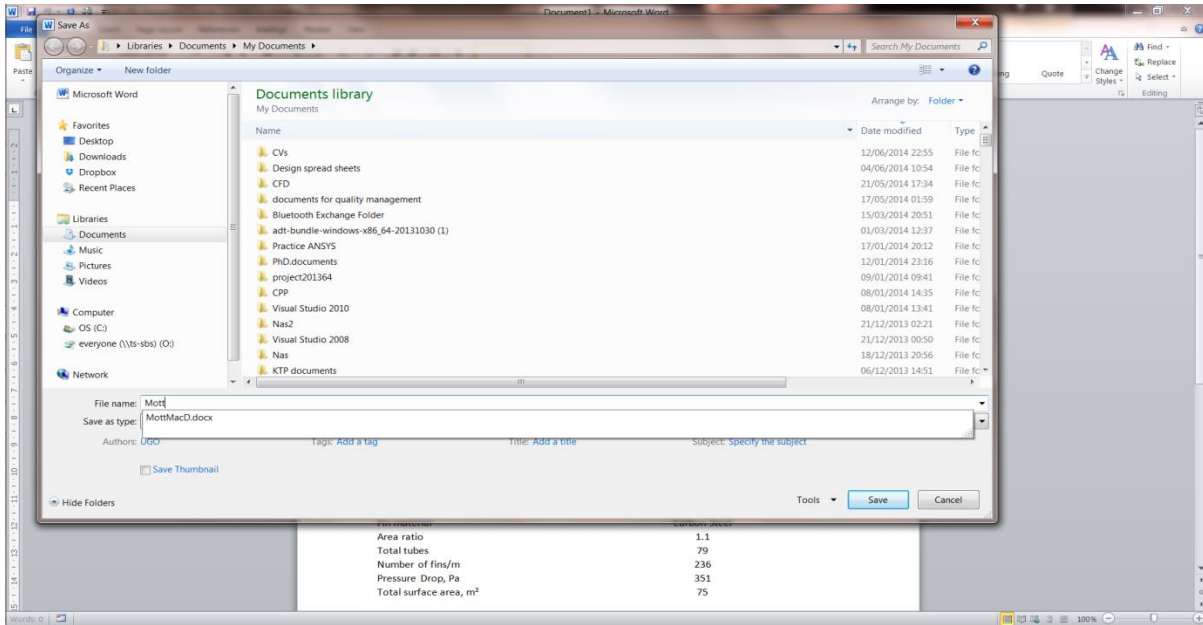C. Designer must then navigate to the preferred folder for saving documents. Name the file and click Save.

Figure 48: Saving the results sheet

D. This is the final produced screen, and designer just needs to close this by clicking the red box at the top right hand corner of the screen. Indicated below.
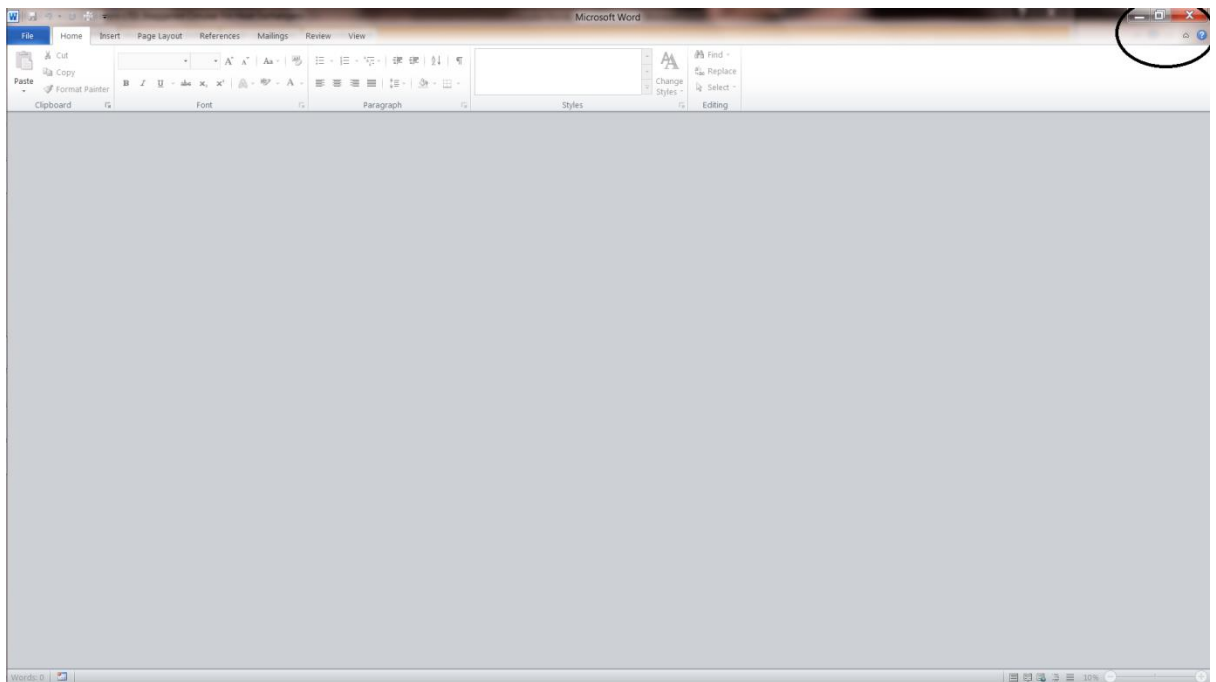

Figure 49: Closing the calculation result sheet

WARNING: IF THE DESIGNER OPTS NOT TO SAVE THE GENERATED DATA, HE MUST SELECT A "NO" ANSWER AT STEP 1. IF THE CANCEL BUTTON IS CHOSEN AT STEP 3, THE TOOLKIT IS BOUND TO DEVELOP PROBLEMS.

Troubleshooting

This section explains common type problems experienced with the toolkit, and ways to fix them.

To ensure that immediate issues are not encountered, designer must ensure that the thermal fluids software REFROP is installed on their individual computer systems. To install REFPROP, user should double-click the installation file and follow the instructions. Once installed, user should follow the steps below to ensure that REFPROP is properly linked to the spread sheets.

The following outlines the procedure for using REFPROP within any spreadsheet in Office 2007 or 2010:

1. Open REFPROP.xls and save it as an add-in, REFPROP.xla or REFPROP.xlam, in the main REFPROP folder, C:\Program Files\REFPROP.

2. Go to File/Options/Trust Centre/Trust centre Settings (bottom at bottom right).

3. Select "Trusted Locations" on the left. Click "Add new location". Browse to C:\Program Files\REFPROP, select "Subfolders of this location are also trusted", and click "OK".

4. Go to File/Options/Add-Ins and select "Excel Add-ins" in the Manage drop-down box at the bottom, and click Go

5. Click "Browse", and navigate to C:\Program Files\REFPROP, select REFPROP.xlam and click "OK". IMPORTANT: Do not simply select REFPROP.xlam when it first comes up, as this will be in the wrong folder (c:\Documents and Settings\Username\Application Data\Microsoft\Addins), which is not trusted and will not work.

6. Select the Data tab, and click on Edit Links. Select REFPROP.xlam. Click on "Change Source" and navigate to C:\Program Files\RREFPROP. Select REFPROP.xlam there and click "OK". This is just to make sure you are connected to the correct Add-in. If the Data tab is greyed out, start typing in a REFPROP command such as; "=Density ("water", "TP", 300, 1)" and the button should become active.

7. Once you have the .xla or .xlam file set up, you can open a brand new workbook and the functions should be available to you. Do not continue working with the REFPROP.xls file since it still contains the VB code that is also in the .xlam file. In this manner, future updates from NIST of the REFPROP.xls file can be resaved as the .xlam file, and all of your workbooks will have access to the most recent code.

Tips

1. In some cases, the macros may not work. Try saving the file as A MACRO-ENABLED WORKBOOK (under Save As…)

2. The .xls file distributed with version 9.0 sometimes will give false answers depending on the sequence of calculations if multiple .xls files are open. Switching between the open files may cause the initial setup to be lost. The updated .xls file given above fixes this.

3. For inputs that do not require a 5th parameter, Excel may require the comma at the end. For example: =Pressure ("water", "TVAP", "SI", 298).

4. If Excel cannot find the REFPROP fluid files, you can copy the *.FLD and HMX.BNC files into a default directory: C:\REFPROP\FLUIDS. When the program fails to find the fluid files, it will look to see if a C:\REFPROP\FLUIDS (or D :) is available, and if so, it will use the files from that source.

5. If you see dual entries for each function in your workbook, then you have either saved two .xla file, or you are working with a file that still contains the VB code. Start with a blank workbook to eliminate the dual entries for the latter case.

Common causes of calculation failure:

- Running the toolkit with another one open
- Incomplete fields in the toolkit.
- Using values not conforming to the SI unit format on which the toolkit has been built

Error Messages

1. Not enough system resources to display completely: This is probably the most common error message shown while the toolkit is being used. An example is displayed below. Designer is simply to ignore this message, by clicking the "OK" button and continue with the design exercise.
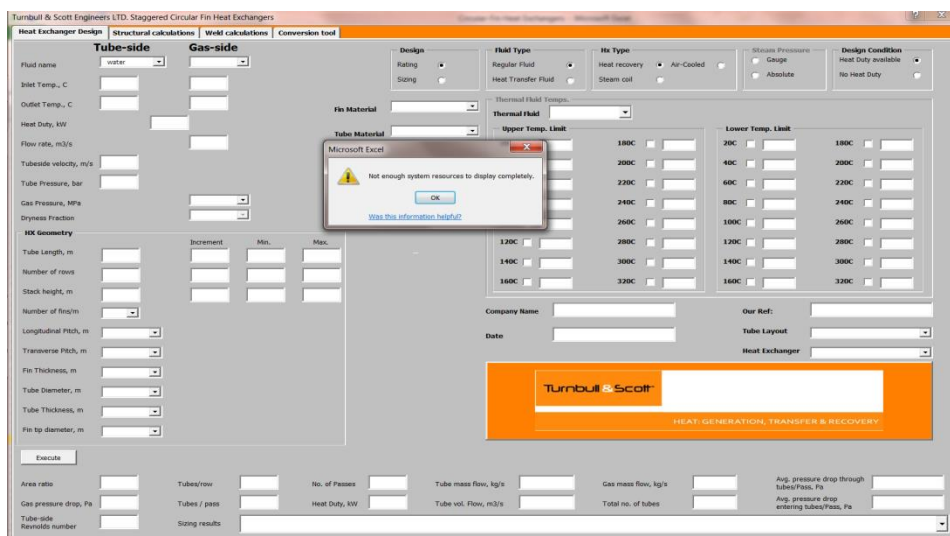

Figure 50: Error message display

Common Errors

1. Excel is not very smart and this also unfortunately applies to the developer who worked with it. Therefore, Designer must ensure that the other calculation sheets are closed before running any calculation or at least activate the user-form from the buttons located on the excel sheets titled "sizing".

2. Not filling all the necessary fields before the "**Execute button**" is hit. This is bound to cause errors in the computer program.